Technische Universität München
Lehrstuhl für Technische Chemie II

Selective liquid phase oxidation of *o*-xylene by spherical silica based transition metal catalysts

Tobias Förster

Vollständiger Abdruck der von der Fakultät für Chemie der Technischen Universität München zur Erlangung des akademischen Grades eines

Doktors der Naturwissenschaften (Dr. rer. nat.)

genehmigten Dissertation.

Vorsitzender:	Univ.-Prof. Dr. K.-O. Hinrichsen
Prüfer der Dissertation:	
	1. Univ.-Prof. Dr. J. A. Lercher
	2. Univ.-Prof. Dr. K. Köhler

Die Dissertation wurde am 06.10.2010 bei der Technischen Universität München eingereicht und durch die Fakultät für Chemie am 09.12.2010 angenommen.

„So eine Arbeit wird eigentlich nie fertig, man muss sie für fertig erklären,
wenn man nach Zeit und Umständen das Mögliche getan hat.“

Johann Wolfgang von Goethe (1749 – 1832)

Acknowledgements

After the work has been done I want to thank all who contributed and helped in any kind of way to the success of this thesis in the past years.

First of all I want to thank Johannes (Prof. Dr. J. A. Lercher) for offering me the opportunity to work in his group. The invitation to perform my Ph.D. thesis in your international and prestigious group was a great pleasure for me.

Additional I want to acknowledge my senior scientist supervisor Andy (PD Dr. A. Jentys). The discussions with you helped me very much and you where there whenever I had any kind of question all over the time.

Especially I want to thank Dr. Stephan Schunk from *hte company* in Heidelberg for giving impulses in the field of radical analysis and for interesting and stimulating discussions during the publication process and for helping with words and deeds.

Thanks to Xaver Hecht and Andreas Marx for all the help in building set-ups and solving technical problems whenever necessary and Martin Neukamm for the BET and AAS measurements. For help in all administrative matters Steffi Maier, Helen Lemmermöhle and Katharina Thies are gratefully acknowledged.

For creating a productive and friendly working atmosphere I want to thank Ana Hrabar, Sonja Wyrzgol, Daniela Hartmann, Stephan Reitmeier, Florian Schüßler, Robin Kolvenbach, Michael Salzinger, Oliver Gobin, Yongzhong Zhu, Roberta Olindo and all other members of TCII which I did not mention here. It was a great pleasure to work together with you.

Furthermore I want to thank Gabi Raudaschl-Sieber and Oksana Sterchova for good advice and help with any problem with MAS NMR spectroscopy.

I also want to thank all students who worked in the field of technical chemistry under my supervision. First I want to mention Sarah Maier who made her diploma thesis in the field of the liquid phase oxidation of *o*-xylene. Furthermore I want to mention the bachelor students Irene Raitmeir, Michael Pschenitza, David Schlereth, Henriette Mahler and Simon Pedron and all the students performing during their “Mitarbeit am Arbeitsplatz” Sanna Zimmer, Björn Askevold, Sebastian Hock, Johannes Daprá and Andreas Wirth.

My dear friends Manuela and Richard: I want to thank the two of you for all the funny and entertaining hours we spent together. I think the working hours gained a lot of attraction because of you.

Last but not least I want to express my deep gratitude to each member of my family for supporting me in all circumstances during the whole time of my studies. Thank you very much, without you this work would not have been possible!

Table of contents

Chapter 1

General Introduction

1.1. Motivation

Oxidation products of the two xylene isomers p- and o-xylene play an outstanding role for the broad spectrum of value products in the field of polymer chemistry. Terephthalic acid which is gained as its ethyl ester from p-xylene is the main component in polyethylene terephthalate (PET) used as a large scale material for plastics, mainly bottles. But also phthalic acid is an important component for the production of plastics. It is mostly used as plasticizer for example in the production of PET.

In the first industrial processes phthalic anhydride was gained by the oxidation of naphthalene. This process is still applied nowadays very rarely depending on the available feedstocks. During this reaction route by definition two carbon atoms per molecule of reactant are lost. This fact led to a further development of the oxidation reaction because it is economical and ecological not favorable. The most widely spread process for the production of phthalic anhydride these days is the direct oxidation of *o*-xylene by air over vanadia-titania catalysts:

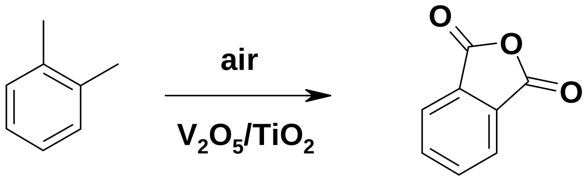

Scheme 1-1: Oxidation of o-xylene to phthalic anhydride over vanadia/titania catalysts.

In terms of carbon efficiency this process is a clear improvement to the original. But still there is room for further development. The major drawback of the direct oxidation of *o*-xylene lays in the limited selectivity of approximately 85% at a conversion of 100%. The rest mainly results in the total oxidation product CO_2 and thus is lost as a value product. One possible starting point to improve the yield of the desired phthalic anhydride is the partition of the process into two steps.

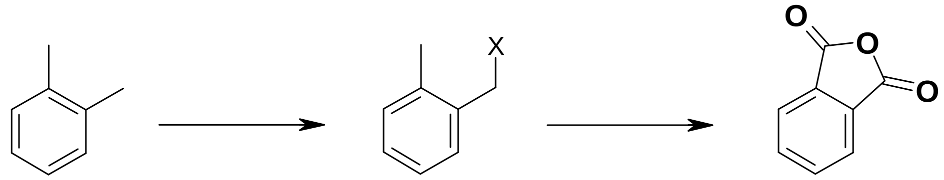

Scheme 1-2: Two step process for the oxidation of *o*-xylene to phthalic anhydride. Note that X stands for oxygenate and is not further defined.

In a first step *o*-xylene is oxidized to a mixture of oxidation products of one of the two methyl groups. Further oxidation of these oxygenates is performed in a second reaction step in which the existing catalyst technology can be applied. The advantage of this two step process is that the reaction parameters as temperature, residence time and catalyst activity can exactly be tuned depending on the composition of the oxygenate mixture. With this tuning possibility the oxidation can be performed under milder conditions and thus the overall selectivity towards phthalic anhydride can be increased.

One possibility for the selective oxidation of one methyl group is the application of a liquid phase oxidation route. Typically Co and/or Mn based systems are applied as catalysts for these reactions being considered as radical chain reactions. It is most likely for this type of reaction that it will stop at the mono acid because of its high stability. Applications are known for the liquid phase oxidation of *p*-xylene to terephthalic acid. In this process an additional source of Br is added to increase the activity of the initiator system and thus also oxidize the second methyl group of the molecule.

The target of the research is to optimize a liquid phase route for the selective oxidation of one methyl group in *o*-xylene. Further requirements to the developed process are the use of heterogeneous catalyst system and the prevention of the use of solvents. One solution for this is the use of transition metal catalysts embedded in organically modified hydrophobic silica materials which are applied in a solvent free process.

1.2. Scope of this thesis

This doctoral thesis aims at the detailed description of the selective liquid phase oxidation of one of the two methyl groups of *o*-xylene by heterogeneous transition metal catalysts. In this context the development of the materials which are suitable as catalyst and initiator systems is as important as the understanding of elemental reactions during the oxidation reaction.

Synthesizing materials in a defined macroscopic shape in a one step procedure which offer catalytic activity is a challenging task of high potential for application in industrial processes. In this work the incorporation of catalytically active transition metal components into a network of hydrophobic polysiloxane was developed. An optimized procedure to synthesize spherical particles is described by varying relevant parameters such as type of precursor compounds, precursor composition or the application of the various catalysts. The incorporation of several kinds of transition metals is described. The complexation to an amino group which is fixed to the silica matrix and the accessibility of transition metals were studied by FT-IR spectroscopy. Furthermore the impact of the transition metal addition on the specific surface area and the condensation behaviour of the spheres were elucidated.

Due to the hydrophobic properties of these organically modified transition metal catalysts the selective liquid phase oxidation of *o*-xylene to partially oxygenated intermediates is a suitable application for these materials. By using gaseous oxygen a potentially industrial applicable bubble column reactor system was developed. Scientifically the focus was on the investigation of the reaction steps and on the understanding of the course of the radical chain reaction mechanism of the catalyst modified oxidation reaction. Thus the influence of the catalyst composition and the type of transition metal on the reactivity and the selectivity towards oxygenates is elucidated. Upon the most attractive transition metals cobalt and manganese are considered to be especially promising.

Next to the development of active catalysts the description of the reaction network was a major focus of the presented work. The primary product of the present reaction is supposed to be 2-methylbenzyl hydroperoxide which is challenging to be quantified due its thermal instability. Therefore, a method to selectively reduce it to the alcohol before analysis was adopted from literature and improved. The major products at low *o*-xylene conversions were *o*-tolualdehyde and 2-methylbenzyl alcohol.

Illustrating the described reaction network by mathematical simulations is a further aspect of the thesis. The quantitative comparison of the most promising cobalt and manganese catalysts to their homogeneous counterparts plays a decisive role. Moreover an analysis of spent catalysts after reaction will be performed in order to follow changes during the reaction and investigate the catalysts' stability.

Chapter 2

Theoretical considerations

2.1. Selective oxidation of hydrocarbons

Among petrochemical processes oxidation reactions are one of the most important group of reactions. Especially when oxygen is introduced into hydrocarbon molecules oxidation is the most favorable choice.

Oxidation is defined as a reaction which increases the formal oxidation number of the reactant. For oxidation reactions of organic molecules, in principle, two types of reactions can be differentiated. On the one hand the dehydrogenation and on the other hand the introduction of heteroatoms like O, N or Cl into the molecule. In both reactions the oxidation number of carbon increases. Selective oxidations of organic compounds by oxygen thus offer a cheap route to incorporate functional groups which are the reason for the added value of chemical compounds. Examples for functional groups are alcohols, aldehydes, acids, esters or ethers. When carbon containing molecules react with oxygen the thermodynamic most stable product is CO_2, which is of no value for the chemical industry. Oxygenates are industrially most attractive and thus interesting in research. As these molecules are intermediate products with respect to the thermodynamics. Therefore, selective oxidation reactions are a sensitive interplay of finding the right balance of activity to reach a sufficient yield of the desired product and not to over oxidize the reactant to CO_2 (see Figure 2-1).

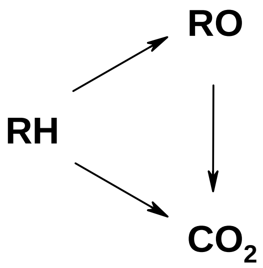

Figure 2-1: Formation of oxygenates during the oxidation of hydrocarbons.

A very illustrative explanation of the selective oxidation principle is given in by C. H. Bartholomew. [1] The partial oxidation is compared to “toasting marshmallows on a campfire; the trick is to find the perfect conditions near the red hot coals and to allow just enough time to reach a nice gold-brown without burning them to a tasteless black crisp." Translated to science this means to find appropriate catalysts showing high selectivity towards partial oxidation products compared to complete combustion and furthermore to find the right reaction conditions particularly the temperature to avoid loss of selectivity.

Table 2-1: Overview of some important industrial applications of selective oxidation reactions. Adopted from [1]

Selective oxidation product	1994 world-wide production (10^3 t *p.a.*)	Principal uses
Acetic acid	3.1	Intermediate for vinyl acetate, acetic anhydride, esters
Methyl-*t*-butyl ether	25.5	Gasoline additives
Methanol	29	Intermediate for formaldehyde, methyl chloride, solvents
Phthalic anhydride	3	Dyes, polymers, plasticizers, polyesters
Vinyl chloride	18	Polyvinyl chloride

For selective oxidation reactions numerous different catalyst systems are known. Most of the materials used for heterogeneous gas phase reactions are based on metal oxides. As a second component a redox active (transition) metal is present which undergoes the actual transfer of electrons. A very prominent example is V_2O_5 which is typically used on oxidic supports like TiO_2. By applying special synthesis procedures these catalysts have a very high activity for the respective reaction. Next to the main component many additives can be inserted to improve the activity, selectivity towards the desired product or the stability of the catalyst.

When oxides are applied as catalyst in oxidation reactions the mechanism commonly follows the Mars-van-Krevelen type mechanism. The reactant is oxidized by reacting with an oxygen atom from the catalyst surface (see Figure 2-2):

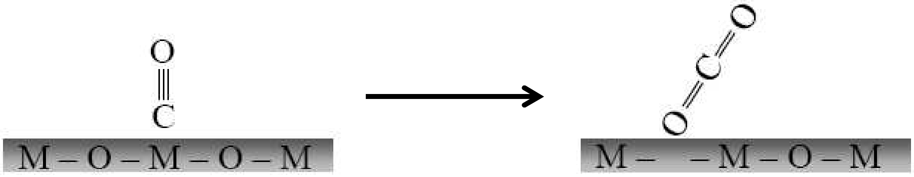

Figure 2-2: Reduction and regeneration of the oxide surface by the reactant during the Mars-van-Krevelen mechanism.

After the reaction product desorbs from the catalyst the regeneration of the surface is performed by oxygen which comes from the oxidant. In most cases this is molecular oxygen from air. This principle reaction mechanism is also called defect site mechanism because a defect site in the catalyst surface is created during the reaction.

From the mechanistic understanding it is obvious that the bond strength of the metal oxygen bond plays a key role for the catalyst's performance. If the bond is too strong, hydrocarbon oxidation will not take place, and if it is too weak, overoxidation to CO_2 will occur. Grasselli described this correlation in an overview article of selective oxidation reactions with the following scheme: [2]

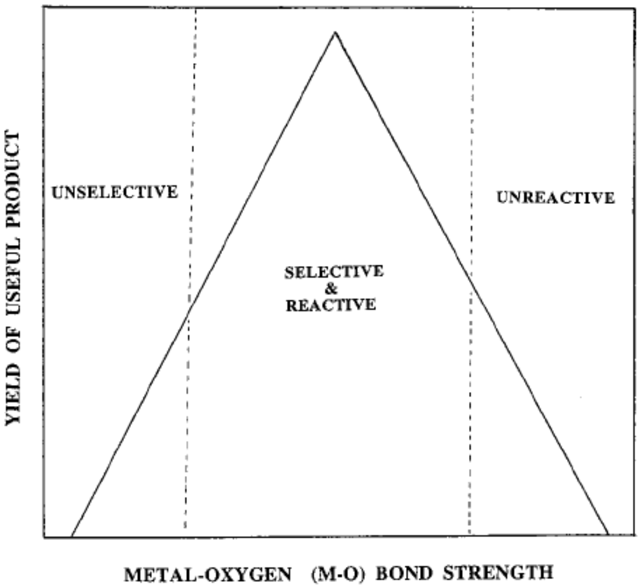

Figure 2-3: Dependence of theoretical product yields on the metal-oxygen bond strength (Adopted from [2]).

As the most appropriate materials Grasselli mentions oxides which have covalent or amphotheric bond character, e.g. molybdates, antimonates or vanadates. Grzybowska-Swierkosz specifies this in her review article in a more detailed way. [3] The M-O bond energy for unselective catalysts is approximately 100 kJ/mol. This bond strength is typically found in transition metal oxides, e.g. NiO, Co_3O_4 or MnO_2. These oxides are known to promote the total oxidation because the oxygen is readily donated to the reactant. For selective oxidation catalysts the M-O bond energy is in the range of 300 kJ/mol. If the bond becomes too strong on the other hand no catalytic activity will be observed (see Figure 2-3).

2.2. Selective oxidation of xylene isomers

2.2.1. Free radical chain reactions

Radical reactions are combinations of a series of principle steps which include initiation, radical chain propagation and termination.

$$In_2 \longrightarrow 2\,In^{\bullet}$$

$$In^{\bullet} + RH \longrightarrow R^{\bullet} + InH$$

$$R^{\bullet} + O_2 \longrightarrow ROO^{\bullet}$$

$$ROO^{\bullet} + RH \longrightarrow R^{\bullet} + ROOH$$

$$2\,ROO^{\bullet} \longrightarrow O_2 + \text{Oxygenates}$$

Scheme 2-1: Basic reactions of a free radical chain oxidation.

During the initiation the first radicals are formed via homolytic bond cleavage in an initiator molecule. Initiators can be added to the reaction in form of labile compounds which decompose at certain temperatures. Alternatively impurities, mainly small amounts of hydroperoxides present in the reactant can support the initial radical formation. Thus this step is crucial for the start up of the reaction and the build up of a certain radical concentration to keep the chain reaction running. If no catalyst is used the initiation mainly proceeds via the bond cleavage of the primary formed hydroperoxide which decompose to two radicals (alkoxy and hydroxy) from one starting molecule as the bond strength of the O-O bond is only approximately 150 kJ/mol. [4]

The chain propagation step consists of two principle reactions. An addition of molecular oxygen to an alkyl radical is the first of these. The resulting alkylperoxy radical abstracts a hydrogen atom from a reactant molecule to form a hydroperoxide and an alkyl radical to close the circle of the chain reaction. The selectivity of the reaction is determined by the C-H bond strength. Hydrogen is preferentially abstracted from the weakest C-H bond. In the case of alkyl substituted aromatics this is the alkyl chain. In the toluene molecule for example the dissociation energy of the C-H bond is 465 kJ/mol and 370 kJ/mol for the aromatic and the alkyl C-H bond respectively. [5] In principle it can be concluded that the selectivity of the process is lower the more reactive the attacking radical is. As an alkylperoxy radical shows only modest reactivity, it has a relatively high preference to attack the weakest C-H bond. On the contrary the hydroxy radical is a very reactive and thus unselective radical.

Termination of radical reactions is the combination of radicals to non radical products which accompanies with a net decrease of the radical concentration. Generally combination of any present radical species can occur and terminate the reaction. In the case of recombination of two alkylperoxy radicals products are alcohols and aldehydes under oxygen liberation.

Autoxidation reactions can be catalyzed by transition metals. Next to the acceleration of the initiation step, which is not a real catalytic function, transition metals are able to catalyze the decomposition of the hydroperoxide. This catalytic pathway is known as the Haber-Weiss mechanism: [6]

$$\mathrm{ROOH} + \mathrm{M}^{n+} \longrightarrow \mathrm{RO}^{\bullet} + [\mathrm{M}^{(n+1)+} \cdot \mathrm{OH}^{-}]$$

$$\mathrm{ROOH} + [\mathrm{M}^{(n+1)+} \cdot \mathrm{OH}^{-}] \longrightarrow \mathrm{ROO}^{\bullet} + \mathrm{M}^{n+} + \mathrm{H_2O}$$

$$2\,\mathrm{ROOH} \longrightarrow \mathrm{RO}^{\bullet} + \mathrm{ROO}^{\bullet} + \mathrm{H_2O}$$

Scheme 2-2: Haber-Weiss mechanism for the catalytic decomposition of hydroperoxides over transition metals.

Transition metals that are capable to perform the decomposition of hydroperoxides are those which readily change between two successive oxidation states like Co or Mn. Scheme 2-2 gives only a representative overview of the function of the transition metal during the process. In the case of a non catalyzed decomposition the neat result is equal. But this route proceeds via a free OH radical which very reactive. Therefore the role of the transition metal can also be described as a stabilization of the OH radicals. Furthermore the transition metal enhances the formation rate of radicals by creating alkyl radicals. [7]

Organic molecules usually are present in a singlet ground state. The oxygen molecule as a biradical in its ground state is a triplet. A direct reaction of oxygen and a hydrocarbon is very slow at room temperature due to the fact that reactions of singlet and triplet states are spin forbidden. A concerted insertion of oxygen to C-C or C-H bonds can thus be neglected. To transfer the hydrocarbon into a triplet state two possibilities are available. First the transfer of an electron from the organic substrate to oxygen or to a catalyst can occur. More likely is the direct abstraction of a hydrogen atom by the biradical oxygen or by another radical species, e.g. an initiator.

2.2.2. Radical based oxidation route

The oxidation of xylene to the corresponding acid follows a route of consecutive reactions via the formation of alcohol and aldehyde (see Scheme 2-3). In this sequence the acid is the thermodynamically favored product. If intermediates are desired as value products the reaction has to be stopped at the maximum yield of the desired product, which is for example the case in pharmaceutical applications. Additionally, this can be achieved by adding the corresponding stoichiometric amount of oxidizing agent to the reaction or by removing the product from the reactor.

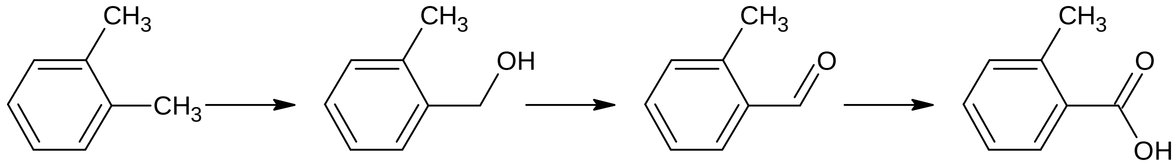

Scheme 2-3: Product sequence of oxidation reactions of *o*-xylene as an example for alkyl aromatics.

A key step during the side chain oxidation of xylene is the formation of benzylic radicals and their further reactions. The formation can occur via homolytic bond cleavage or by a redox process (Scheme 2-4).

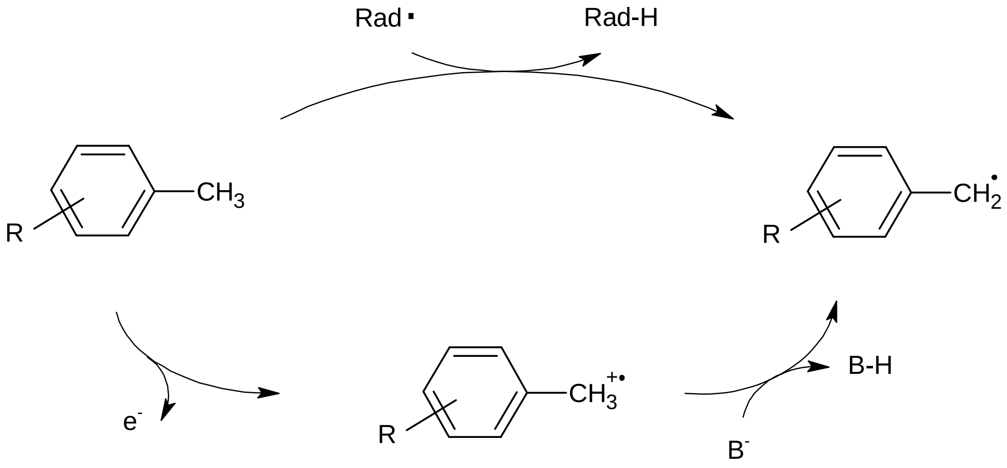

Scheme 2-4: Formation of benzyl radical from an alkyl substituted aromatic.

A homolytic bond cleavage of the C_α-H bond can occur when a radical **R** attacks the reactant. This radical can be a radical initiator which is added to the reactant or a radical from an ongoing radical chain reaction. A hydrogen atom in the benzylic position is abstracted by the **R**. The reactivity is defined by the dissociation energy of the C_{α}-H bond and the stability of the formed radical. In the case of a redox process the aromatic is first oxidized to a radical cation by electron transfer from the π-system. By a base this cation is deprotonated and a charge neutral radical is formed. The reactivity via this route is defined by the ionization potential of the aromatic and the acidity of the radical cation. Consecutive reactions of the benzyl radical are radical substitution, recombination of radicals and the oxidation of the radical.

The liquid phase oxidation of methyl substituted aromatics is performed with air as oxidizing agent on industrial scale. Originally cobalt or manganese compounds, or a mixture of both, were used as catalysts. During the production of terephthalic acid the further oxidation of *p*-toluic acid is a big problem. Due to the deactivating effect of carboxy group the oxidation of the mono acid was very slow. A first improvement was the esterification of the first carboxy group with methanol to enhance the mono acid's reactivity. [8] An alternative was shown in the Eastman-Kodak-process. There acetaldehyde or propanone were used as a co-oxidizing agent. [9] A way to improve the activity of the initiator system was introduced by the Amoco in the late 1950s. It was shown that the addition of any kind of bromine source to the reaction significantly increased the yield of terephthalic acid. The use of Co(II)/Mn(III)/Br^- as initiator system is known as the Amoco-MC (MC stands for *mid-century*) process. [7] This system was further developed in the past years and it was found that the selectivity towards terephthalic acid was increased by additives like hafnium, zirconium, cerium or molybdenum. [7, 10, 11]

2.2.3. Industrial gas phase process

An example of a very well studied process in chemical industry is the gas phase oxidation of *o*-xylene to phthalic anhydride. [12-16] Typically vanadia-titania catalysts are used in this process. As the reaction is highly exothermic catalyst with low specific surface areas (ca. 10 $m^2 g^{-1}$) are used also to make consecutive reactions less favored. Typically 2 wt. % V_2O_5 are grafted on anatase. On industrial scale the process is performed in multitubular fixed bed reactors at temperatures of around 400°C. The conversion of *o*-xylene is very close to 100% with a phthalic anhydride selectivity of approximately 85%.

In the gas phase oxidation of *o*-xylene a broad variety of catalyst additives are known in literature. [3, 16, 17] This makes the catalyst system to an almost alchemistic mixture of many components and every company which is conducting this reaction has its own recipe for the best available catalyst. One of the secrets obviously is to find the right form of surface species (see Figure 2-4).

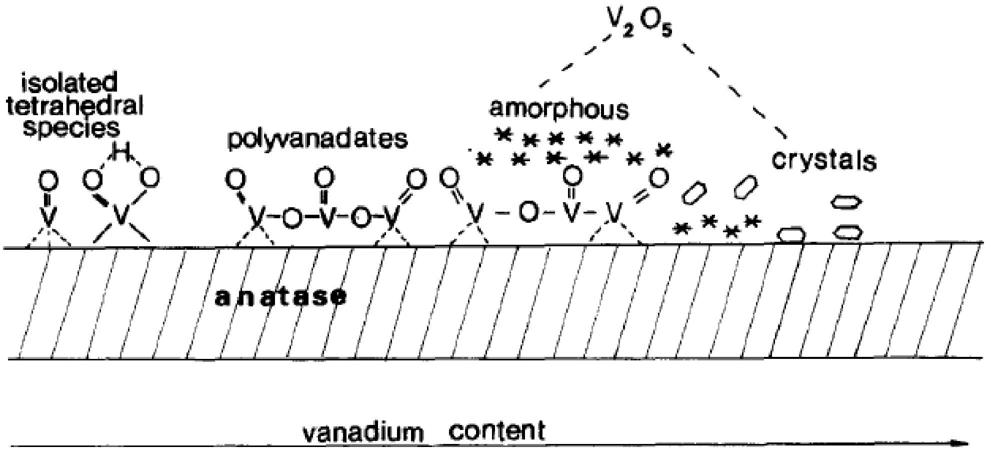

Figure 2-4: Different V_xO_y species on TiO_2 anatase support. [13]

The different species increase in particle size with the concentration of vanadium on the support. With growing particle size the outer surface and thus the relative number of active vanadium atoms decreases. If one mono layer of V_xO_y is exceeded amorphous or crystalline V_2O_5 is formed which shows the lowest activity. Highest catalytic activity is observed for isolated species. Finding the balance between active isolated species which occur at very low loadings and a sufficient concentration of vanadium in the catalyst is the key challenge in producing highly active catalysts. One way is to insert additives which are able to stabilize the most active species even at higher vanadium contents. Further functions of additives are: the prevention of anatase rutile transformation (e.g. Mo), decrease of byproduct formation (e.g. K), reduction of the surface acidity to improve the adsorption of xylene (alkali promoters) or enhancement of the surface acidity to reduce the adsorption of acid reaction products. [18]

2.2.4. Recent developments

In recent process developments sustainability and environmental considerations play a key role. Not only to improve the carbon efficiency but also to increase the energetic economics of chemical processes are important fields in the chemical engineering area. Moreover the chemistry itself might be changed to reach those noble goals. Basically three possibilities are available. Firstly the reactant itself can be substituted to a more suitable precursor for value products. This especially is interesting if carbon is lost during the reaction. Also the catalysts can be modified in a way that the selectivity to the desired product is increased. And finally the solvents used can be changed to environmentally friendly i.e. better recycling or for example substitution by water or supercritical CO_2. But the most environmentally friendly solvent is – no solvent.

2.3. Principle of sol-gel transformations

The sol-gel process is a synthesis procedure for non metallic inorganic polymers which can result in pure oxides or contain organic fragments. Sol-gel technology offers a useful tool to vary material properties in a very broad range with relatively low experimental effort. [19-21] These properties include the polarity, mechanical stability, acidity, introduction of special functionalities and many other features. [22-27] In principle reactions of Si, Al, Zr or Ti are performed as sol-gel reactions as suitable precursors of these are available and stable under atmospheric conditions. Upon these elements Si is the most frequently and best understood component. This is the reason why in the following explanations are based on Si. The principle reactions include the hydrolysis of precursors, the condensation and the formation of the gel.

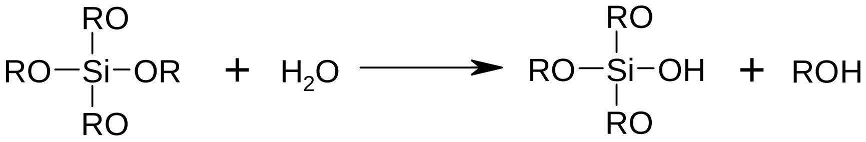

Scheme 2-5: Hydrolysis reaction of silicon alkoxides.

In the hydrolysis step reactive hydroxy intermediates of the metal are formed. The precursor thus consists of compounds that have at least one hydrolysable bond; most frequently alkoxides are used. As the Si-C bond is stable against hydrolysis and temperatures below 100°C are applied during the reaction organic functional groups can be introduced into the material via utilizing precursors carrying one to three organic side groups.

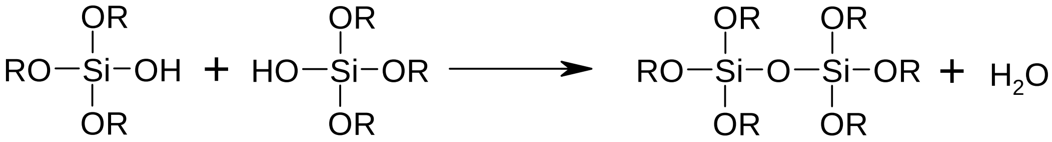

Scheme 2-6: Condensation of silanol intermediates.

The hydrolysis is followed by condensation of the intermediately formed hydroxy species. Condensation can also occur with alkoxy groups resulting in one equivalent of alcohol. The formed inorganic polymer first forms a sol consisting of very small colloidal particles. Agglomeration of these is called gelation. A gel is defined as a solid which includes a liquid phase usually the solvent or condensation product. After drying the sol is called aerogel or xerogel depending on the way of drying. The polymerization to macroscopic particles includes three steps: polymerization of monomers, particle growth and combination of particles to chains and networks.

Both basic steps, hydrolysis and condensation, can be accelerated by catalysts. It should also be mentioned that these reactions are not separated but take place parallel. Generally it can be concluded that acids increase the rate of hydrolysis and basic catalysts enhance the condensation reaction. [28] Another type of reaction accelerator is based on dialkyl tin compounds having two hydrolysable groups. The silanol reacts with the tin compound to an ether like species which then reacts with a further silanol molecule. By this the OH group is transformed into a better leaving group and thus the condensation is accelerated.

2.4. Synthesis method of spherical silica

Catalysts applied in industrial processes need to have macroscopic shapes. After catalytic active materials have been synthesized the materials undergo a molding process to fulfill this requirement. Only few synthesis procedures are known in which a direct formation of applicable shapes is performed. One example is the production of spherical polysiloxane support materials in the millimeter range.

Spherical particles are formed from droplets in a water atmosphere while different ways to create stable droplets are known. The simplest way is to inject a hydrophobic precursor mixture into a vessel with stirred water. A drawback of this method is the unequally distributed drop size. This will end in a very broad particle size distribution of the resulting solid spheres. In order to overcome this problem a method was developed by Witossek *et al.* [29, 30] in which droplets are created on the end of a needle by a water flow with constant flow rate.

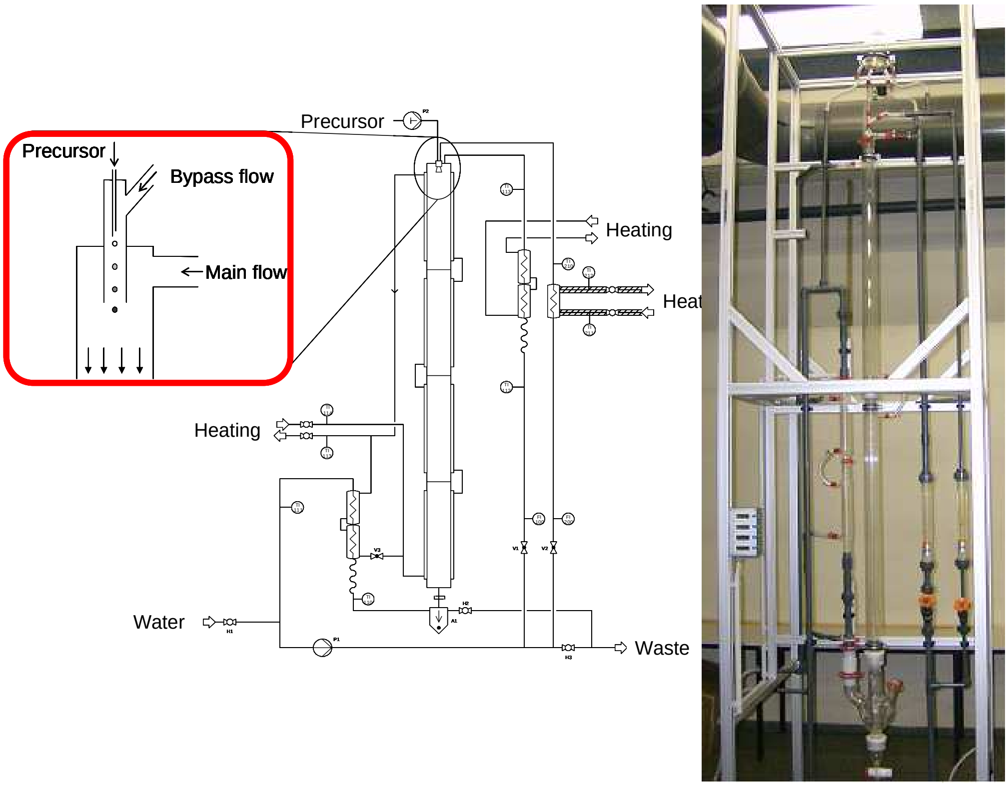

Figure 2-5: Set up for the synthesis of spherical polysiloxane particles.

A precursor mixture is introduced on top of the reactor system by a syringe pump via a needle. By a constant bypass flow in the reactor droplets with equal diameters are formed (see magnification in Figure 2-5). With the bypass flow the droplets are transported into the main part of the water filled, heated reactor column. As the mixture of precursors is hydrophobic the droplets remain stable in the water surrounding. Since the density of the reactant solution is below the density of water the droplets tend to ascend. But because of the down flow of water they are kept in balance until their density is increased since the degree of polymerization is growing. When a certain extent of solidification is reached particles sink to the bottom of the reactor and are collected in a storage container.

Besides the hydrophobicity of the precursor solution the velocity of the bypass flow is of great importance for the appropriate formation of drops (see Figure 2-6).

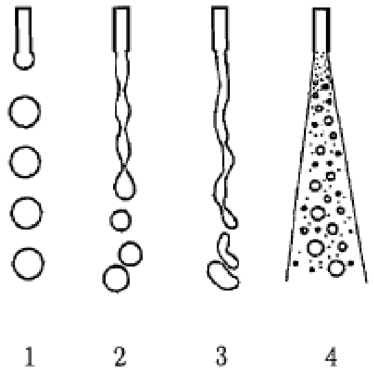

Figure 2-6: Different types of drop formation. [31]

In Figure 2-6 different regimes of droplet formation are illustrated whereas the flow rate is increasing from 1 to 4. At very high bypass flows (case 4) the precursor solution is atomized from the needle resulting in very small drops without any defined size distribution. If the bypass flow rate is reduced a jet is formed. This can result in undefined drop shapes (case 3) or spherical droplets (case 2) can be formed which do not show evenly size distributions. Best results are reached when the flow velocity is further decreased and single drop formation is observed. Only in this mode a monodispers size distribution can be achieved.

Within the regime of single drop formation, which can only be achieved under laminar bypass flow conditions, the diameter of synthesized polysiloxane spheres depends on the velocity of the bypass flow (see Figure 2-7).

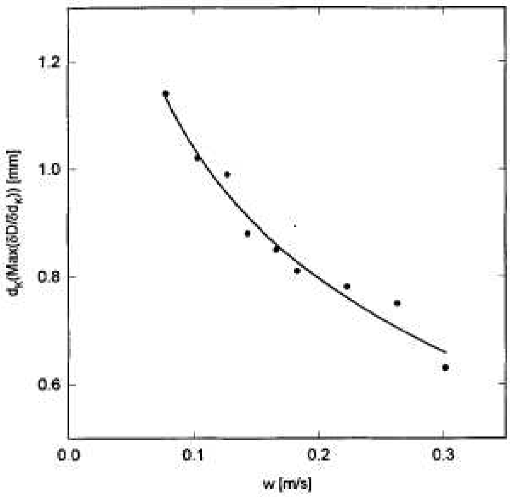

Figure 2-7: Dependence of the particle size on the bypass flow rate. [29]

Generally all types of silane precursors can be used in this synthesis procedure as long as conditions can be found which assure a sufficient polymerization velocity. This is one of the key points in the presented process as the reaction rate has to be well balanced. On the one hand it has to have a minimal rate to assure solidification. On the other hand the velocity has to be below a certain value at which the polymerization already starts on the top of needle resulting in a blockage of the precursor supply.

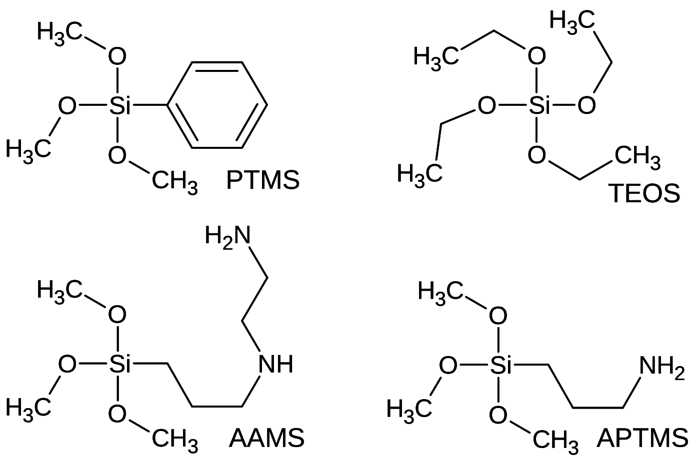

Scheme 2-7: Most frequently used silane precursors (PTMS: phenyltrimethoxysilane, TEOS: tetraethyl orthosilicate, AAMS: 3-(2-aminoethylamino)propyl]trimethoxy-silane, APTMS: 3-aminopropyl-trimethoxysilane)

Mixtures which fulfill these requirements best consist of the network building component TEOS and an amino group carrying silane like AAMS or APTMS. The network building component is necessary to guarantee a satisfactory mechanical stability of the spheres and the basicity of the amino group is required to assure a sufficient reaction rate. The rate is additionally adjusted by adding tin compounds which are known to accelerate polycondensation reactions of silanes.

2.5. Introduction of transition metals

The sol-gel process generally allows an incorporation of different metals into the framework via hydrolysis and condensation of alkoxide precursors; examples are Zr, Ti or Al. Via this route oxides of different metals are created resulting in interesting properties such as acidity. As the precursors of different metals have very different reaction rates an even distribution of the hetero metals is very ambitious to reach. Also it is questionable whether these metals show any catalytic activity.

A more general way to introduce transition metals into the matrix is the anchoring of those via organic functionalities on the polysiloxane surface. Due to its electron donating property the amino group is the most suitable among those. Via this bonding position metals can be incorporated. In general two options exist: a direct addition of transition metal precursors to the reaction mixture of the silanes or inclusion by an impregnation procedure with synthesized polysiloxane supports.

2.6.References

[1] C. H. Bartholomew, *Fundamentals of Industrial Catalytic Processes*, Chapman & Hall, **1997**.

[2] R. K. Grasselli, *Top. Catal.* **2002**, *21*, 79.

[3] B. Grzybowska-Swierkosz, *Appl. Catal. A-Gen.* **1997**, *157*, 263.

[4] R. A. Sheldon, J. K. Kochi, *Metal-Catalyzed Oxidations of Organic Compounds*, Academic Press, New York, **1981**.

[5] *Handbook of Chemistry and Physics*, 90 ed., CRC Press, **2009**.

[6] F. Haber, J. Weiss, *Naturwissenschaften* **1932**, *20*, 948.

[7] W. Partenheimer, *Catal. Today* **1995**, *23*, 69.

[8] H.-J.-A. K. Weissermel, *Industrielle Organische Chemie. Bedeutende Vor- und Zwischenprodukte*, 5 ed., Wiley-VCH, Weinheim, **1996**.

[9] P. Raghavendrachar, S. Ramachandran, *Ind. Eng. Chem. Res.* **1992**, *31*, 453.

[10] W. Partenheimer, *Advanced Synthesis & Catalysis* **2004**, *346*, 297.

[11] W. Partenheimer, V. V. Grushin, *Advanced Synthesis & Catalysis* **2001**, *343*, 102.

[12] G. C. Bond, *J. Chem. Technol. Biotechnol.* **1997**, *68*, 6.

[13] B. GrzybowskaSwierkosz, *Appl. Catal. A-Gen.* **1997**, *157*, 263.

[14] A. K. Suresh, M. M. Sharma, T. Sridhar, *Ind. Eng. Chem. Res.* **2000**, *39*, 3958.

[15] M. S. Wainwright, N. R. Foster, *Catal. Rev.-Sci. Eng.* **1979**, *19*, 211.

[16] C. R. Dias, M. F. Portela, G. C. Bond, *J. Catal.* **1995**, *157*, 344.

[17] B. Grzybowska-Swierkosz, *Top. Catal.* **2000**, *11*, 23.

[18] V. Nikolov, D. Klissurski, A. Anastasov, *Catal. Rev.-Sci. Eng.* **1991**, *33*, 319.

[19] R. Murugavel, A. Voigt, M. G. Walawalkar, H. W. Roesky, *Chemical Reviews* **1996**, *96*, 2205.

[20] P. D. Lickiss, *Advances in Inorganic Chemistry* **1995**, *42*, 147.

[21] M. J. Vanbommel, T. N. M. Bernards, A. H. Boonstra, *J. Non-Cryst. Solids* **1991**, *128*, 231.

[22] E. J. A. Pope, J. D. Mackenzie, *J. Non-Cryst. Solids* **1986**, *87*, 185.

[23] J. D. Mackenzie, E. P. Bescher, *J. Sol-Gel Sci. Technol.* **1998**, *13*, 371.

[24] J. D. Mackenzie, Q. X. Huang, T. Iwamoto, *J. Sol-Gel Sci. Technol.* **1996**, *7*, 151.

[25] B. V. Zhmud, J. Sonnefeld, *J. Non-Cryst. Solids* **1996**, *195*, 16.

[26] M. Guibergiapierron, G. Sauvet, *European Polymer Journal* **1992**, *28*, 29.

[27] G. Helary, G. Sauvet, *European Polymer Journal* **1992**, *28*, 37.

[28] L. L. Hench, J. K. West, *Chemical Reviews* **1990**, *90*, 33.

[29] H. Witossek, E. Bratz, *Chem. Eng. Technol.* **1997**, *20*, 429.

[30] E. Yacoub-George, E. Bratz, H. Tiltscher, *J. Non-Cryst. Solids* **1994**, *167*, 9.

[31] J. Schwarzer, N. Rabiger, A. Vogelpohl, *Chemie Ingenieur Technik* **1986**, *58*, 696.

Chapter 3

One step synthesis of organofunctionalized transition metal containing mesoporous silica spheres

Hydrophobic mesoporous silica spheres containing transition metals coordinatively bound to aminosilane groups are synthesized in a one-step procedure from functionalized silicon alkoxides. In situ IR spectroscopy shows the presence of amino groups in the solid. These amino groups are critical to bind transition metals such as Co, Cu, Fe, Mn or V by complexation. The accessibility of the transition metals is shown by IR spectra of adsorbed CO. The method described provides a scalable approach to synthesize tailored transition metal containing structured micro and mesoporous organofunctionalized silica spheres, which show great potential for catalytic applications.

3.1. Introduction

Silica based inorganic polymers are intensely studied because of their potential use in catalysis, sorption, separation, membrane technology, microelectronics and optics. [1-7] As catalysts and adsorbents, these materials have to be formed into various shapes such as spheres, pellets, extrudates or monoliths tailored to their dedicated use in a particular process. This forming step adds not only cost to the process of making the final active material, it poses also a challenge with respect to the scalability of complex catalyst preparation. Thus, a one-step synthesis procedure, which encompasses the incorporation of the catalytic function and the formation of a macroscopic body, is conceptually promising.

The emulsion technique [8] appears to be a particularly interesting route to synthesize spherical particles varying in size from nanometer to millimeter diameter realizing such different materials as nano-sized metals [9, 10] or oxide particles [11, 12]. However, it has also been reported for the synthesis of macroscopic silica spheres. Starting from tetraethyl orthosilicate (TEOS) in an oil-in-water emulsion, Schacht *et al.* [13] were able to synthesize silica hollow spheres in the range of 1 to 100 µm. Their strategy was based on controlling the oil-water interface by adding surfactants. Huo *et al.* [14] extended the size of the silica spheres from the micrometer to the millimeter range. In their work beads in the range from 0.1 to 2 mm were synthesized by adding the reactive precursor mixture into a stirred tank reactor.

In order to form silica spheres in an oil-in-water emulsion, the key point is the control of the interface between the hydrophobic silicon precursor and the water phase. The hydrolysis and, thus, the solidification of the reactive silanes starts at this interface due to the contact with water. By diffusion of water into the droplet, hydrolysis and condensation reactions proceed as illustrated in Scheme 3-1. The formed emulsion can be stabilized by adding surfactants [15, 16] or by mechanical means, i.e., application of a flow in combination with a rapidly starting gelation process. [7, 17]

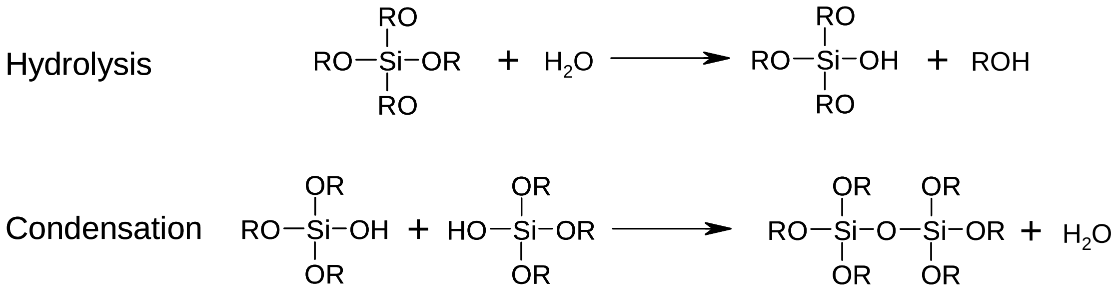

Scheme 3-1: Hydrolysis and condensation reaction during the sol-gel process. OR= alkoxy group.

Pure silica materials are catalytically inactive. To incorporate catalytic activity components such as functional groups (e.g. amino-, hydroxyl-, alkyl-, phenyl- or carboxy groups) or metals have to be introduced. Replacing one or two alkoxy groups of the silane by organic moieties is a useful tool to synthesize organofunctionalized silica since the Si-C bonds are maintained during hydrolysis and condensation. [18-20]

Within these functionalized materials, amino functionalized polysiloxane materials are particularly suited as anchoring groups for transition metals.[21] El-Ashgar *et al.* reported, for example, the application of aminopropylsilane as a ligand for the pre-concentration of Cu(II) in ion chromatography procedure.[22] In terms of catalytic applications it is interesting to note that the thermal stability of amino containing polysiloxanes increases by the complexation of a transition metal.[21]

Stimulated by these reports, we developed a one-step synthesis procedure for highly functionalized materials containing transition metal cations. Here, we describe the synthesis of transition metal containing spherical amino functionalized polysiloxanes with millimeter size diameters under continuous operating conditions.

3.2.Experimental

3.2.1. Chemicals

3-Aminopropyltrimethoxysilane (APTMS) (>97%), tetraethyl orthosilicate (TEOS) (>99%), phenyltrimethoxysilane (PTMS) (97%), [3-(2-aminoethylamino) propyl]trimethoxysilane (AAMS) (>98%), butanol (>99.5%), dibutyltin dilaurate (DBTDL) (95%) and metal acetyl acetonates (97%) were purchased from Sigma Aldrich. All chemicals were used as received from the supplier.

3.2.2. Synthesis apparatus

The principle procedure for the synthesis of macroscopic spherical silica particles utilized in this work was first described by Witossek *et al.* [17] A schematic overview of the reactor employed for the synthesis is presented in Figure 3-1.

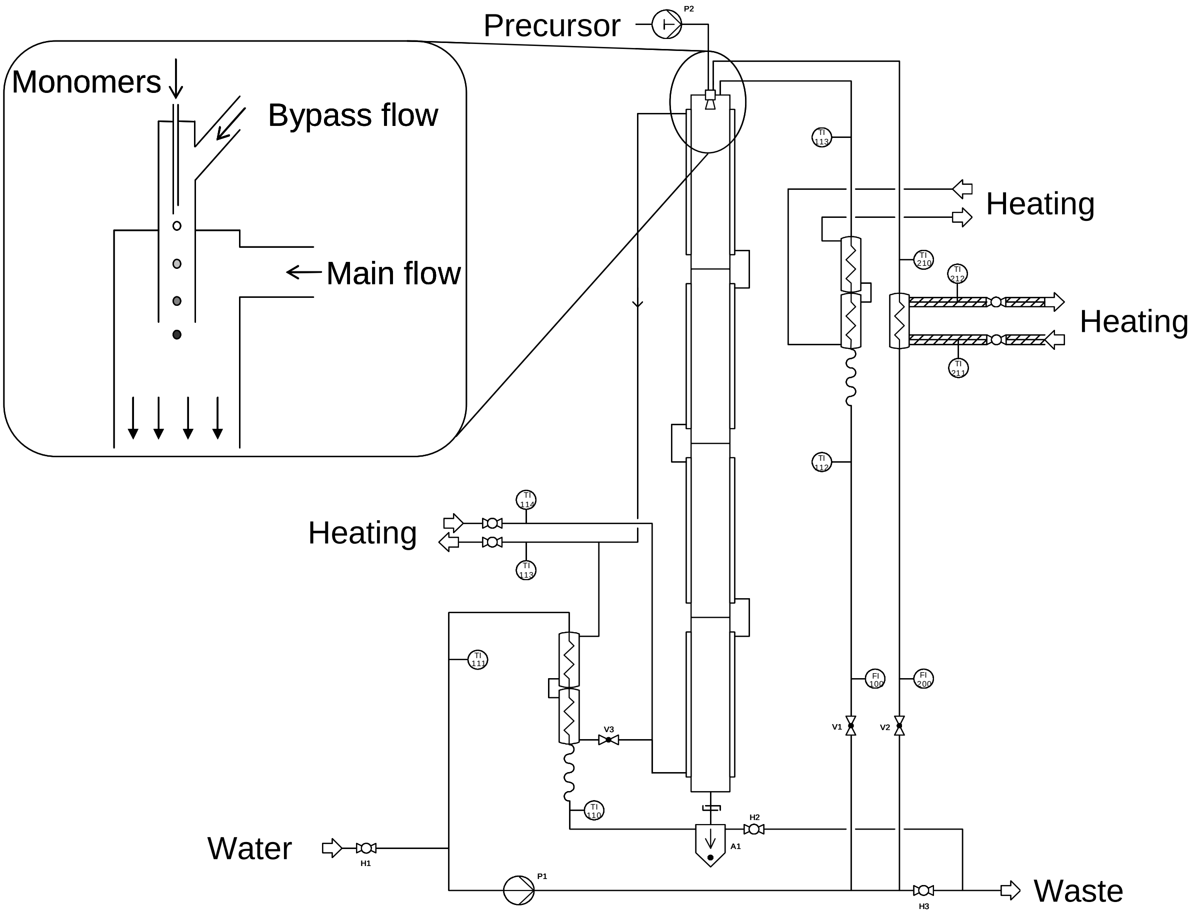

Figure 3-1: Schematic overview of the water filled column used for the synthesis of silica beads.

The precursor solution is injected at the top of the water filled reaction column. Droplets are created and transported into the main part of the column by the bypass flow. In the main stream they are forced to move downwards with optimized velocity. This procedure allows a continuous production of spherical particles. The droplet diameter is controlled by the linear velocity of the bypass flow. Their size furthermore defines the dimension of the resulting spherical solid. Overall it should be noted that the formation of stable droplets is very sensitive to the flow, temperature and the precursor composition.

3.2.3. Preparation of porous silica spheres

Porous silica spheres were synthesized using the setup displayed in Figure 3-1. Two mixtures of silanes were used as precursor for the production of silica spheres. The components of the synthesis mixture S1 were TEOS, AAMS and PTMS in the molar ratio of 5 : 2 : 3. Synthesis mixture S2 contained TEOS and APTMS in the molar ratio of 2 : 1. In both cases 1-butanol (10 vol. %) was used as solvent and DBTDL as catalyst. The mixtures of silanes, solvent and DBTDL were stirred for 30 min to assure a homogeneous solution before being continuously injected into the column via a syringe. For every experiment the rate of injection was remained constant at 15 mL min^{-1}. The water temperature was 333 K and the linear velocity of the carrying water flow was in the range of 0.03 to 0.3 m s^{-1}. After the synthesis procedure, the silica spheres were aged in water at ambient temperature for 12 h followed by washing with deionized water and *i*-propanol. The materials were freeze-dried after washing.

To synthesize metal containing silica spheres, cobalt, manganese, copper or vanadium acetyl acetonate was added directly to the precursor mixture. The concentration of transition metal was controlled in the range from 1.9 to 5.0 mol % with respect to Si in the precursor mixture.

3.2.4. Characterization

IR spectroscopy was used to evaluate the structure and adsorption ability of the resulting materials on a Bruker IFS88 spectrometer in the region from 400 to 4000 cm^{-1} with a resolution of 4 cm^{-1}. Before measurement, samples were prepared as self-supporting wafers with a weight of approximately 5 mg cm^{-2} and inserted in a vacuum cell with a geometry optimized for transmission IR spectroscopy. For structural studies, samples were dried under vacuum ($p = 10^{-6}$ mbar) at 723 K (heating increment 10 K min^{-1}) for 1 h before each measurement. For CO adsorption experiments, wafers were dried at 723 K under vacuum prior to the CO adsorption and spectra were recorded at ambient temperature at CO pressures of 1.5 mbar. Water was adsorbed at 323 K in a pressure range from 10^{-4} to 1 mbar.

The content of silicon and the metal component was determined by atomic absorption spectroscopy (AAS) using a UNICAM Solaar M5 Spectrometer. Typically, 20-40 mg of the sample was dissolved in a mixture of 0.5 ml of hydrofluoric acid (48%) and 0.1 ml of nitro-hydrochloric acid at the boiling point of the mixture (about 383 K). The specific surface areas were derived from N_2 adsorption measurements carried out at 77.4 K using a PMI automated BET sorptometer. Prior to the measurements, all samples were outgassed at 523 K for 2 h. The specific surface areas as well as the mesopore and micropore distributions were calculated according to the BET and BJH theory and t-plot analysis.

Scanning electron microscope (SEM) images were measured on a JEOL 500 SEM at 25 kV. Transmission electron microscope (TEM) images of the materials were recorded with a JEM-2010 JEOL transmission electron microscope operating at 120 kV. The samples were grinded, suspended in ethanol and ultrasonically dispersed. Drops of the dispersions were applied on a copper grid-supported carbon film.

For solid-state MAS NMR experiments, samples were packed into 4 mm ZrO_2 rotors. ^{29}Si MAS NMR measurements were performed on a Bruker AV500 spectrometer (B_0 = 11.75 T) using a spinning rate of 12 kHz. Chemical shifts are reported relative to $Si(SiMe_3)_4$ for ^{29}Si (δ_{Si} = - 9.84 ppm).

3.3. Results

3.3.1. Synthesis of spherical silica particles

The polysiloxane materials were synthesized by combination of controlled hydrolysis and condensation of respective silane precursor compounds. The network building component TEOS was partially substituted by organofunctionalized silanes in order to fine tune the hydrolysis and condensation rate of the mixture and to introduce amino groups. Various mixtures of silane precursor were explored and optimized for the synthesis of polysiloxane beads. After screening, two types of polysiloxane materials, S1 derived from TEOS : AAMS : PTMS = 5 : 2 : 3 and S2 based on TEOS : APTMS = 2 : 1, were found to be suitable for the synthesis of well-formed and mechanically stable silica spheres. Their respective elemental composition is summarized in Table 3-1.

Table 3-1: Elemental composition of the synthesized polysiloxane materials.

Sample Name	*Precursors composition*	*Elemental concentration [wt. %]*[a]				
		Si	*C*	*H*	*N*	*M*[b]
S1	TEOS/AAMS/PTMS = 5/2/3	24.0	34.0	3.7	1.1	-
Co-S1	TEOS/AAMS/PTMS = 5/2/3	24.1	38.0	3.6	1.2	0.4
V-S1	TEOS/AAMS/PTMS = 5/2/3	23.5	39.7	4.0	1.0	0.4
Cu-S1	TEOS/AAMS/PTMS = 5/2/3	23.9	38.6	3.9	1.3	0.4
S2	TEOS/APTMS = 2/1	31.7	8.2	2.8	2.1	-
S2-3	TEOS/APTMS = 3/1	35.5	8.8	3.1	1.3	-
S2-4	TEOS/APTMS = 4/1	36.2	9.2	2.8	1.6	-
S2-5	TEOS/APTMS = 5/1	35.8	7.5	2.5	1.3	-
S2-6	TEOS/APTMS = 6/1	35.7	8.7	2.8	1.7	-
S2	TEOS/APTMS = 2/1	31.7	8.2	2.8	2.1	-
Mn-S2	TEOS/APTMS = 2/1	30.9	12.7	3.4	3.9	0.9
V-S2	TEOS/APTMS = 2/1	31.3	12.6	3.5	3.2	0.9
Co-S2	TEOS/APTMS = 2/1	31.1	10.9	3.2	2.9	1.0
Cu-S2	TEOS/APTMS = 2/1	31.7	10.3	3.5	3.1	1.0

Co11-S2	TEOS/APTMS = 2/1	28.5	11.9	3.6	3.4	1.1
Co13-S2	TEOS/APTMS = 2/1	28.7	11.7	3.5	3.0	1.3
Co16-S2	TEOS/APTMS = 2/1	26.7	15.0	3.3	3.1	1.6
Co20-S2	TEOS/APTMS = 2/1	27.5	12.6	3.6	3.1	2.0
Co25-S2	TEOS/APTMS = 2/1	26.9	16.0	3.7	3.9	2.5

a: The silicon and the metal amount were determined by AAS and the C, N, H concentration by elemental analysis
b: M refers to the respective transition metal species

The set of materials S1 had a relatively higher carbon concentration in the range 34-40 wt. % while the carbon content in the series of S2 was only between 7-16 wt. %. This significant difference is related to the nature of the silanes added to the precursor solutions. To introduce amino groups into the final product, amino group carrying precursors, AAMS for S1 and APTMS for S2, were used in the synthesis mixtures. In the materials S2, the detected N concentrations were approximately 60% of the expected value; however, only 20% of the expected N was left in materials of type S1. While the concentration of nitrogen in the solid polysiloxane obtained via both routes is below the value expected, the higher concentration of amino groups in type S2 materials (derived from APTMS) is related to the lower solubility of this aminosilane in water. In consequence, the detailed studies described below are based on type S2 materials.

3.3.2. Structural properties of the spherical materials

The spherical shape of the polysiloxanes is illustrated in Figure 3-2. The pure silicon precursors resulted in white spheres with uniform diameter of 0.5-1 mm. Incorporation of a transition metal into the precursor solution did neither change the morphology nor the size of the resulting spheres. However, the color of the spheres varied depending on the nature of metal and its oxidation state. Introduction of Co led to blue spheres, Mn to brown and V to green-colored. In the case of Co a characteristic change in color from violet into blue was observed during the condensation process, indicating a coordination of Co to the amino groups in the polysiloxane network.

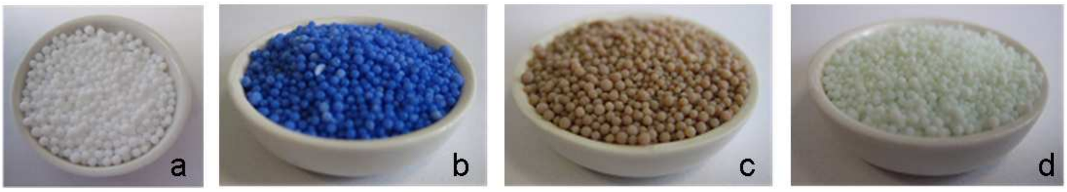

Figure 3-2: Photographs of spherical materials S2 in the absence (a) and in presence of metal ions (b) Co, (c) Mn and (d) V.

A detailed examination of the surface morphology and structure of the polysiloxane spheres was performed by scanning electron microscopy (see Figure 3-3). The measurements show spherical particles (Figure 3-3a) with a rough and macroscopically dense surface (Figure 3-3b).

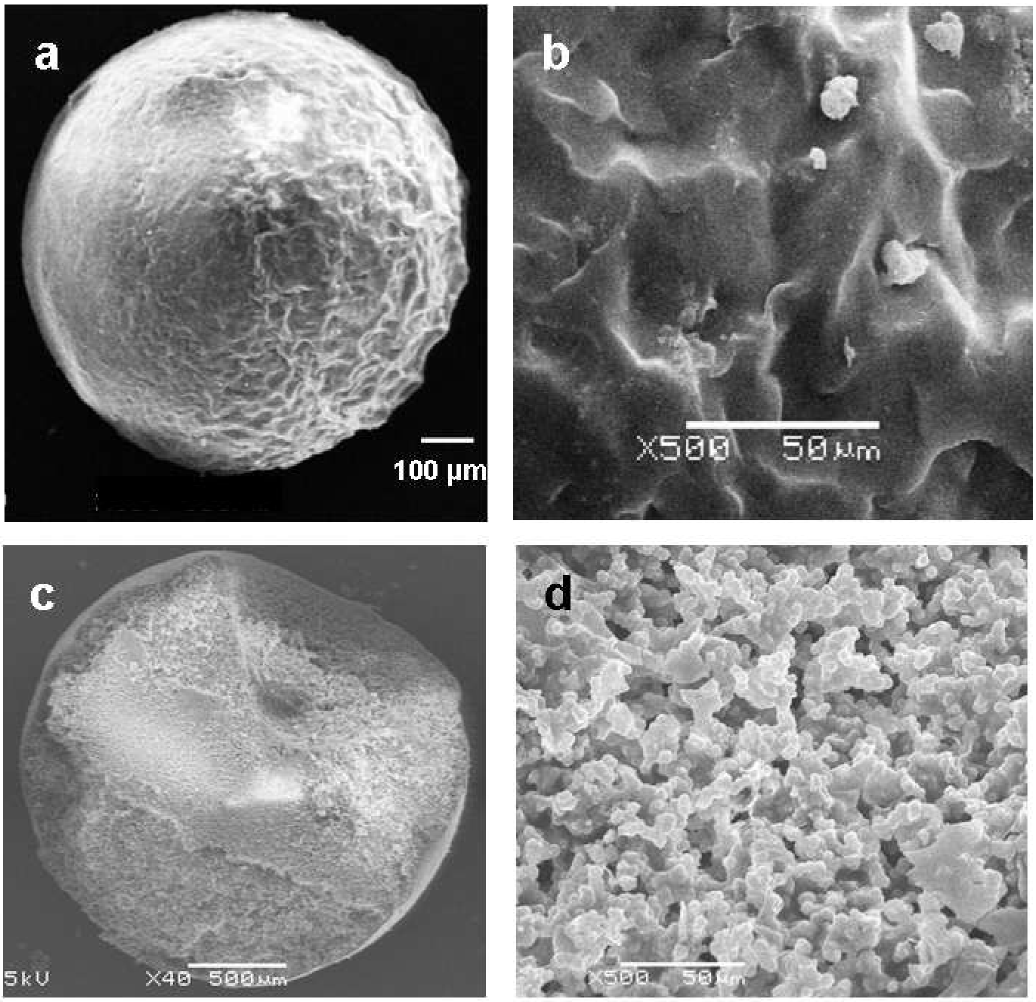

Figure 3-3: SEM images of S1 type silica spheres as synthesized (a), of a sphere surface (b), of a cross-section of a sphere (c) and of the inner primary particles of a sphere (d).

To study the structure of the spheres, a bead was cut into hemispheres and the cross-section was analyzed by scanning electron microscopy (see Figure 3-3c). It is seen that two different states of silica were formed, i.e., a dense layer forming the surrounding shell and a second region consisting of macroporous silica. The inner part of the sphere consists of primary particles of 5 µm in diameter (see Figure 3-3d). TEM and XRD showed that the synthesized materials were completely amorphous and a long range structure was not developed.

The particle size distribution of the beads was determined by a laser particle counter. Exemplary, the result of one batch is presented in Figure 3-4.

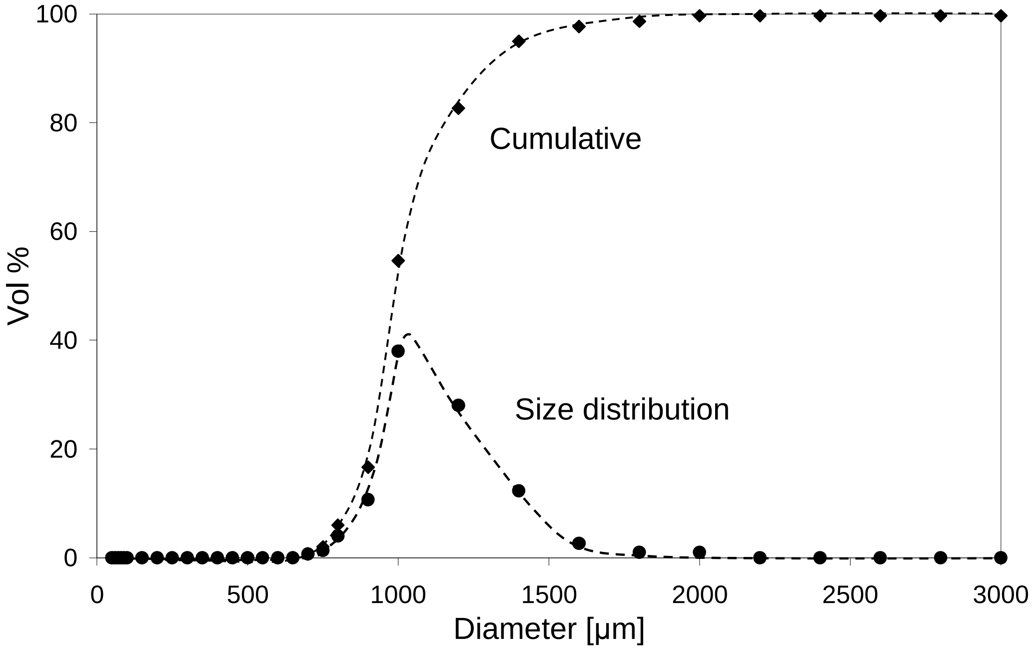

Figure 3-4: Particle size distribution of the sample S2.

A sharp monodisperse peak at 1000 µm was observed demonstrating the uniformity of the bead size distribution. Indeed, the bead size can be tuned in the range from 600 to 1200 µm by changing the flow rate in the injection part under otherwise identical conditions. In general, the sphere diameter increased with decreasing flow rates. This dependence of the sphere diameter on the injection rate is in good agreement with the results described by Witossek *et al.* [17]

3.3.3. Textural properties

The textural properties of the resulting silica beads were evaluated using N_2 physisorption. At first, the influence of the precursor composition and especially of the organosilane content in the precursor was studied. For TEOS/APTMS ratios between 2 and 6, the specific surface area increased from 103 $m^2 g^{-1}$ to 143 $m^2 g^{-1}$ as the TEOS/APTMS ratio increased from 2 to 6 indicating that higher concentrations of APTMS leads to decrease of the specific surface area (see Figure 3-5). As APTMS contains one amino group it acts as a base which catalyzes the hydrolysis and condensation of TEOS resulting in more condensed materials.

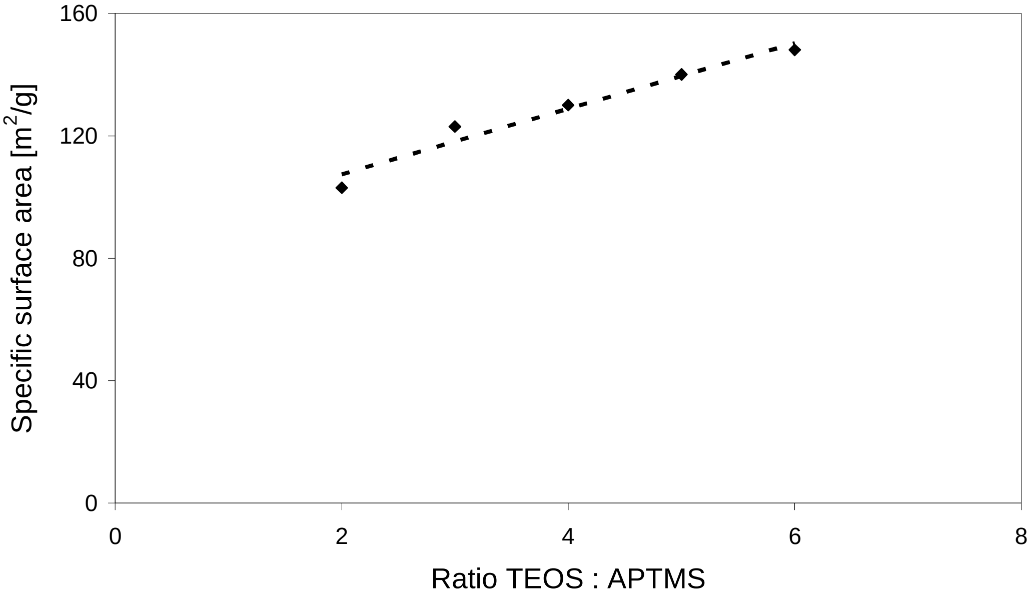

Figure 3-5: Specific surface areas of silica materials based on the S2 sample in dependence of the TEOS/APTMS ratio.

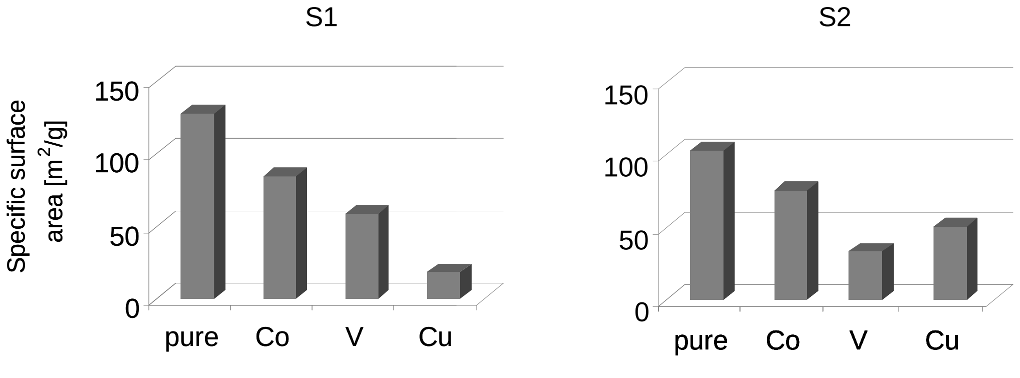

Figure 3-6: Comparison of the specific surface areas determined by BET analysis of nitrogen isotherms for the two types (S1 and S2) of polysiloxane materials. The amount of transition metal was 0.4 wt. % for the S1 series and 1 wt. % for the S2 series.

Addition of transition metal components to the precursor mixture had a significant influence on the bead formation rate of and is reflected on the specific surface area. The effect derived from the transition metal component on the specific surface area for materials S1 and S2 is presented on Figure 3-6. The specific surface area of the S1 material was larger than in the case of S2 system, if no transition metal is added to the system. Both types show the tendency that the specific surface area was lowered by the addition of a transition metal (Co, V or Cu) independent of the kind of transition metal. In the case of Cu, the specific surface area was reduced to 14% of the value found in the absence of the metal component. The addition of V to the mono amino type precursor solution resulted in a reduction of the specific surface area to 32%. A general trend of the influence of the type of transition metal on the specific surface area of the resulting functionalized silica spheres cannot be deduced from this.

To investigate the influence of the concentration of transition metal, Co^{2+} was introduced in different concentrations to otherwise identical precursor solutions. The specific surface areas of the resulting spheres are shown in Figure 3-7. While the incorporation of 2 mol % Co in the polysiloxane led to a reduction of the surface area from 103 m^2g^{-1} to 58 m^2g^{-1} compared to the pure silica spheres, further increase of the loading of Co from 2 mol % up to 5 mol % led to a linear increase of the specific surface area from 58 m^2 g^{-1} to 85 m^2 g^{-1}.

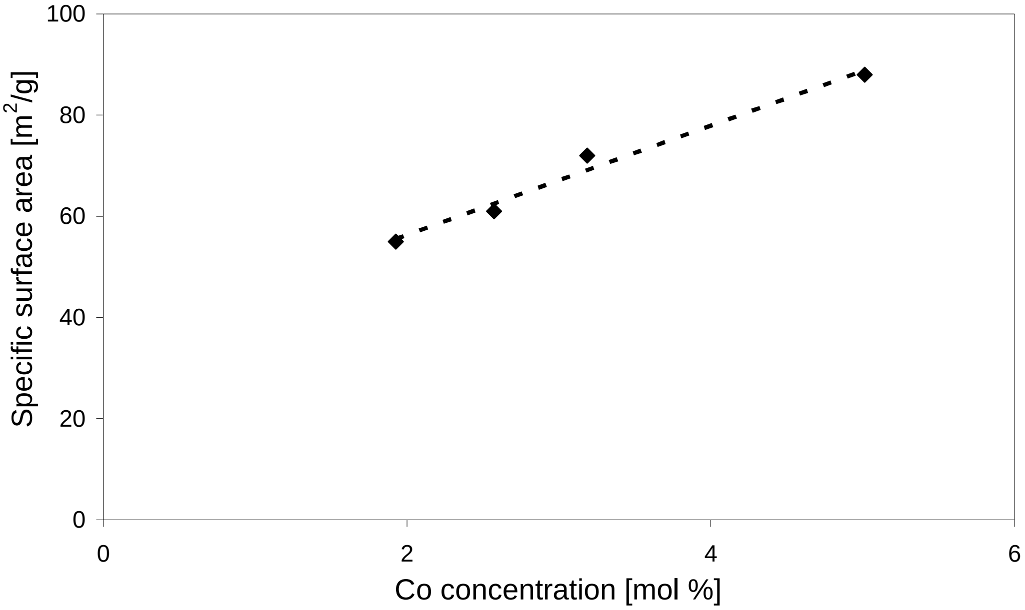

Figure 3-7: Effect of Co concentration on specific surface areas of polysiloxane materials S2.

3.3.4. ^{29}Si MAS NMR spectroscopy of silica materials

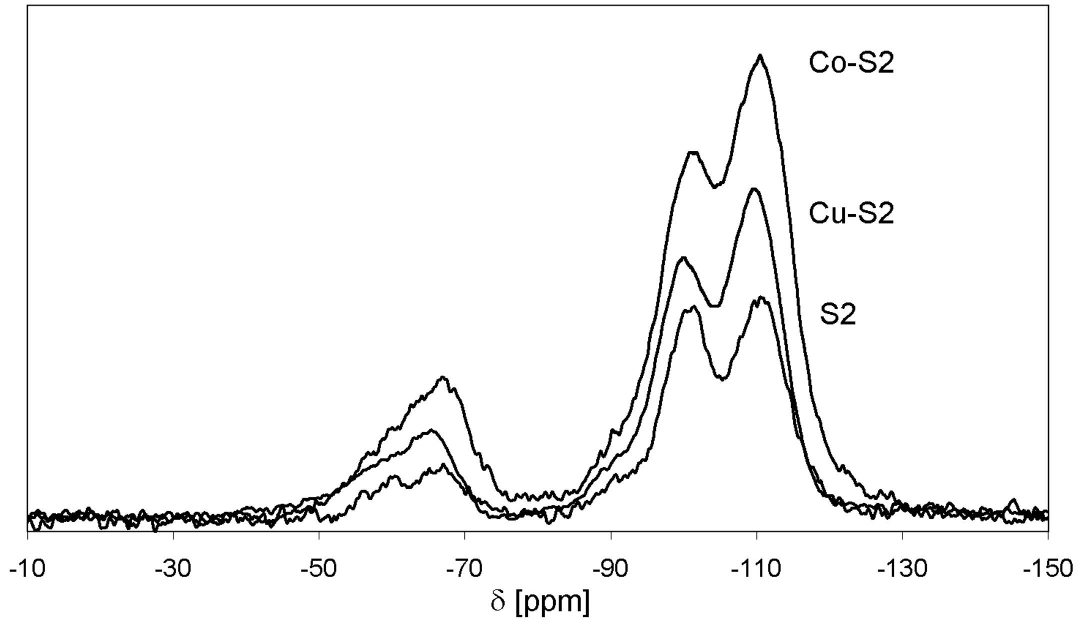

Figure 3-8: ^{29}Si MAS NMR spectra of a transition metal (Co or Cu) containing polysiloxane material compared to the pure silica material. The displayed silica materials are of the S2 type. NMR spectra were recorded at ambient conditions.

To determine the degree of polymerization of the polysiloxane the local environment of Si was investigated by ^{29}Si MAS NMR spectroscopy. Typical ^{29}Si MAS NMR spectra of investigated samples are displayed in Figure 3-8, while attribution and relative intensity of the bands are compiled in Table 3-2. Two groups of signals are observed in Figure 3-8. The signals in the range from -40 to -60 ppm are assigned to silicon with three oxygen neighbors (T species), whereas the group in the range from -70 to -110 ppm corresponds to silicon in the environment of four adjacent oxygen atoms (Q species). Deconvolution of the superposed signals lead to three subspecies of T and Q species respectively.

Table 3-2: Relative intensities of Si-species occurring in the polysiloxane network for materials of the composition TEOS : APTMS = 2 : 1.

Chemical shift (ppm)	Si-species	relative intensity		
		S2	Cu-S2	Co-S2
-55	T^1	0.016	0.022	0.022
-60	T^2	0.022	0.069	0.078
-68	T^3	0.093	0.081	0.080
T total		0.131	0.172	0.180
-92	Q^2	0.076	0.072	0.092
-100	Q^3	0.326	0.307	0.249
-110	Q^4	0.466	0.449	0.480
Q total		0.868	0.828	0.821
T/Q		0.151	0.208	0.219
Q^4/Q^3		1.429	1.463	1.922

The T species result from the aminopropyl silane, whereas the Q species result from TEOS. A comparison of the ratio of T species reveals that the addition of transition metal results in a lower degree of condensation of the organofunctionalized Si species. But this fact is neutralized by the fact that the relative concentration of T sites increases as concluded by the observation that the ratio of the sum of T and Q species increases after metal addition from 0.151 to 0.208 and 0.219 respectively. This is accompanied by a higher concentration of nitrogen in the material. The ratio of Q^4 to Q^3 is shifted towards the totally condensed Si, when transition metals are introduced to the system indicating that the degree of condensation of TEOS increased.

3.3.5. IR spectroscopy of synthesized materials

The amino functional group incorporated into the polysiloxane network and its influence on the anchoring of the transition metal component to the silica framework was characterized by IR spectroscopy. The IR spectra of Co containing and pure polysiloxane spheres are compiled in Figure 3-9.

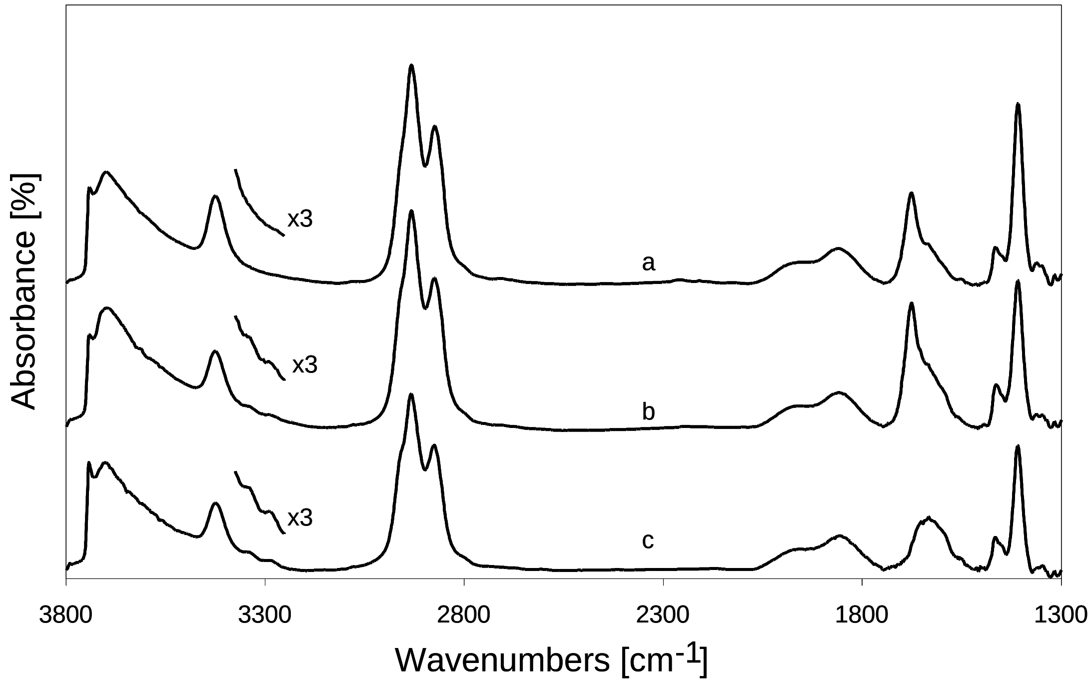

Figure 3-9: IR spectra of polysiloxane materials with no Co (a, sample S2), 1.1 wt. % Co (b, sample Co11-S2) and 2.0 wt. % Co (c, sample Co20-S2) loading.

As shown in Figure 3-9, all spectra indicate a peak at 3740 cm^{-1}, which is assigned to the stretching vibration of terminal silanol groups. The broad peak at 3700 cm^{-1} is attributed to the perturbed OH groups resulting from hydrogen-bridge bonding in the material. The presence of aminosilane is indicated by the band of unperturbed NH groups at 3420 cm^{-1} in every spectrum. In the presence of Co additional bands at 3338 cm^{-1} and 3284 cm^{-1} appear (see magnification in Figure 3-9). These two bands were observed independently of the method Co was introduced to the silica matrix, i.e., direct incorporation during the sol-gel process or incipient wetness impregnation of synthesized silica beads with Co salt solution. These bands also appear independently of the solvent and the counter ion used during the impregnation.

The bands between 2800 and 3000 cm^{-1} are attributed to the C-H stretching vibrations of the organic side groups. The bands at 1740 – 2090 cm^{-1} are attributed to vibrations of the Si-O bonds in the framework. At lower wavenumbers (1520 – 1740 cm^{-1}) the N-H deformation vibrations were observed. A change of the shape of this band from the Co free sample to the material with higher Co content indicates the complexation of the metal ion by the amino groups. Between 1320 and 1500 cm^{-1} originate from the deformation vibrations of CH-, HCN- and HNC functional groups. [6]

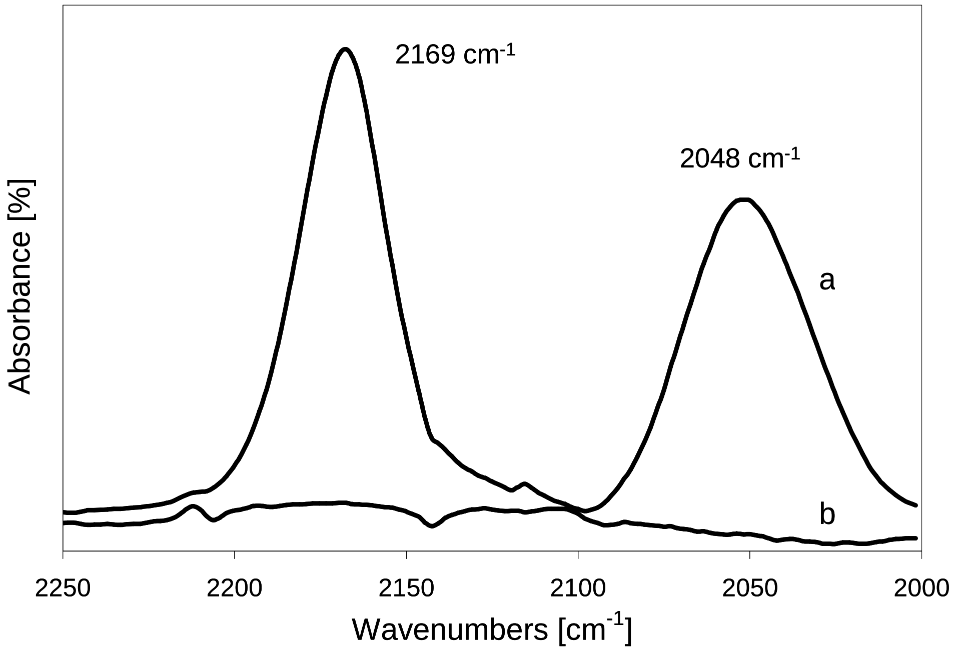

Figure 3-10: IR spectra of adsorbed CO on the Co containing sample Co20-S2 (a) and the spectrum of Co free polysiloxane S2 at 303 K and 1.5 mbar CO.

In order to test the accessibility of transition metals CO was adsorbed to Co containing materials. Figure 3-10 shows the IR spectrum of CO adsorbed on the sample Co20-S2 at ambient conditions compared to the spectrum of pure silica (S2). Adsorbing CO to Co containing materials results in two bands in the spectrum at 2048 cm^{-1} and 2169 cm^{-1}. The first one is characteristic of terminal stretching vibrations of CO in carbonyls, while the band at 2169 cm^{-1} is attributed to CO adsorbed on Co^{2+} cations.[23] Both bands appear in all Co containing silica spheres.

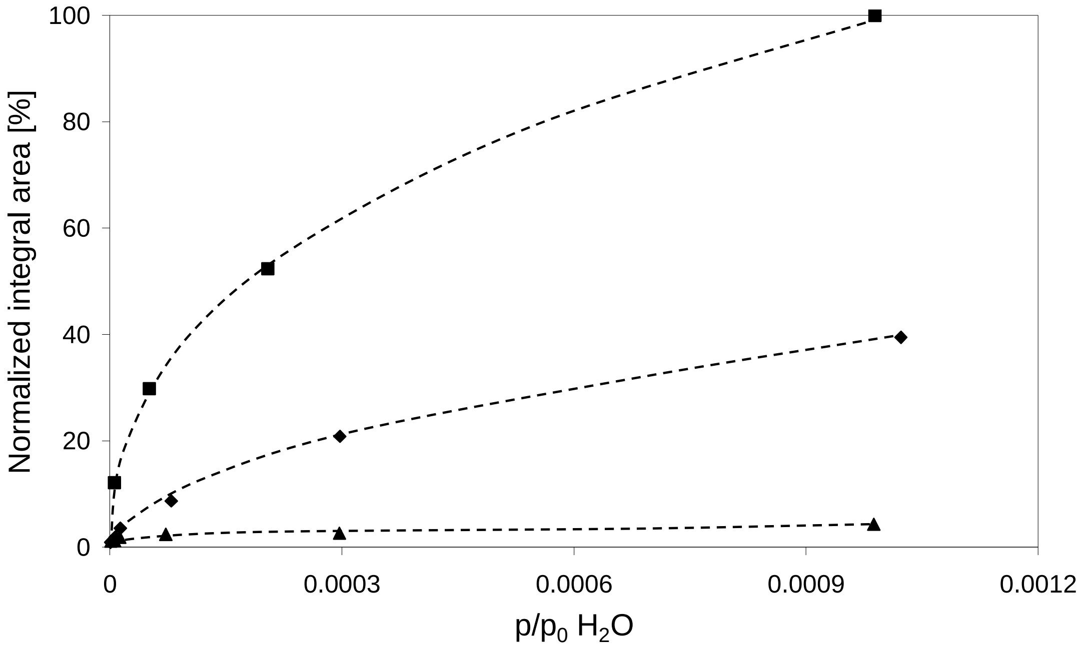

Figure 3-11: Normalized absorption of the band 1630 cm^{-1} caused by water adsorbed to the material. The S1 material (▲) was compared to S2 material (♦) and to the corresponding calcined material without organic side groups (■) (adsorption of water was recorded by IR at 323 K).

To identify the adsorption of water to the polysiloxane network IR experiments at different water partial pressures were conducted. Figure 3-11 shows the uptake of water, which is based on the normalized intensity of the H-O-H deformation vibration band at 1630 cm^{-1} in the IR spectra. Here, the water uptake was used as indicator for the hydrophobicity of the synthesized materials. Synthesized polysiloxane materials were compared to an oxidic reference sample (100% water adsorption capacity) which was created by treating a polysiloxane in air at 873 K. A comparison of resulting water isotherms shows that sample S1, containing 34 wt. % C, has lower water uptake capacity (4%) compared to sample S2 which contains 9 wt. % C and shows a water uptake capacity of 39%. To quantify this trend of hydrophobicity water uptake measurements were performed by thermogravimetry under identical conditions. The oxidic reference sample showed the highest water uptake (100% corresponds to 74 mg g^{-1}_{solid}). Sample S1 only reached 13% of maximum water uptake, whereas sample S2 shows a water uptake capacity of 47%, which is in good agreement with the IR experiments. Summarizing the water adsorption experiments, it is observed that the reference sample which does not contain organic groups shows the highest water uptake and, thus, is considered as the most hydrophilic one.

3.4. Discussion

The combined experiments show that an upper limit of around 30 mol % APTMS in the mixtures consisting of TEOS and APTMS exists with respect to a sufficient stability of the resulting solid spheres. If the concentration of APTMS is higher, the spheres formed collapse to fine particles during the drying procedure. This is attributed to the formation of an insufficient concentration of Si-O-Si bridges in case of a higher concentration of non-condensable silica components.

The presence of basic amino groups and of a catalyst (DBTDL) is beneficial for the forming of the silica network and the complexation of the metal. The basicity of the amino group accelerates the hydrolysis and increases the gel formation rate due to hydrogen-bridge bonds between the amino group and hydroxyl groups already formed on the silica surface. [24] The dialkyl tin catalyst containing two hydrolysable functionalities acts as a leaving group, which can be created from the intermediately formed silanol, increasing in consequence the condensation rate. The crucial point in the present synthesis strategy is to subtly adjust the condensation rate. High reaction rates are unfavorable with respect to the formation of uniform spheres and blockage of the injection system, but too low rates on the other hand limit the formation of mechanically stable beads.

The particle diameter of the spheres can be adjusted by controlling the droplet forming process via the water flow rate and the injection velocity of the precursor solution, which both define the size of drops of reactive monomers and so the diameter of the resulting sphere allowing a narrow size distribution of the particles. As a quantitative measure the dimensionless Weber number ($We = \delta\, w^2\, d\, \sigma^{-1}$) is used. It describes the fluid inertia compared to its surface tension. The lower the We values the closer the droplet geometry approaches a perfect sphere. For a standard experiment ($\delta = 0.95$ g cm^{-3}; $w = 0.15$ m s^{-1}; $d = 1000$ µm; $\sigma = 0.02$ N m^{-1}) the value is calculated to $We = 1.1$. As comparison it should be mentioned that droplets, which provide Weber numbers above 13 disintegrate in gas phase processes.

It was observed that the concentration of amino groups is below the expected depending on the precursor mixture. This is attributed to the water solubility of amino containing silanes and the formation of oligomers from aminopropyl silanes, which are water soluble.[25] When di-amino silanes are applied the resulting concentration of N is lower than in the case of the mono-amino mixture. Due to the presence of two polar amino groups, it is assumed that AAMS and the oligomers formed from it show a higher tendency to dissolve in water than the mono-basic amine. Although the amine concentration is below the expected value an incorporation of amino groups into the polysiloxane network was shown by IR spectroscopy.

The hydrophobicity of the synthesized materials was directly proportional to the carbon content, and the hydrophobicity of the organic groups. In oxide materials, OH surface groups allow the adsorption of water and, thus, a relatively high hydrophilicity is generated. If a certain fraction of ester groups in the precursor mixture is replaced by organo-functionalized side groups, the concentration of surface OH-groups of the resulting material in the sol-gel process is reduced, because hydrophobic groups are substituting hydrophilic ones. When phenyl groups are introduced (material S1) an even more pronounced decrease of the water adsorption capacity is observed since the phenyl ring itself is less polar than the amino propyl group.

The complexation of the metals by the amino group is verified by IR spectra of cobalt containing polysiloxane spheres. Two bands appear in the IR spectra at 3338 cm^{-1} and 3284 cm^{-1}, which are assigned to NH vibrations. Note that the lower wavenumber compared to the NH vibration in the absence of cobalt indicates an interaction with the metal cations. Additionally, the change of the band in the region of the deformation vibration of the NH supports the assumption of the bonding of Co to the amino groups of the framework. The same effect can be observed in the IR spectrum when an amino group containing polysiloxane is exposed to an incipient wetness impregnation procedure where an aqueous solution of a Co salt is added to the polysiloxane support.

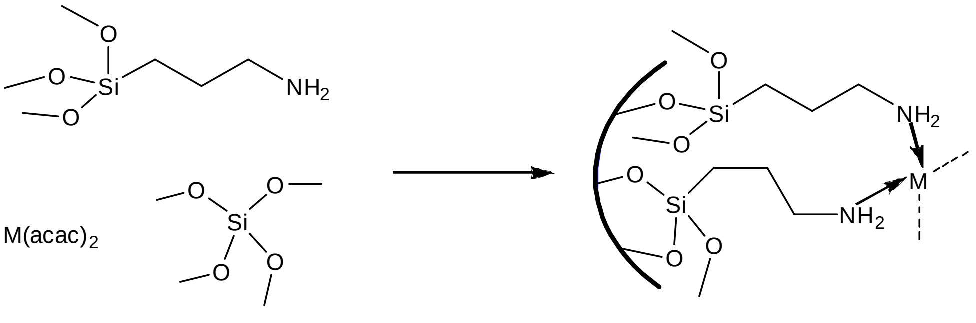

Scheme 3-2: Schematic representation of the coordination of a metal species to the polysiloxane network via amino containing side groups.

A further indicator of the complexation is the fact that the transition metal acetyl acetonate is hardly soluble in TEOS or the solvent used for the synthesis, but in the amino silane it dissolves readily. One or more amino containing silane molecules form a complex with the Co species resulting in a bulky structure. Starting from these *in situ* formed nuclei the condensation will start readily resulting in an enhanced overall reaction rate. As a result the conversion into solid particles was faster, when metal compounds were added to the reaction solution. During the incorporation of Co into the polysiloxane matrix a change in color from violet to blue in the resulting solid polysiloxane is attributed to the change of coordination of Co. In the violet starting material Co^{2+} is tetrahedrally coordinated by the acetyl acetonate ligands. During the synthesis procedure Co is coordinated by an amino group. Therefore the coordination sphere is supposed to change to octahedral which accompanies with an increased splitting of the energy levels. It is also noted that in general amino groups are known to split up the energy levels more pronounced. Higher splitting in turn leads to absorption of light of shorter wavelengths, which corresponds in a red shift of the appearing color.

Besides the complexation of the metal ions, amino functionalized silanes remarkably influence the condensation behavior. By varying the APTMS concentration in the S2 mixture it was shown that higher base concentrations accelerate the overall reaction rate and lead to a decrease of the specific surface area. The reason for this is that the higher concentration of amino groups causes a higher concentration of water inside the droplet. This is supported by the more pronounced leaching of AAMS compared to APTMS as

AAMS has higher basicity and hydrophilicity. In the case of the AAMS precursor, the barrier for water diffusing into the droplet is lower than in the case of the less hydrophilic APTMS. Although the higher basicity of AAMS (due to two amino groups) and a higher hydrophilicity compared to APTMS allow a faster condensation of the polysiloxane network, it was observed that the specific surface area of S1 materials was higher than of S2 materials. This is explained by the fact that the organic side chains of AAMS and PTMS have a higher steric demand which circumvents a dense packing of the polysiloxane.

The degree of condensation is also affected by the presence of transition metals. ^{29}Si MAS NMR spectroscopy shows that the concentration of highly condensed Si Q4 species increased in the presence of transition metals compared to Q3. We attribute this to the complexation of the metal by the amino group of the silane precursor and the accompanied increased overall reaction rate by the formation of condensation nuclei. As a second fact, it is observed that the specific surface area is decreased as soon as transition metals are added to the polysiloxane. Taking these facts together it is concluded that a denser network is formed, when transition metal is added.

Starting from the Co concentration of 1.9 mol % the specific surface area is decreased to 53% compared to the equivalent material without Co. If the Co concentration in the precursor mixture is raised above this level, however, the specific surface area increases linearly. The reason for this might be the reduction of the absolute concentration of (basic) amino functions. By the complexation of Co the amine is blocked and is no longer available as a base to enhance the silane condensation.

Although a more rigid network was created by incorporating transition metals, the transition metal was still accessible by CO as a probe molecule (CO did not adsorb on Co free polysiloxane). The adsorption of CO to the catalyst shows that at least one coordination position on the Co cation is accessible indicating that it is coordinatively unsaturated. Under the applied synthesis conditions water fills all coordination places in the Co surrounding and is replaced by CO during the adsorption experiments. In a potential catalytic application the thermal activation procedure will free this site and allow access to the transition metal cation.

3.5. Conclusions

A one step method for the synthesis of millimeter-sized silica spheres covered with organic functional groups and containing accessible transition metal cations is presented. Through tailoring the initial silicon precursor composition and injection rate it is possible to prepare spherical silica beads and control their macroscopic size as well as their pore structure. Amino silane functional groups introduced into the polysiloxane networks are not only important for the successful formation of beads and adjusting the textural properties and hydrophobicity of the resulting materials, but are also the sites for anchoring transition metals such as Co, Cu, Fe, Mn and V. The method described allows the synthesis of catalytic active moieties already incorporated in a tailored macroscopic shape.

3.6. Acknowledgments

The authors thank the German Bundesministerium für Bildung und Forschung (BMBF) for partial financial support of the presented work (Project No. 03X2007A). Furthermore we are grateful to Dipl.-Ing. Xaver Hecht for carrying out BET measurements and Dipl.-Ing. Martin Neukamm for performing AAS analytics. The authors acknowledge fruitful discussions in the framework of the network of excellence IDECAT.

3.7. References

[1] R. Murugavel, A. Voigt, M.G. Walawalkar, H.W. Roesky, *Chemical Reviews* **1996**, *96*, 2205.

[2] M.M. Collinson, *Mikrochim. Acta* **1998**, *129*, 149.

[3] P.D. Lickiss, *Adv. Inorg. Chem.* **1995**, *42*, 147.

[4] J.D. Mackenzie, E.P. Bescher, *J. Sol-Gel Sci. Technol.* **1998**, *13*, 371.

[5] J.D. Mackenzie, Q.X. Huang, T. Iwamoto, *J. Sol-Gel Sci. Technol.* **1996**, *7*, 151.

[6] B.V. Zhmud, J. Sonnefeld, *J. Non-Cryst. Solids* **1996**, *195*, 16.

[7] E. Yacoubgeorge, E. Bratz, H. Tiltscher, *J. Non-Cryst. Solids* **1994**, *167*, 9.

[8] J. Israelachvili, *Colloids Surf. A* **1994**, *91*, 1.

[9] D.H. Chen, S.H. Wu, *Chem. Mater.* **2000**, *12*, 1354.

[10] S.Q. Qiu, J.X. Dong, G.X. Chen, *J. Colloid Interface Sci.* **1999**, *216*, 230.

[11] K.S. Finnie, J.R. Bartlett, C.J.A. Barbe, L.G. Kong, *Langmuir* **2007**, *23*, 3017.

[12] I. Miletto, A. Gilardino, P. Zamburlin, S. Dalmazzo, D. Lovisolo, G. Caputo, G. Viscardi, G. Martra, *Dyes Pigm.* **2010**, *84*, 121.

[13] S. Schacht, Q. Huo, I.G. VoigtMartin, G.D. Stucky, F. Schuth, *Science* **1996**, *273*, 768.

[14] Q.S. Huo, J.L. Feng, F. Schuth, G.D. Stucky, *Chem. Mater.* **1997**, *9*, 14.

[15] Q.S. Huo, D.I. Margolese, U. Ciesla, D.G. Demuth, P.Y. Feng, T.E. Gier, P. Sieger, A. Firouzi, B.F. Chmelka, F. Schuth, G.D. Stucky, *Chem. Mater.* **1994**, *6*, 1176.

[16] Q.S. Huo, D.I. Margolese, U. Ciesla, P.Y. Feng, T.E. Gier, P. Sieger, R. Leon, P.M. Petroff, F. Schuth, G.D. Stucky, *Nature* **1994**, *368*, 317.

[17] H. Witossek, E. Bratz, *Chem. Eng. Technol.* **1997**, *20*, 429.

[18] M. Oubaha, P. Etienne, S. Calas, R. Sempere, J.M. Nedelec, Y. Moreau, *J. Non-Cryst. Solids* **2005**, *351*, 2122.

[19] D.A. Loy, B.M. Baugher, C.R. Baugher, D.A. Schneider, K. Rahimian, *Chem. Mater.* **2000**, *12*, 3624.

[20] S. Sankaraiah, J.M. Lee, J.H. Kim, S.W. Choi, *Macromolecules* **2008**, *41*, 6195.

[21] K. Moller, T. Bein, *Chem. Mater.* **1998**, *10*, 2950.

[22] N. El-Ashgar, I. El-Nahhal, *J. Sol-Gel Sci. Technol.* **2005**, *34*, 165.

[23] S.K. Bhargava, D.B. Akolekar, *J. Colloid Interface Sci.* **2005**, *281*, 171.

[24] U. Schubert, G. Kickelbick, N. Husing, *Molecular Crystals and Liquid Crystals* **2000**, *354*, 695.

[25] I.S. Khatib, R.V. Parish, *J. Organomet. Chem.* **1989**, *369*, 9.

Chapter 4

Selective liquid phase oxidation of *o*-xylene with gaseous oxygen by Cobalt containing silica initiator-catalyst-systems

Polysiloxanes containing Co or Mn act as initiators and catalysts in the selective liquid phase oxidation of o-xylene by oxygen under solvent free conditions. Their hydrophobic character allows the fast desorption of polar products resulting in a higher activity compared to the benchmark system Co naphthenate. Besides the acceleration of the initiation Co or Mn catalysts efficiently decompose the intermediate 2-methylbenzyl hydroperoxide. The decomposition ratio of the products o-tolualdehyde and 2-methylbenzyl alcohol can be controlled by the type of the transition metal, i.e., Co increases the selectivity towards the aldehyde, while Mn cations favor the formation of alcohol.

4.1. Introduction

The direct insertion of oxygen into organic molecules generates important chemical functionality with high atom efficiency. This makes selective oxidation reactions very attractive for industrial applications. Important examples of liquid phase oxidation reactions carried out on industrial scale are the oxidation of *p*-xylene and related aromatic educts to the corresponding acids (especially the production of terephthalic acid from *p*-xylene [1]) and the oxidation of cyclohexane to the corresponding ketone and alcohol.[2] The resulting products are important intermediates or monomers for the production of nylon and polyethylene terephthalate (PET) respectively. These autoxidation processes have in common that the reactions are carried out in the liquid phase using oxygen as terminal oxidant. Both proceed via a radical reaction pathway in presence of Co and Mn compounds, which act as initiators for the formation of radicals. In case of the *p*-xylene oxidation a halogen source (i.e., HBr) is typically introduced to increase the activity of the system via enhancing radical formation. [3, 4]

The mechanism of autoxidation reactions is described as free radical chain reactions [5], consisting of initiation, chain growth and termination steps. The chain growth is sustained by the formation of hydroperoxides, which are thermally or catalytically decomposed over transition metals (e.g., Co or Mn) to oxygenates. This decomposition is generally described as the Haber-Weiss mechanism. [6] Alternatively, the hydroperoxide can also be dehydrated to an aldehyde over an acid functionality. The central role of the transition metal species lies (a) in the generation of organic entities in the form of radicals via hydrogen abstraction and (b) the catalytic decomposition of hydroperoxide compounds to the corresponding alcohols and aldehydes. [5]

For the oxidation of cyclohexane on an industrial scale typically mixtures of cobalt and manganese naphthenates are employed. The limitations of this process are the low conversion usually achieved and the undesired high cyclohexanol yields. The ratio of cyclohexanone and cylohexanol can be tuned and is known to strongly depend on the type of transition metal of the catalyst. [7] Co enhances the formation of cyclohexanone, whereas Mn catalysis increases the selectivity towards cyclohexanol. For the commercial oxidation of *p*-xylene mixtures of Co, Mn and Br initiators are applied as initiators with acetic acid as solvent. Due to the presence of bromine and acid the mixture is highly corrosive and special precautions have to be taken to handle it on an industrial scale.

As an alternative heterogeneous initiator and catalyst systems are available for liquid phase oxidations in the presence of oxygen, which may potentially combine the benefits of easy separation with the advantage of non corrosive reactions mixtures. Several examples for the successful application of heterogeneous initiator/catalyst systems for the oxidation of alkyl substituted aromatics are described in the literature, however, in depth insight on the prevailing reaction mechanisms is limited. [8, 9]

Thomas *et al.* used heterogeneous AlPO-36 systems loaded with Co, Mn or Fe for the liquid phase oxidation of *p*-xylene to *p*-toluic acid, 4-formylbenzoic acid and terephthalic acid under varying conditions. [8] These materials, however, are up to date only of academic interest, because they do not reach the productivity of the industrially used Co/Mn/Br systems.

MnAPO-5 was studied by Moden *et al*. [10] for the decomposition of hydroperoxides during the selective oxidation reaction of cyclohexane. The investigated catalyst systems were proven to act as heterogeneous catalysts by decomposing the intermediate hydroperoxide. [10, 11] Ramanathan *et al.* developed an amorphous mesoporous cobalt containing silicate (Co-TUD-1) as an effective catalyst for the decomposition of cyclohexyl hydroperoxide to cyclohexanol and cyclohexanone. [12]

The selective oxidation of *o*-xylene to phthalic anhydride is carried out as a gas phase process using vanadia-titania catalysts on industrial scale. [13, 14] A large number of reports on the reaction conditions, catalyst compositions and reaction mechanism exists in the open literature for this gas phase reaction. [13, 15] The main limitation of this process is the selectivity of ca. 80-85% to phthalic anhydride at almost 100% conversion. Separating the process into two consecutive steps was presented as possible solution to increase the selectivity to 88% in the patent literature. [16] In a first step *o*-xylene is oxidized over Co naphthenate to *o*-toluic acid, which is converted to phthalic anhydride by a subsequent partial oxidation step using a vanadia catalyst. Recently, we described a polysiloxane based material that is capable for the selective liquid phase oxidation of one of the methyl groups of *o*-xylene under solvent free conditions. [17] In the present contribution these solid Co^{2+} and Mn^{3+} cation containing hydrophobic initiator catalyst systems are used for the mechanistic description of the reaction network of this liquid phase oxidation. The formation and consumption of the radicals in the individual elementary steps of the reaction were used to determine the reaction pathways and a complex network of reaction steps was derived to explain the reactivity and selectivity to partially oxygenated substances over Co^{2+} or Mn^{3+} containing initiator catalyst systems.

4.2. Experimental

4.2.1. Catalyst Synthesis

Spherical polysiloxanes were synthesized by applying the sol-gel process [18] using a mixture of (easily hydrolysable) silane precursors and a transition metal source, which was injected into a water filled column. The initially formed stable droplets were converted into spherical particles by polymerization of the silanes in the aqueous phase at 333 K. In order to assure a sufficient condensation rate dibutyl tin dilaurate was added to the solution. The detailed procedure of the synthesis is described elsewhere. [19] After ageing in water at room temperature for 12 h the catalyst materials were washed with deionized water and *i*-propanol. Before their usage the solid materials were dried by lyophilization. The diameter of the synthesized particles was in the range of 800 - 1200 µm. 3-aminopropyltrimethoxysilane (>97%), tetraethyl orthosilicate (>99%), 1-butanol (>99.5%), dibutyltin dilaurate (95%), cobalt (II) and manganese (III) acetylacetonate (97%), triphenyl phosphine (>98.5%) and tetradecane (>99%) used for the catalyst synthesis and the reactant *o*-xylene (>99%) were purchased from Sigma Aldrich and used without any further purification.

The concentration of the metal in the solid catalysts was determined by atomic absorption spectroscopy using a UNICAM Solaar M5 Spectrometer. For this typically, 30-60 mg of the sample was dissolved in 0.5 ml of hydrofluoric acid (10%) at its boiling point (about 383 K).

4.2.2. Liquid phase oxidation of o-xylene

The liquid phase oxidation experiments were carried out in a lab-scale bubble column reactor consisting of a 10 mm inner diameter glass tube loaded with reactant (*o*-xylene) and catalyst without the usage of a further solvent. Prior to each reaction, the reactant was heated to the desired temperature under nitrogen flow using a pressure of 2.4 bar. The gas was directed through a glass frit to form small bubbles in order to minimize the transport resistance of the gas into the liquid. The upper part of the reactor was cooled to 293 K and the entrance gas stream was saturated at the same temperature with *o*-xylene to prevent the loss of reactant via the gas stream. The reaction was started by switching the nitrogen to a mixture of synthetic air (50%) and nitrogen. After the reactor the gas stream was directed through a saturator filled with 0.1 M NaOH to quantify the integral amount of CO_2 formed in the reaction by back titration with hydrochloric acid.

Liquid samples were collected by using a syringe inserted from the top of the reactor. Hexachlorobenzene was used as internal standard to every reaction. To identify the concentration of products a Shimadzu GC-2010 gas chromatograph equipped with a 30 m DB-5 column (0.25 mm inner diameter and 0.25 µm film thickness) and a FID detector was used. Tetradecane was added to each analysis as internal GC standard. To determine the concentration of the 2-methylbenzyl hydroperoxide the procedure described by Shulpin *et al.* [20] was used.

4.2.3. Adsorption of CO followed by IR spectroscopy

The samples were prepared as self supporting wafers (5-10 mg cm^{-2}) and measured in transmission mode using a with a Bruker IFS88 spectrometer using a resolution of 4 cm^{-1}. After activation in vacuum (10^{-6} mbar) at 723 K (heating rate 10 K min^{-1}) for one hour the samples were cooled to 300 K and CO was adsorbed at partial pressure between 10^{-3} mbar and 1 mbar.

4.2.4. ^{1}H NMR spectroscopy

^{1}H NMR spectra of the reaction solutions were analyzed with a Bruker NMR spectrometer operating at 360 MHz, using 5-mm high-resolution liquid probes under ambient conditions. The reaction products were dissolved in $CDCl_3$.

4.3. Results

4.3.1. Catalyst characterization

The chemical composition of the Co and Mn containing catalysts determined by AAS and elemental analysis are summarized in Table 4-1. Before synthesis of the catalysts, the metal compound was mixed with tetraethyl orthosilicate (TEOS) and 3-amino-propyltrimethoxysilane in a ratio of 2 : 1 in 10 vol. % 1-butanol and a Sn containing reaction accelerator was added. The precursor mixture was injected into a water filled column at 333 K. During the polycondensation reaction the density of the injected droplets increased until solid spheres were formed, which sunk to the bottom of the reactor. After removing the solid polysiloxane spheres from the synthesis apparatus the catalysts were stored in water at ambient conditions for 12 h for further ageing and finally freeze dried. The catalysts were used for the oxidation reaction without any further pretreatment. The elemental composition of the catalysts was not affected by the oxidation reaction; especially the N concentration was constant.

Table 4-1: Chemical composition of the Co and Mn containing catalysts. Note that the difference to 100% is balanced by oxygen.

Sample name	Metal loading (wt. %)	C content (wt. %)	Si content (wt. %)	N content (wt. %)	H content (wt. %)
Co-0.3	0.3	6.7	33.6	1.1	2.7
Co-0.8	0.8	7.6	34.2	1.8	2.5
Co-1.1	1.1	8.7	33.1	2.0	2.5
Co-1.9	1.9	8.0	25.7	2.2	3.0
Mn-2.0	2.0	14.3	31.5	3.1	3.7

The loading of Co was varied in the range from 0.3 to 1.9 wt. % by synthesis. The diameter of the spheres was kept constant at 800 µm for all materials. Co containing samples showed blue color and the Mn materials were brown.

4.3.2. Adsorption of CO on the Co containing catalyst

The IR spectra during adsorption of CO on Co-1.9 at 303 K and CO partial pressures between 10^{-3} mbar to 1.5 mbar are shown in Figure 4-1.

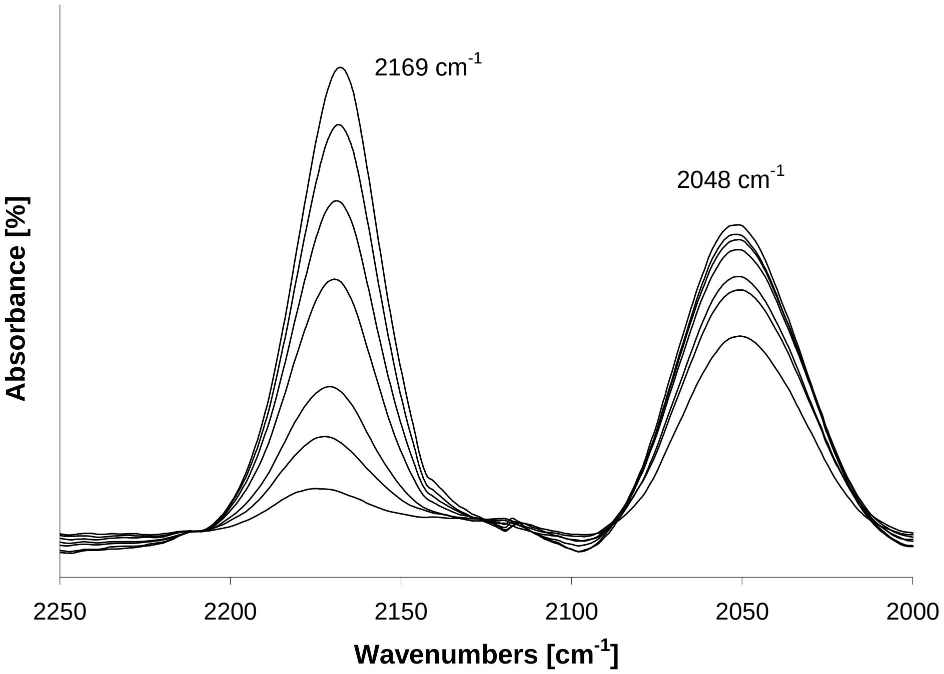

Figure 4-1: Difference IR spectra of CO adsorbed on Co-1.9 catalyst at 303 K and CO partial pressures between 10^{-3} and 1.5 mbar.

Adsorption of CO on the Co containing catalysts led to the formation of two bands at 2048 cm^{-1} and 2169 cm^{-1}, which are characteristic for stretching vibrations of CO in metal carbonyl species and for CO adsorbed on Lewis acidic Co (II) cations. [21] The carbonyl band at 2048 cm^{-1} is more intense at low pressures and increases only slightly with the CO partial pressure. The band at 2169 cm^{-1}, attributed to CO adsorbed on Co (II), increase over the entire pressure range studied and did not reach saturation at the highest pressure applied. Therefore, the saturation coverage was calculated from fitting the coverage with a Langmuir sorption isotherm:

$$Q = Q_{sat} \frac{K \times p}{1 + K \times p}$$

With Θ_{sat} the saturation coverage, K the Langmuir adsorption constant and p the CO partial pressure. The value for K was constant at 3.42 mbar^{-1} for every catalyst sample.

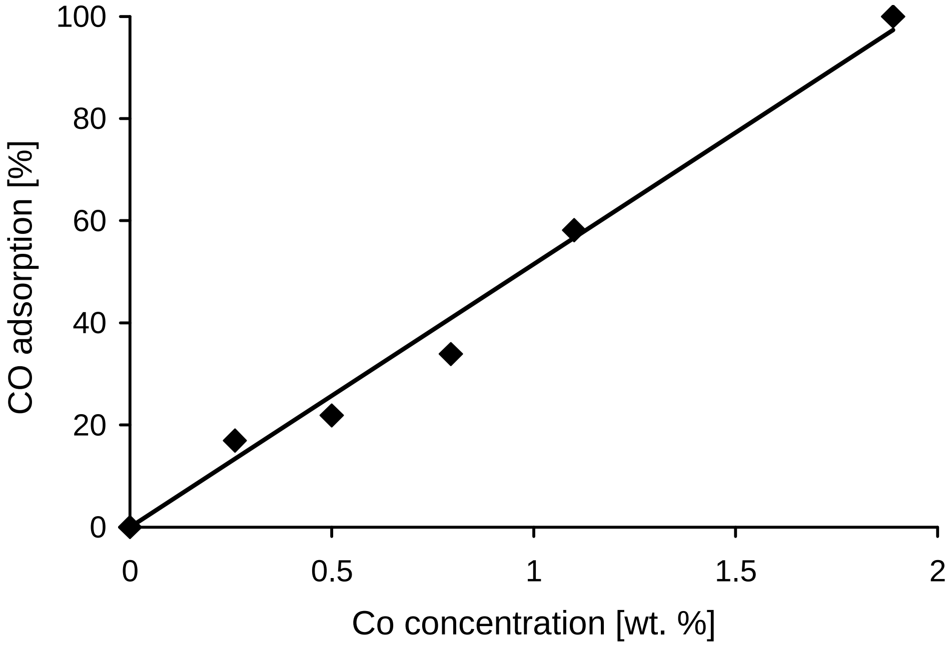

Figure 4-2: Maximum CO coverage (band at 2169 cm^{-1}) as function of the Co loading of the catalysts.

The maximal CO adsorption capacity shows a linear dependency on the Co loading (see Figure 4-2), which indicates that the accessibility and the local structure of the Co^{2+} species is not affected by the metal loading. The support itself did not show any evidence for CO adsorption in the IR spectra.

In order to test the hydrophilicity of the polysiloxane materials water was adsorbed at different partial pressures. The coverage was followed by IR spectroscopy and the intensity of the H-O-H deformation vibration band at 1630 cm^{-1} was used for quantification.

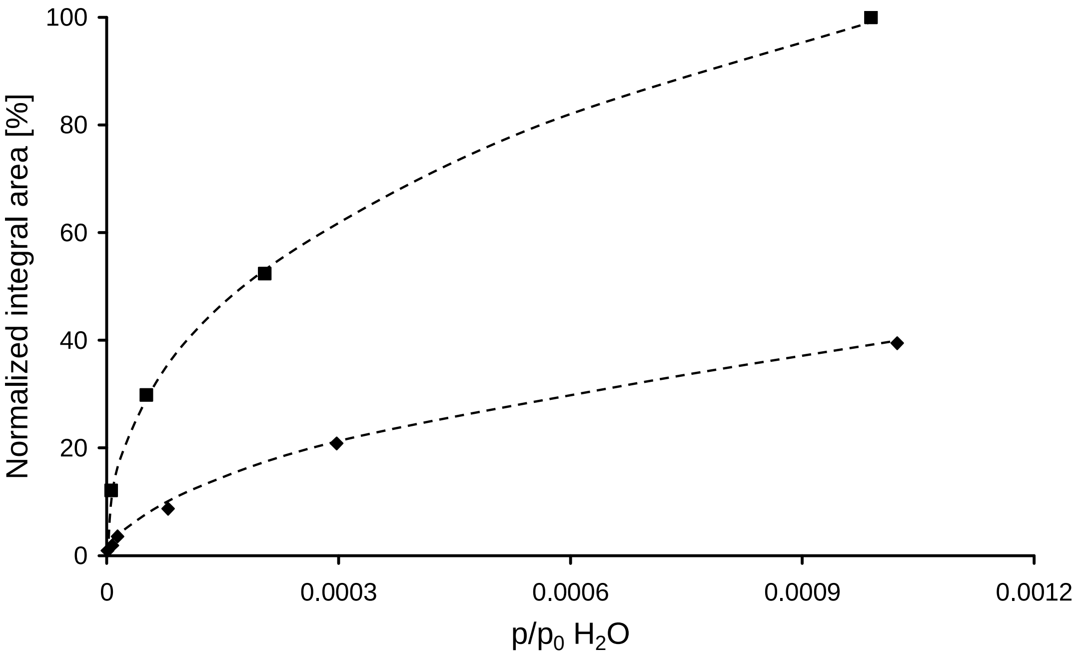

Figure 4-3: Normalized absorption of the band 1630 cm^{-1} caused by water adsorbed to the material. The Co-1.9 catalyst (●) was compared to the corresponding calcined material without organic side groups (■) (adsorption of water was recorded by IR at 300 K).

The hydrophilicity of the Co^{2+} containing polysiloxane material was 40% of the oxidic reference sample, from which organic side groups were removed by treatment at 873 K under air flow (see Figure 4-3).

4.3.3. Thermal decomposition of the hydroperoxide

Hydroperoxides are expected to be formed as reaction intermediates in the partial oxidation reaction of aromatic molecules, however, they cannot be directly detected by GC analysis as they thermally decompose into an aldehyde and an alcohol at temperatures around 473 K (see Scheme 4-1). [20] Therefore, an indirect method has to be applied for the detection of 2-methylbenzyl hydroperoxide.

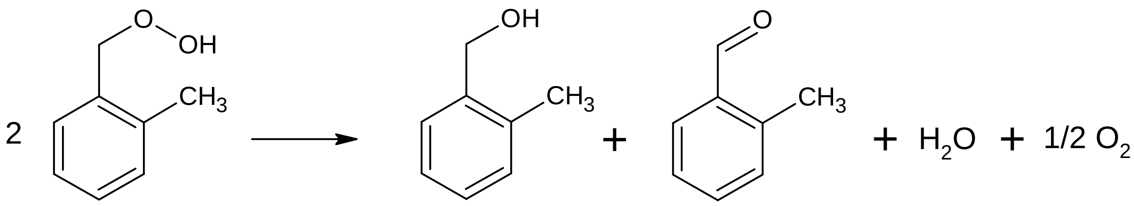

Scheme 4-1: Decomposition of 2-methylbenzyl hydroperoxide to *o*-tolualdehyde and 2-methylbenzyl alcohol.

Using a solution containing 1 mol % 2-methylbenzyl hydroperoxide (in *o*-xylene), prepared by oxidizing *o*-xylene at 398 K with synthetic air for 12 h, a ratio of 7:1 between *o*-tolualdehyde and 2-methylbenzyl alcohol formed by the thermal decomposition in the GC inlet system was determined. For the analysis of the liquid samples a fraction was reduced with triphenyl phosphine to 2-methylbenzyl alcohol (see Scheme 4-2).

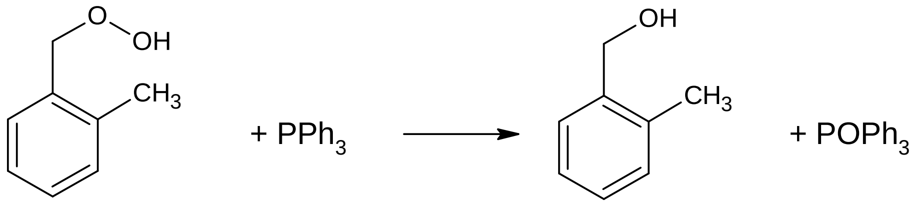

Scheme 4-2: Reduction of the 2-methylbenzyl hydroperoxide to 2-methylbenzyl alcohol by PPh_3.

A second fraction was analyzed directly and by using the ratio between alcohol and aldehyde determined before, the concentrations of alcohol, aldehyde and hydroperoxide in the liquid samples could be determined.

The ratio of *o*-tolualdehyde and 2-methylbenzyl alcohol formed by the thermal decomposition of the hydroperoxide was determined experimentally. The presence of the hydroperoxide was confirmed by ^{1}H-NMR spectroscopy (Figure 4-4).

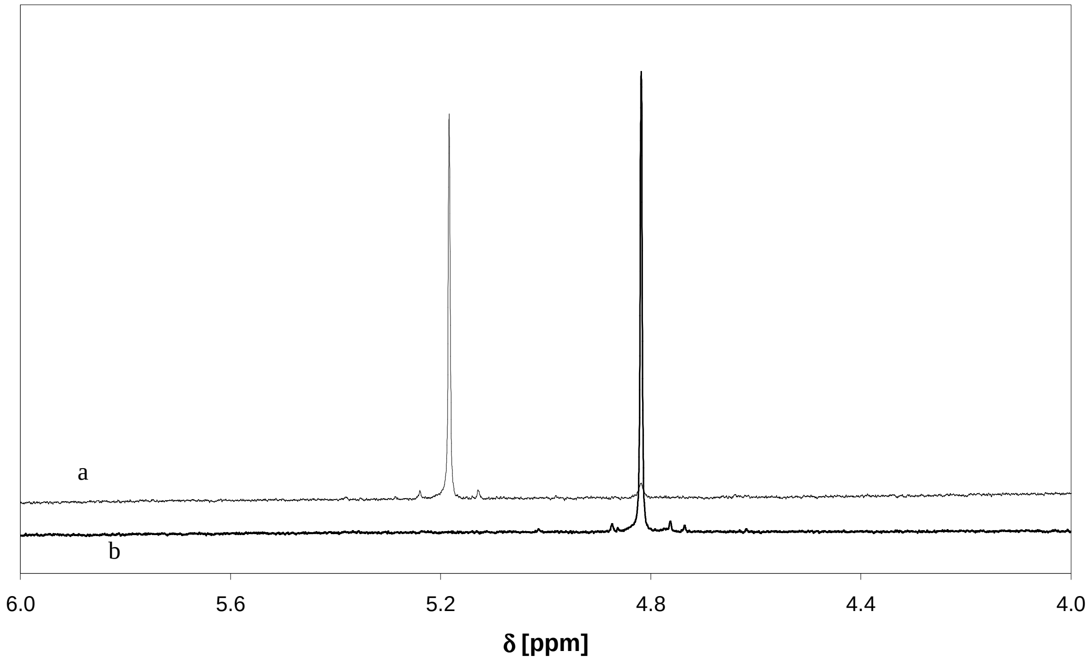

Figure 4-4: ^{1}H-NMR spectra of the untreated 2-methylbenzyl hydroperoxide solution (a) and the solution after reduction with PPh_3 (b) under ambient conditions.

The ^{1}H-NMR spectrum of the 2-methylbenzyl hydroperoxide solution (Figure 4-4a) contains a signal at 5.2 ppm which is assigned to the protons of the α-CH_2-group. Additionally, the mixture contains 2-methylbenzyl alcohol (4.8 ppm) and *o*-tolualdehyde (10.4 ppm, not displayed here) in low concentrations. This solution was injected into the GC and analysis gave a *o*-tolualdehyde to 2-methylbenzyl alcohol ratio of 7 : 1 after correcting for the initially present components.

The hydroperoxide was completely reduced with PPh_3 to 2-methylbenzyl alcohol (Scheme 4-2) which is confirmed by the disappearance of the NMR signal at 5.2 ppm and the increased signal at 4.8 ppm corresponding to the alcohol (Figure 4-4). The intensity of the aldehyde peak remains constant after this procedure.

4.3.4. Influence of the Co concentration on the oxidation of *o*-xylene

The conversion of *o*-xylene as function of the Co concentration was studied at 445 K and a total pressure of 2.4 bar. In all reactions an induction period was observed. Its duration decreased linearly with increasing Co loading. The rate of *o*-xylene conversion for catalysts with Co loadings from 0.3 to 1.9 wt. % is compared in Figure 4-5.

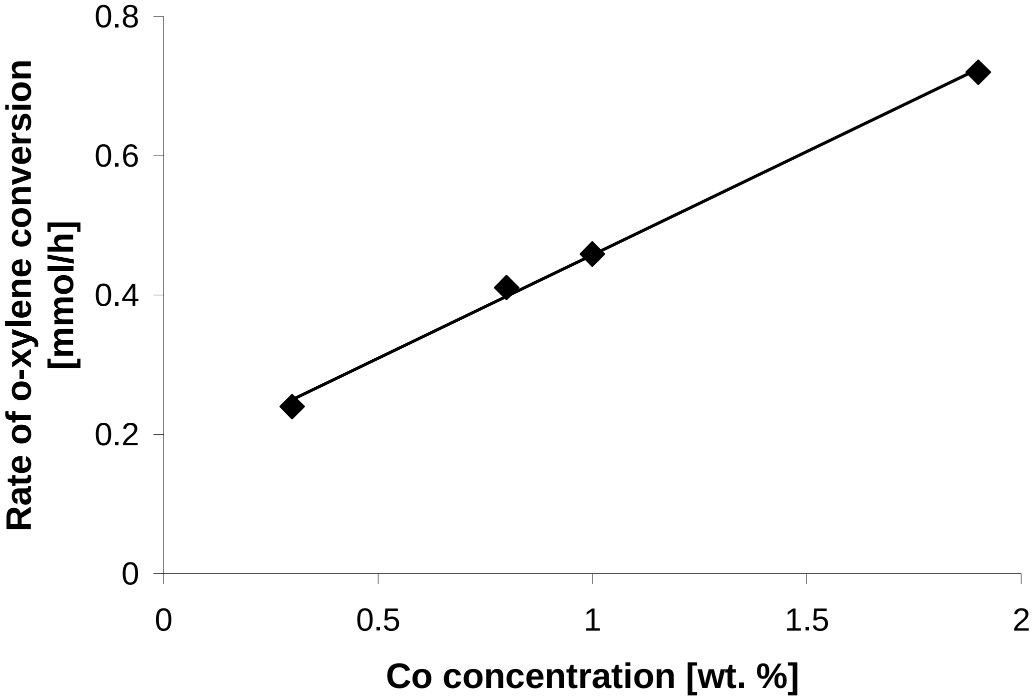

Figure 4-5: Initial rates of *o*-xylene conversion as function of the Co concentration of the polysiloxane catalysts (experimental conditions: 445 K, total pressure 2.4 bar).

The linear relation of the activity of the initiator catalyst systems and the concentration of active transition metal indicates that the chemical nature of the Co^{2+} species is identical for all catalysts. This is supported by the fact that the selectivity towards the oxidation products as function of the *o*-xylene conversion was independent of the cobalt loading. An example of the selectivity as function of the conversion for the Co-1.9 catalyst is shown in Figure 4-6. Initially 2-methylbenzyl hydroperoxide, 2-methylbenzyl alcohol and *o*-tolualdehyde are formed, whereas the selectivity towards *o*-toluic acid only increases when the conversion exceeds 4 mol %. The initial slopes indicate that

2-methylbenzyl hydroperoxide, 2-methylbenzyl alcohol and *o*-tolualdehyde are formed as primary products, while *o*-toluic acid was formed as a secondary product.

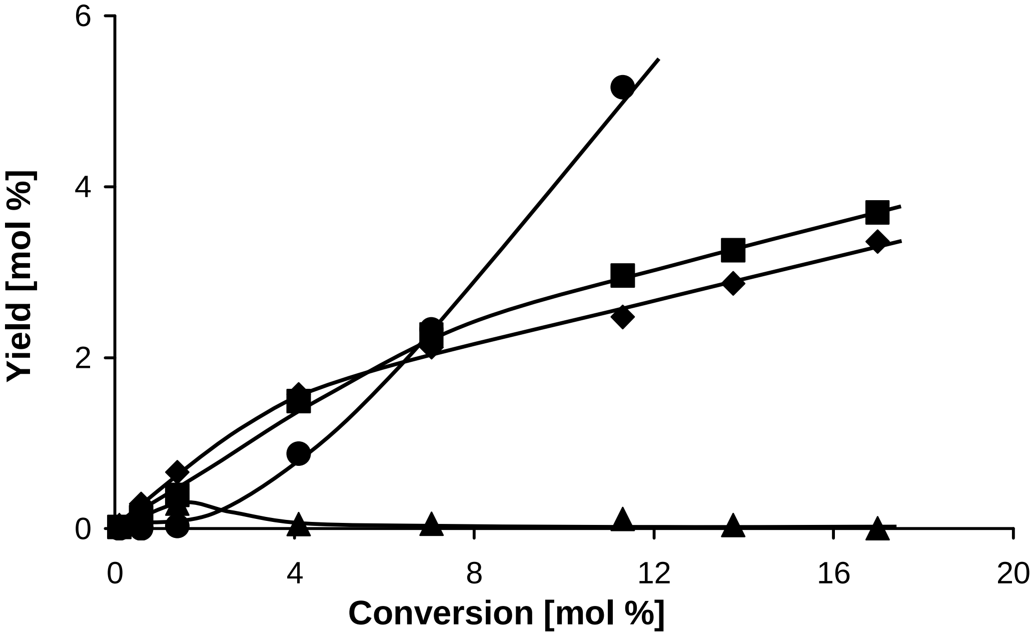

Figure 4-6: Yields of *o*-tolualdehyde (♦), 2-methylbenzyl alcohol (■), 2-methylbenzyl hydroperoxide (▲) and *o*-toluic acid (●) as function of the *o*-xylene conversion (reaction conditions: 445 K, 100 mg Co-1.9 catalyst, total pressure 2.4 bar).

Besides the main products phthalide (yields of 1 mol %) and other side products such as *o*-xylene dimers, esters of *o*-toluic acid and 2-methylbenzyl alcohol, formiates of 2-methylbenzyl alcohol, toluene and phthalic anhydride were detected in minor concentrations (molar yields below 0.4 mol % at conversions above 20 mol %).

The ratio of *o*-tolualdehyde and 2-methylbenzyl alcohol for the application of Co and Mn catalysts are compared in Figure 4-7. This ratio is seen as a measure for the selectivities of the decomposition products of 2-methylbenzyl hydroperoxide. The absolute values for the yield of oxygenates can be seen in Figure 4-6. The ratio between *o*-tolualdehyde and 2-methylbenzyl alcohol decreased from an initial value of 2.5 at low conversion to a constant level between 1 and 0.6 when Co or Mn were applied as catalyst at higher conversion.

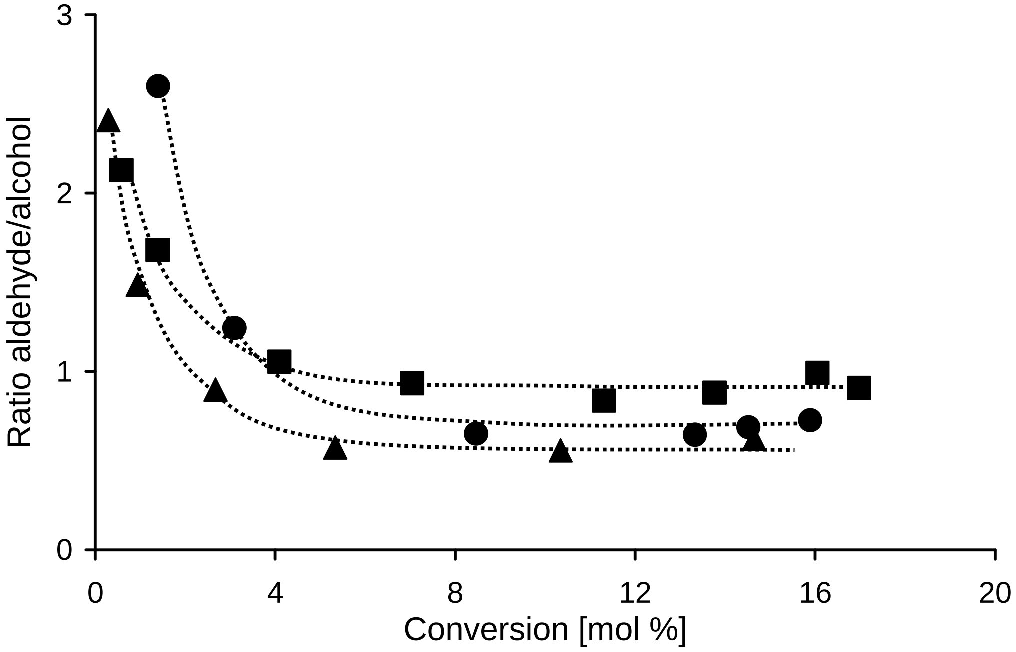

Figure 4-7: Ratio of yields of *o*-tolualdehyde to 2-methylbenzyl alcohol in dependence of the *o*-xylene conversion for the Co-1.9 (■), Mn-2.0 (▲) catalyst and without a catalyst (●) (reaction conditions: 445 K, total pressure 2.4 bar).

Without catalyst the decomposition of the 2-methylbenzyl hydroperoxide occurred only at higher local concentrations, and the ratio of the aldehyde and the alcohol was 0.7.

To verify that the transition metal was not leached from the catalyst during the reaction the Co containing catalyst was used under the typical reaction conditions at 445 K until 2-methylbenzyl hydroperoxide was decomposed, i.e., 8 mol % conversion (Figure 4-8). After reaching this point the catalyst was removed from the liquid phase by filtration at 353 K and the solution returned into the reactor for further reaction at 445 K.

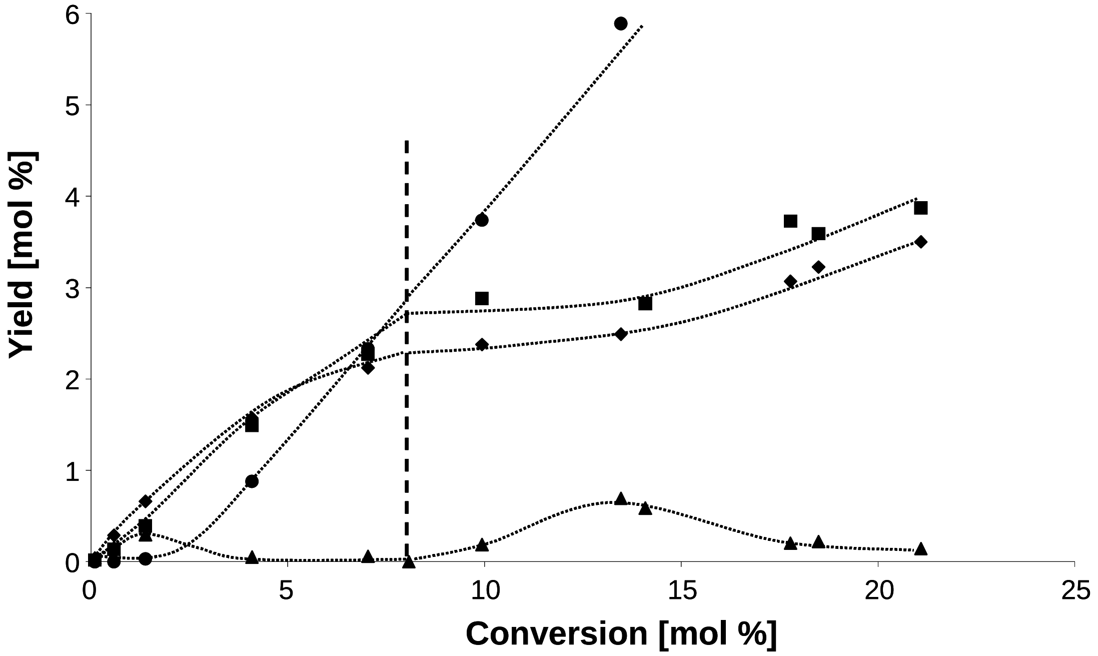

Figure 4-8: Yields of the oxygenates *o*-tolualdehyde (♦), 2-methylbenzyl alcohol (■), 2-methylbenzyl hydroperoxide (▲) and *o*-toluic acid (●) as function of the *o*-xylene conversion (reaction conditions: 445 K, 100 mg 1.9 wt% Co catalyst, total pressure 2.4 bar). The Co catalyst was removed from the reaction mixture when the concentration of 2-methylbenzyl hydroperoxide was below 0.03% (at conversion of 8%) which is indicated by the vertical line.

The concentration of 2-methylbenzyl hydroperoxide increased again after the catalyst was removed from the reaction mixture, while the concentration of *o*-tolualdehyde and 2-methylbenzyl alcohol remained constant until the maximum hydroperoxide concentration was 0.7 mol %. At this concentration the decomposition rate of the hydroperoxide in the liquid phase became larger than the formation rate (similar to the reaction carried out without catalyst (see Figure 4-10) and accordingly the concentrations of the alcohol and aldehyde started to increased further. Interestingly, the formation of the acid was not affected by the removal of the catalysts, which indicates that the formation of *o*-toluic acid from *o*-tolualdehyde does not require the presence of the catalyst. Additionally, the concentration of 2-methylbenzyl hydroperoxide is below the concentration compared to the reaction of pure *o*-xylene. This is attributed to the presence of oxygenates, which inhibit the formation of new radicals.

To further assure that Co is not leached into the liquid phase an AAS analysis of the liquid phase after the oxidation reaction was performed, confirming the absence of Co in the solution. Additionally a reaction without the use of any catalyst was performed using the concentration of the reaction products corresponding to a conversion of 8 mol % (see Figure 4-8). The profile of reaction products was equal to the reaction where the catalyst was removed at conversion of 8 mol % giving an additional evidence for the absence of Co in the solution.

4.3.5. Influence of temperature on 2-methylbenzyl hydroperoxide decomposition

The effect of the reaction temperature on the decomposition rate of the 2-methylbenzyl hydroperoxide was studied over Co-1.9 at 2.4 bar pressure. The maximal yield of 2-methylbenzyl hydroperoxide and the corresponding o xylene conversion at which this maximum yield has been reached are shown in Figure 4-9.

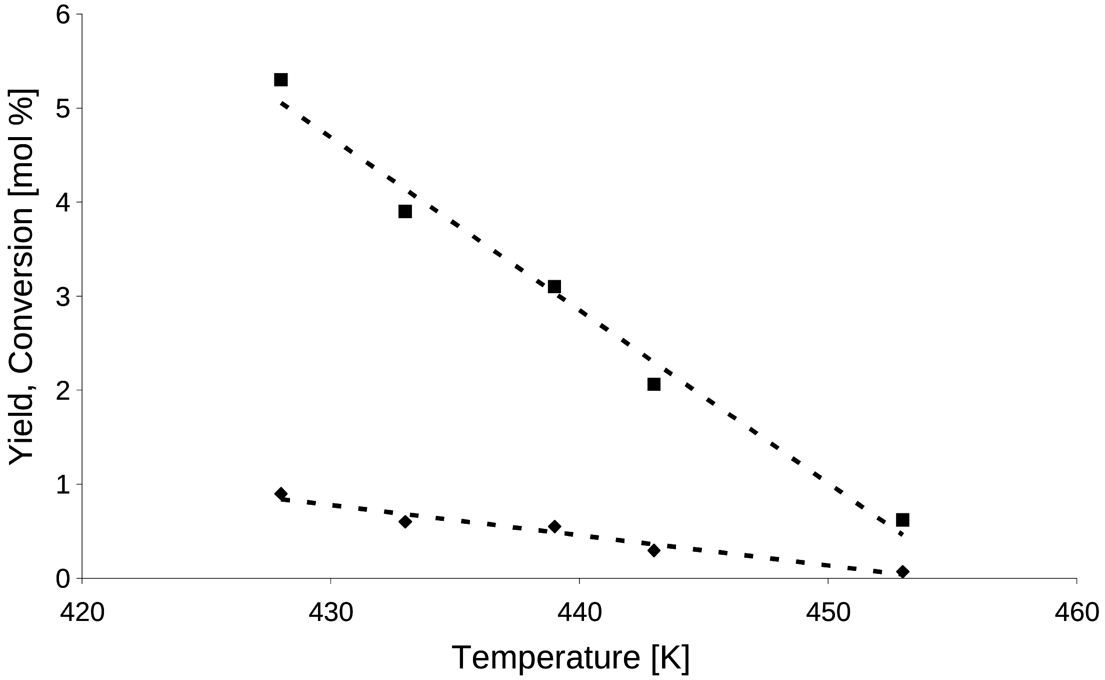

Figure 4-9: Maximum yield of 2-methylbenzyl hydroperoxide (♦) and the corresponding *o*-xylene conversion at which this yield has been reached (■) (experimental conditions: 100 mg Co-1.9 catalyst, total pressure 2.4 bar).

The maximum concentration of 2-methylbenzyl hydroperoxide in the liquid phase decreased when the reaction temperature increased. While the maximum hydroperoxide yield was reached at low temperature, the selectivity at the conversion this has been reached remained approximately constant for all reaction temperatures. This indicates that the activity of the catalyst for decomposing 2-methylbenzyl hydroperoxide has a higher apparent energy of activation than the formation of the hydroperoxide.

At a reaction temperature of 445 K the maximum 2-methylbenzyl hydroperoxide yields were reached at 2.0 mol % and 2.7 mol % conversion of *o*-xylene for Co^{2+} and Mn^{3+} catalysts, respectively, indicating that the hydroperoxide was decomposed more effectively on Co.

Normalizing to the concentration of the transition metal species the TOF for the Co polysiloxane catalysts was 4.0 min^{-1} and 3.5 min^{-1} for the Mn cation containing materials. This is twice as high as the benchmark system Co naphthenate (TOF = 2.0 min^{-1}). With the benchmark catalyst the yield of *o*-tolualdehyde was the highest tested (5 mol % *o*-xylene conversion; see Table 4-2).

Table 4-2: Yields (in mol %) of main oxygenates with different catalyst systems (experimental conditions: 445 K, total pressure 2.4 bar, 5 mol % conversion).

Compound	Co-naphthenate	Co-1.9	Mn-2.0
o-tolualdehyde	2.3	2.0	1.4
2-methylbenzyl alcohol	0.2	1.8	2.4
o-toluic acid	0.8	1.1	0.1

The yield of 2-methylbenzyl alcohol is the highest with Mn based catalysts, while in the case of Co based catalysts the selectivities towards *o*-tolualdehyde, 2-methylbenzyl alcohol are nearly equal (2.0 and 1.8 mol %, respectively). When Co naphthenate is used 1 mol % of the diester of *o*-toluic acid and 2-methylbenzyl alcohol is formed. Note that the yield of 2-methylbenzyl hydroperoxide is very low (< 0.1 mol %) at conversions of

5 mol %, as it already decomposed to a large extent. As additional product phthalide is formed with every catalyst used, which also balances the sum of yields to 5 mol %.

The role of the transition metals for the decomposition of 2-methylbenzyl hydroperoxide was examined by comparing the reaction with and without addition of a Co containing catalyst at 445 K as show in Figure 4-10.

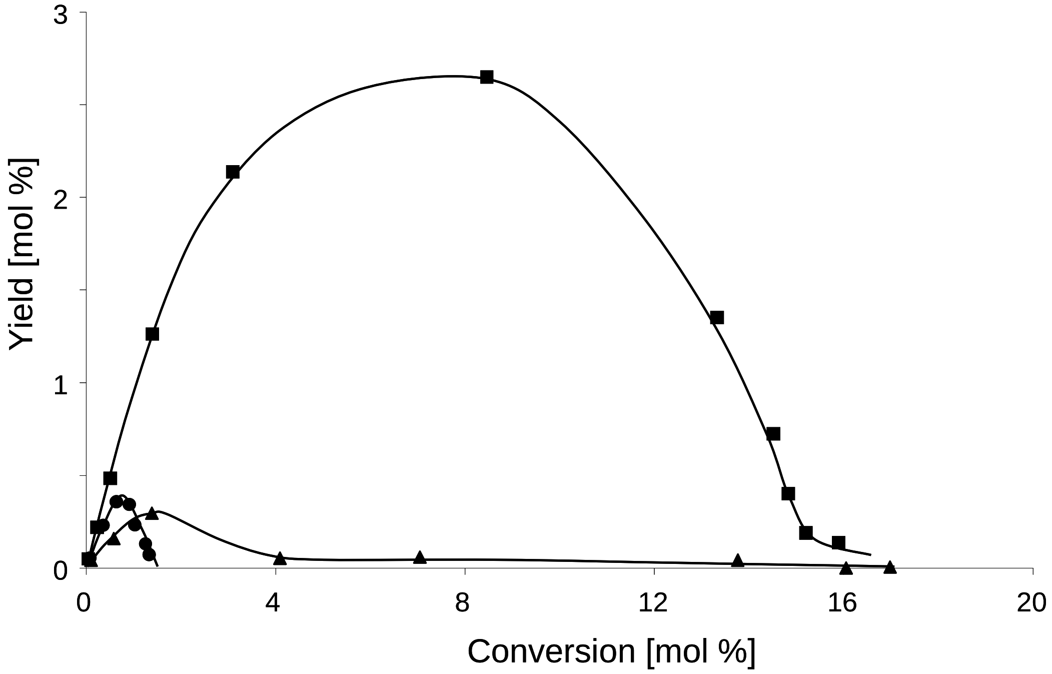

Figure 4-10: Yield of 2-methylbenzyl hydroperoxide in dependence of the *o*-xylene conversion in absence (■) and presence of a catalyst (Co-1.9) (▲) and with support material (●) (reaction conditions: 445 K, total pressure 2.4 bar).

The formation of 2-methylbenzyl hydroperoxide is detected as soon as oxygen is added into the reactant gas mixture. In the absence of a catalyst the 2-methylbenzyl hydroperoxide yield increased to 2.6 mol %, while in the presence of Co-1.9 the hydroperoxide was rapidly decomposed on the catalyst leading to a significantly lower concentration. The maximum yield of 2-methylbenzyl hydroperoxide (2.6 mol %) can be considered as a maximal yield, before the decomposition to *o*-tolualdehyde and 2-methylbenzyl alcohol exceeds the formation rate in the liquid phase without the application of a catalyst. When the support material without any transition metal was tested under reaction conditions the maximal 2-methylbenzyl hydroperoxide yield was 0.5 mol % and the conversion was limited to 1.5 mol %.

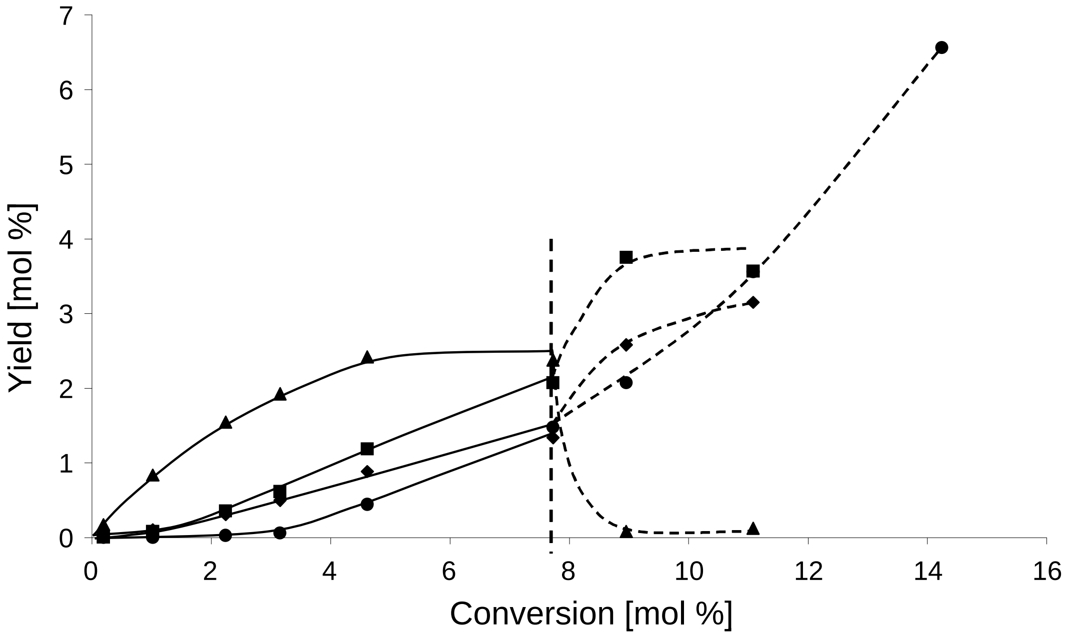

Figure 4-11: Yields of *o*-tolualdehyde (♦), 2-methylbenzyl alcohol (■), 2-methylbenzyl hydroperoxide (▲) and *o*-toluic acid (●) in dependence of the *o*-xylene conversion without catalyst in the initial phase of the reaction. The Co-1.9 catalyst was added after a defined time (vertical line) (reaction conditions: 445 K, total pressure 2.4 bar).

To further investigate the function of the catalyst, the reaction was initially started without catalysts and only after the 2-methylbenzyl hydroperoxide yield reached a constant level Co-1.9 was added. The concentration profiles of the oxidation products are shown in Figure 4-11. In the initial phase the yield of 2-methylbenzyl hydroperoxide increases to 2.4 mol % before the Co^{2+} catalyst was added. In the presence of the catalyst the yield of 2-methylbenzyl hydroperoxide decreased rapidly and simultaneously the yields of the decomposition products *o*-tolualdehyde and 2-methylbenzyl alcohol increased at almost the same rate. Note that the increase of *o*-toluic acid yield rises after the addition of the catalyst due to the creation of *o*-tolualdehyde by the decomposition of 2-methylbenzyl hydroperoxide.

4.3.6. Reaction with intermediate products

To elucidate the reaction network and to study the influence of the concentration of the reaction intermediates *o*-tolualdehyde and 2-methylbenzyl alcohol on the reaction, each of them was added into the reactant before starting the reaction. The yield of *o*-tolualdehyde after adding 2-methylbenzyl alcohol or *o*-tolualdehyde is illustrated in Figure 4-12.

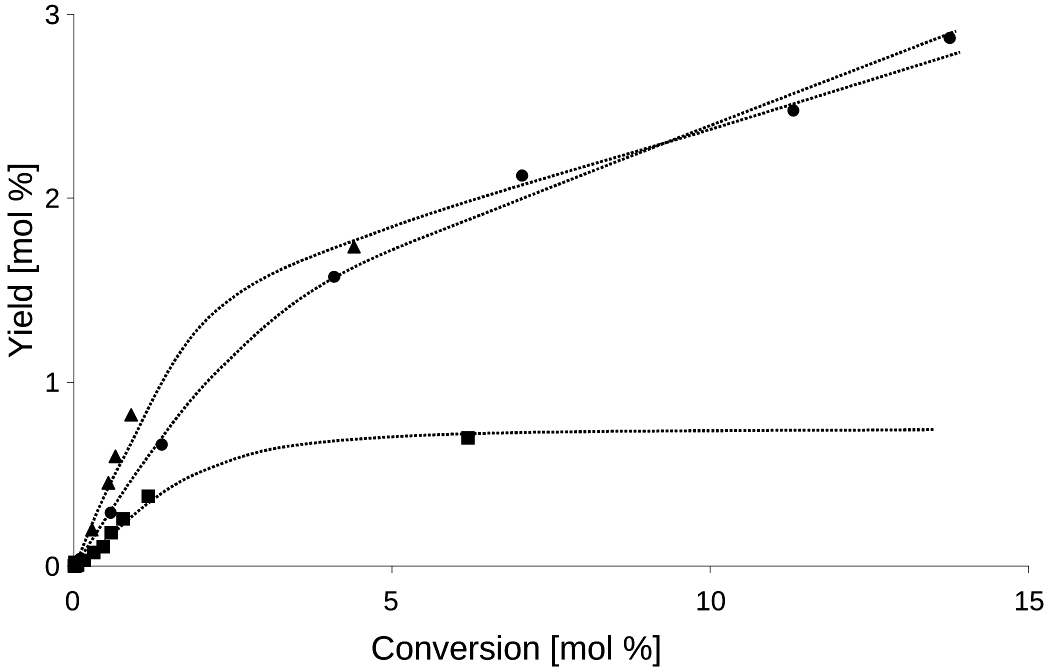

Figure 4-12: Yields of *o*-tolualdehyde after adding 1.8 mol % 2-methylbenzyl alcohol (▲) or 1.6 mol % *o*-tolualdehyde (■) to the reactant and for the reaction of *o*-xylene (●) (reaction conditions: 443 K, 100 mg Co-1.9 catalyst, total pressure 2.4 bar).

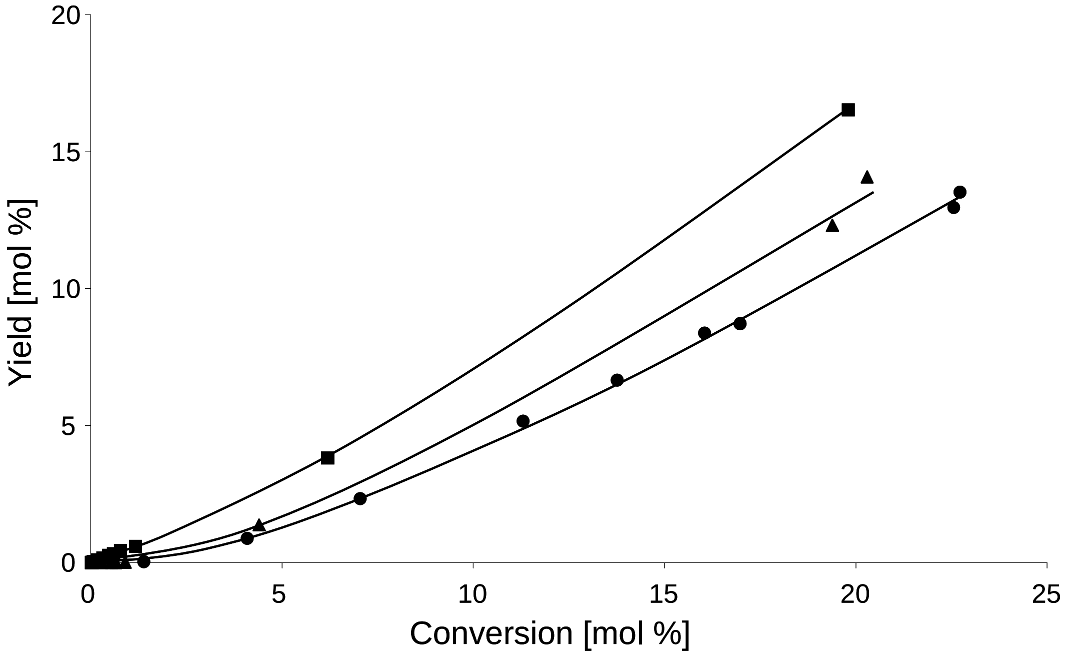

Figure 4-13: Yields of *o*-toluic acid after adding 1.8 mol % 2-methylbenzyl alcohol (▲) or 1.6 mol % *o*-tolualdehyde (■) to the reactant and for the reaction of *o*-xylene (●) (reaction conditions: 443 K, 100 mg Co-1-9 catalyst, total pressure 2.4 bar).

At low conversion levels the yield of *o*-tolualdehyde increased after adding 2-methylbenzyl alcohol, while at higher conversion levels the addition of 2-methlybenzyl alcohol did not change the yield of *o*-tolualdehyde compared to the oxidation of neat *o*-xylene. This confirms that *o*-tolualdehyde is a consecutive product of 2-methylbenzyl alcohol. On the contrary, the addition of *o*-tolualdehyde into the reactant significantly lowered its formation in the reaction.

The influence of adding *o*-tolualdehyde and 2-methylbenzyl alcohol on the formation of *o*-toluic acid was investigated at 445 K at 2.4 bar using the Co-1.9 catalyst (see Figure 4-13). Adding 2-methylbenzyl alcohol to the reactant had a positive effect on the yield of *o*-toluic acid. The addition of *o*-tolualdehyde leads to an even more pronounced enhancement of the yield in *o*-toluic acid. Adding the intermediate reactants *o*-tolualdehyde and 2-methylbenzyl alcohol into the reactant generally increased the induction period, which implies that the formation of radicals is retarded when oxygenates (i.e., aldehydes or alcohols) are present. After adding the intermediate products not only the selectivity towards the consecutive products but also the rate of o-toluic acid formation is increased in the sequence *o*-xylene, 2-methlybenzyl alcohol addition, *o*-tolualdehyde addition.

4.3.7. Catalytic activity in the oxidation of methyl substituted aromatics

To test the general catalytic activity of Co^{2+} containing polysiloxane spheres also toluene and 1,3,5-trimethyl benzene (mesitylene) were tested. The experimental conditions were kept equal to those of *o*-xylene oxidation, i.e. 100 mg of the catalyst was used and the reaction temperature was 445 K.

The spectrum of oxidation products of toluene included benzyl alcohol and benzaldehyde. Benzoic acid was observed in very low yields under the applied reaction conditions. In case of the oxidation of mesitylene products were 3,5-dimethylphenyl methanol, 3,5-dimethylbenzaldehyde and 3,5-dimethylbenzoic acid. The reactivity increased in the row toluene, mesitylene and *o*-xylene which is in good agreement with the predicted initial rate of oxygenation summarized by Partenheimer. [5]

4.4. Discussion

The results clearly indicate that the selective oxidation of *o*-xylene over transition metal based catalysts proceeds via radical reaction pathways. A linear correlation of the Co^{2+} loading and the initial reaction rate was observed, which implies that the active center for the initiation reaction is the transition metal. The accessibility of the Co^{2+} by CO showed a linear correlation to the Co^{2+} concentration in the material which further strengthens this assumption. The stability of the catalyst materials was shown by an unchanged elemental composition of the polysiloxanes after the oxidation reaction. Furthermore the CO adsorption behavior of used catalysts was equal to that of fresh materials proving that the accessibility of the transition metal was not reduced.

The formation and decomposition of 2-methylbenzyl hydroperoxide can be seen as the initial step followed by a series of radical based reactions leading to *o*-tolualdehyde, 2-methylbenzyl alcohol and *o*-toluic acid. To evaluate the formation and consumption of radicals by the individual reactions along the reaction route the most feasible reactions occurring in the oxidation of *o*-xylene via a radical based reaction mechanism are summarized in Table 4-3. The reactions included in this table contain the routes to the main products observed, i.e., 2-methylbenzyl hydroperoxide, *o*-tolualdehyde, 2-methylbenzyl alcohol and *o*-toluic acid.

Table 4-3: Radical reactions during the oxidation of *o*-xylene. **In** stands for initiator species, **R** symbolizes radicals species.

1.0 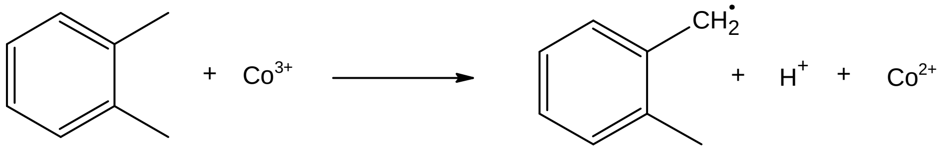

1.1 $Co^{2+} + O_2 + H^+ \longrightarrow Co^{3+} + \bullet OOH$

1.2 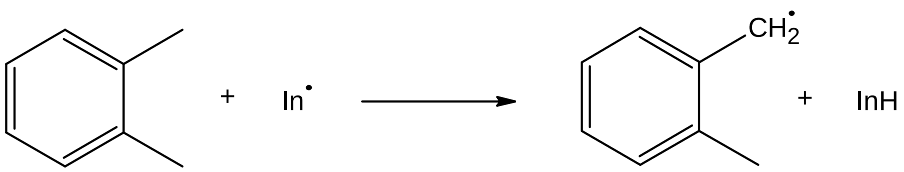

1.3

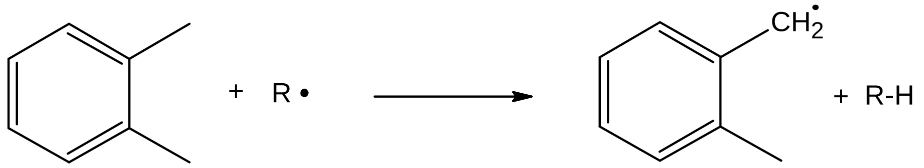

2.0

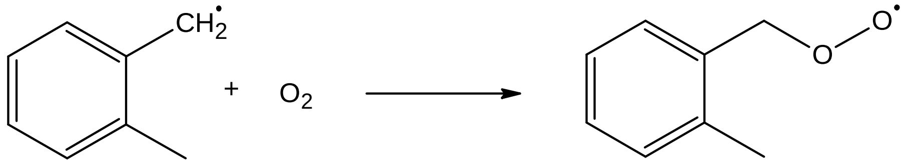

3.0

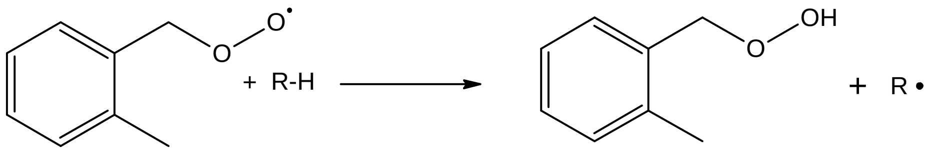

4.0

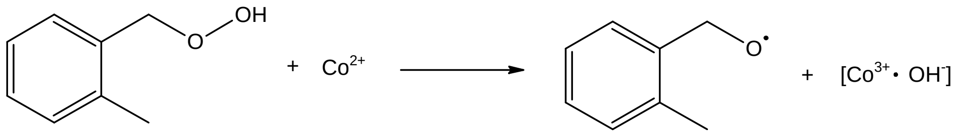

4.1

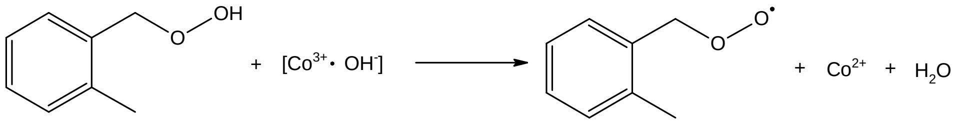

5.0

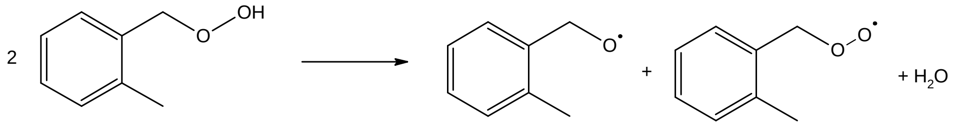

5.1

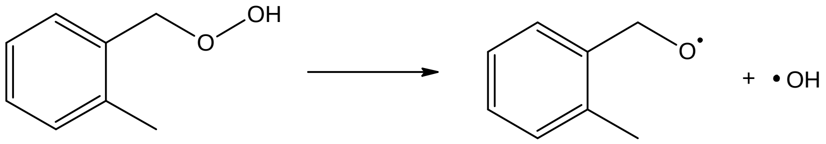

6.0

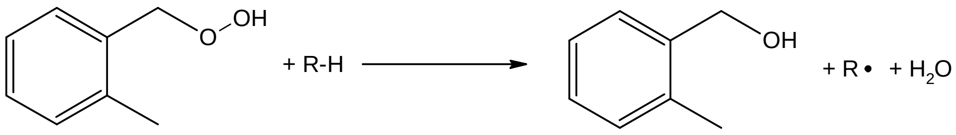

6.1

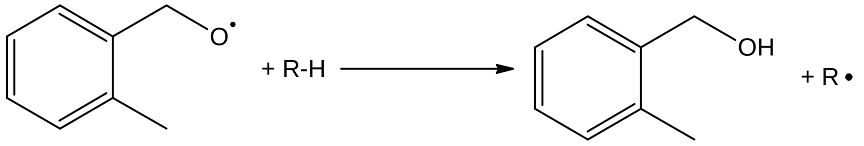

6.2

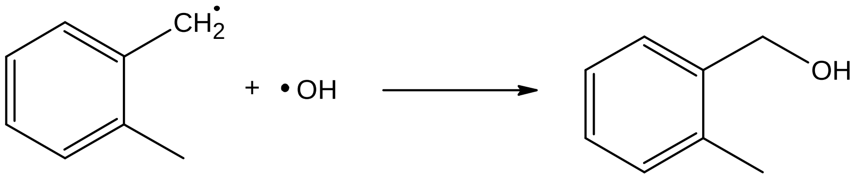

7.0

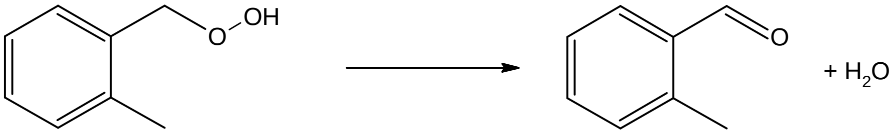

7.1

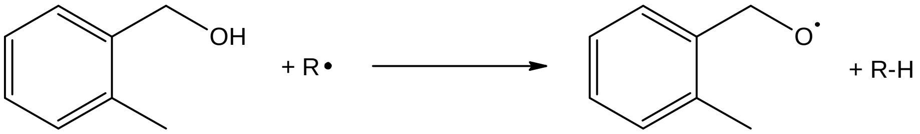

7.2

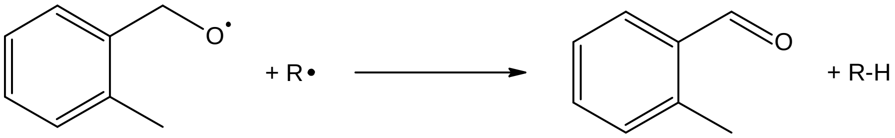

8.0

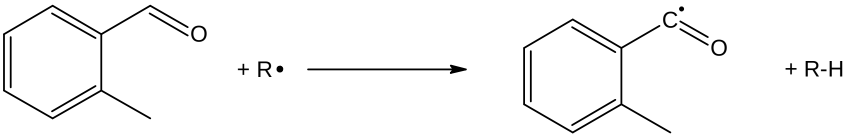

8.1

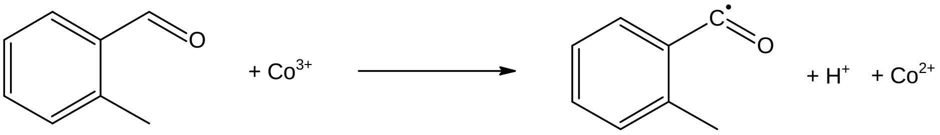

8.2 $Co^{2+} + O_2 + H^+ \longrightarrow Co^{3+} + \bullet OOH$

9.0

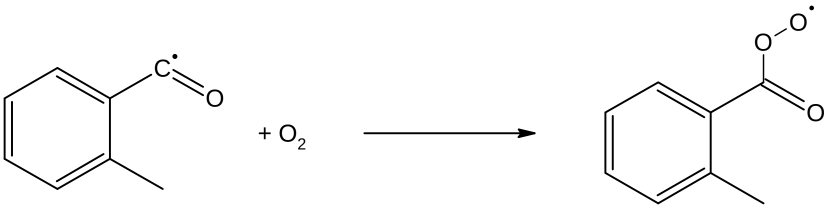

10.0

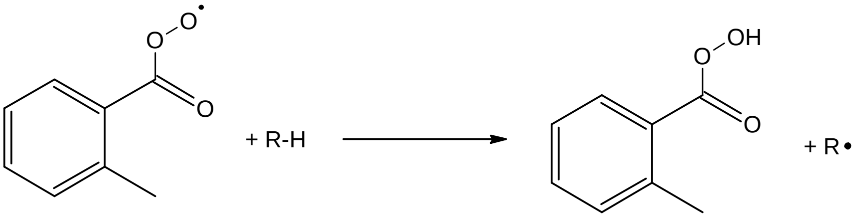

11.0 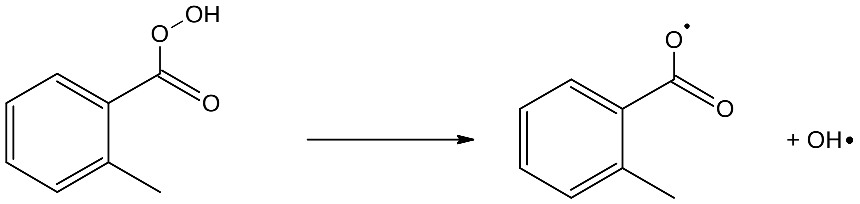

11.1 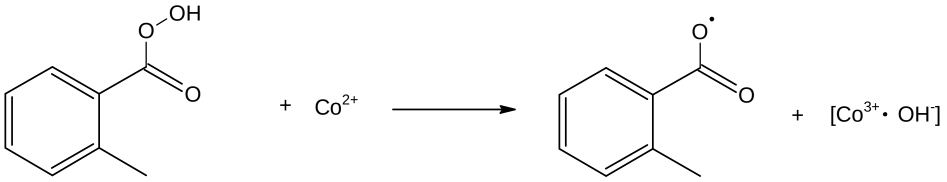

11.2 $R\text{-}H + [Co^{3+}\cdot OH^{-}] \longrightarrow R\bullet + Co^{2+} + H_2O$

The formation of 2-methylbenzyl alcohol can proceed via five possible pathways. Four of these routes proceed via the formation of 2-methylbenzyl hydroperoxide (reactions 1.0, 1.2 or 1.3 in combination with 2.0 and 3.0) followed by its thermal or catalytic decomposition (reactions 5.0 and 6.1, 5.1 and 6.1, 4.0 and 6.1 or 3.0 and 6.0). Alternatively, it can be formed from a benzylic radical by a recombination with an OH-radical (reaction 6.2). This OH-radical originates from the decomposition of a hydroperoxide.

For the formation of *o*-tolualdehyde three pathways are possible. One is the direct route starting from *o*-xylene, which proceeds via the dehydration of 2-methylbenzyl hydroperoxide (reaction 7.0). Alternatively *o*-tolualdehyde can be formed from 2-methylbenzyl alcohol as a consecutive product (reactions 7.1, 7.2) or from a 2-methylbenzyl alcohol pathway by the reaction with an alkoxy radical by delivering a hydrogen atom to a carbon based radical (reaction 7.2). The latter step is consuming radicals to a high degree and, therefore, the formation of *o*-tolualdehyde via this pathway has to be seen as highly radical annihilating. A certain initial radical concentration is necessary to propagate the radical chain. When the *o*-tolualdehyde fraction is too large the chain propagation is slowed down strongly because of the consumption of radicals that is necessary for its formation and further conversion and thus is observed as the first main product of the oxidation reaction.

Comparing the oxidation of *o*-tolualdehyde and 2-methylbenzyl alcohol (reactions 7.1, 7.2 and 8.0, 9.0, 8.1, 9.0 followed by 10.0, 11.0, 11.1 and 12.0), it appears unlikely that the oxidation of 2-methylbenzyl alcohol significantly contributes to the formation of *o*-toluic acid. No direct route from 2-methylbenzyl alcohol to *o*-toluic acid is available, because only one step oxidation reactions are observed in radical based mechanisms. This assumption is further supported by the increase in the selectivity towards *o*-toluic acid when *o*-tolualdehyde was added into the reactant. The formation rate of *o*-toluic acid is increased in both cases of intermediate addition although it is more pronounced when *o*-tolualdehyde is added. The presence of aldehydes in radical based reactions is known to shift the reaction pathways into the direction of per-acids, which subsequently react to the corresponding acid. Consequently, the formation of peracidic species, described in the reaction steps 9.0, 10.0, 11.x and 12.0, is enhanced in the case of higher concentration of *o*-tolualdehyde, which is the case at high conversion levels (or when it is directly added to the reactant). The addition of aldehyde first is accompanied by a reduction of the reaction rate because of a radical quenching by the formation of stable oxygen based radicals which do not support the radical chain propagation. A thermodynamic limitation can be excluded here because the equilibrium between aldehyde and acid is not reached yet as much higher *o*-tolualdehyde concentrations have been observed. Also an equilibrium between alcohol and aldehyde is not aspired by the system here otherwise the formation rate of *o*-toluic alcohol would be increased; but this is not observed. A combination of the further reaction of *o*-tolualdehyde and a lower formation rate due to the high degree of radical annihilation leads to a relative increase of 2-methylbenzyl alcohol. Consequently, the ratio of *o*-tolualdehyde to 2-methylbenzyl alcohol decreased with increasing conversion for any type of catalyst.

Within the reaction network the role of the initiator catalyst system is concluded to be a classical initiator for the formation of radical species. [5] The second function of the catalyst is to promote the decomposition of 2-methylbenzyl hydroperoxide to *o*-tolualdehyde and 2-methylbenzyl alcohol.

The ratio of *o*-tolualdehyde and 2-methylbenzyl alcohol starts at values of about 2.5 independent of the used catalyst system. This ratio decreases with increasing conversion until it stabilizes at conversions above 4 mol %. The initial decrease is explained by the further reaction of *o*-tolualdehyde to *o*-toluic acid with a higher rate than the reaction of 2-methylbenzyl hydroperoxide to *o*-tolualdehyde until a constant ratio is reached. The final ratio strongly depends on the transition metal in the catalyst. When Co^{2+} is used as active component the tendency to form *o*-tolualdehyde is increased compared to Mn^{3+} which enhances the formation of 2-methylbenzyl alcohol. This trend was also shown earlier for the selective oxidation of toluene and cyclohexanol. [4, 7]

The decomposition of the initially formed 2-methylbenzyl hydroperoxide over transition metal species to *o*-tolualdehyde and 2-methylbenzyl alcohol is described by the adsorption of the hydroperoxide to the transition metal center as already illustrated for the analogue reaction of *p*-xylene by Partenheimer. [22] This reaction (see Scheme 4-3) proceeds via the cleavage of the O-O bond assisted by the transition metal.

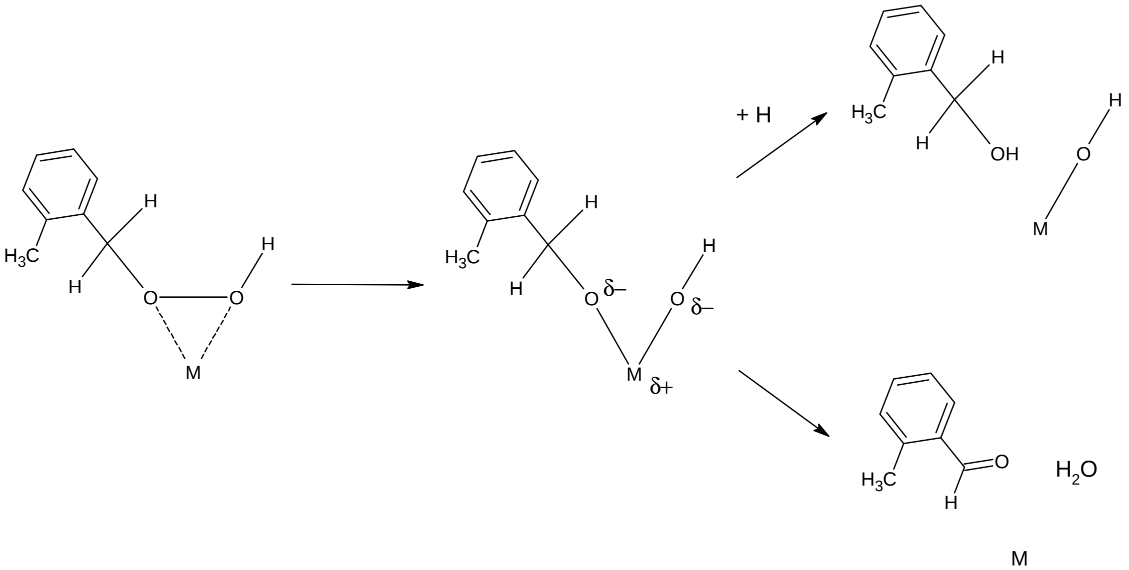

Scheme 4-3: Suggested mechanism for the transition metal catalyzed decomposition of 2-methylbenzyl hydroperoxide to *o*-tolualdehyde and 2-methylbenzyl hydroperoxide.

When 2-methylbenzyl hydroperoxide is bound to a transition metal cation the O-O is weakened and tends to decompose. The description of the decomposition by the Haber-

Weiss mechanism might be simplified too much to understand the different selectivities for different transition metal types. The decomposition leads to *o*-tolualdehyde or 2-methylbenzyl alcohol. If no catalyst is used the decomposition results in more alcohol than aldehyde (ratio aldehyde/alcohol is 0.7) as the radical based route proceeds via alkoxy radicals forming alcohol by H abstraction and thus maintaining the radical chain. The formation of *o*-tolualdehyde via the non transition metal catalyzed route is strongly radical annihilating resulting in a decreased formation rate of the aldehyde. The fact that Co^{2+} favors the formation of *o*-tolualdehyde is explained by the polarization of the intermediately formed metal oxygen bond. The low relative electronegativity of Co^{2+} leads to a very ionic bond character of the metal oxygen bond resulting in an increased electron density on the hydroxy oxygen. By abstracting a proton from the α-C-atom water can be liberated. The metal oxygen bond character is more covalent in the case of Mn^{3+} catalysis as its electronegativity is higher than Co^{2+} resulting in a lower difference in electronegativity of Mn^{3+} and oxygen. [23] The resulting lower negative partial charge of oxygen leads to a stabilization of the OH moiety which can be seen as a transition metal stabilized radical. The cleavage of the O-O bond therefore is homolytic and 2-methylbenzyl alcohol is the consecutive product via this pathway. Note that both routes of 2-methylbenzyl hydroperoxide decomposition occur for all transition metals. In agreement with earlier publications the use of Co^{2+} enhances the formation of the aldehyde species whereas Mn^{3+} increases the formation of 2-methylbenzyl alcohol.

The activity of the presented catalyst exceeds the TOF of the benchmark system Co naphthenate. The water adsorption capacity, and thus the hydrophilicity, of the polysiloxane material is lower compared to materials which were free of organic groups. This hydrophobicity of the polysiloxane surface might be the reason for the enhancement of the reaction rate. The tool of organic surface modification offers the possibility to decrease the adsorption behavior of polar reaction products accompanied by an increased reaction rate compared to materials without hydrophobic moieties. The general catalytic activity of transition metal containing polysiloxane catalysts was shown in the selective oxidation of other alkyl substituted aromatic substrates.

4.5. Conclusions

The presented results show the activity of transition metal containing polysiloxanes in the selective oxidation of methyl substituted aromatics under solvent free conditions. Their function of the active species is the initiation of the radical chain and the decomposition of the intermediately formed hydroperoxide. The activity of both, Co^{2+} and Mn^{3+}, was superior to the benchmark system Co naphthenate as the hydrophobicty of the polysiloxane material enhances the desorption of polar reaction products like *o*-toluic acid. The decomposition of the hydroperoxide depends on the type of transition metal whereas Co^{2+} enhanced the formation of *o*-tolualdehyde and Mn^{3+} increased the selectivity towards 2-methylbenzyl alcohol. The difference in selectivity is explained by the electronegativity difference of the two transition metals resulting in different partial charges at oxygen atoms and thus varying reactivities. The heterogeneous polysiloxane materials are stable under reaction conditions. No leaching of transition metal was observed and the accessibility of active species was not influenced by the oxidation reaction.

4.6. Acknowledgments

The authors thank the German Bundesministerium für Bildung und Forschung (BMBF) for partial financial support of the presented work (project no. 03X2007A). We are very grateful to Dipl. Ing. M. Neukamm for conducting AAS measurements, Dipl. Ing. X. Hecht for operational support and B. Sc. S. Pedron for experimental performance. Furthermore the authors acknowledge fruitful discussions in the framework of the network of excellence IDECAT.

4.7. References

[1] Q. B. Wang, X. Li, L. J. Wang, Y. W. Cheng, G. Me, *Ind. Eng. Chem. Res.* **2005**, *44*, 261-266; P. Raghavendrachar, S. Ramachandran, *Ind. Eng. Chem. Res.* **1992**, *31*, 453-462; Q. B. Wang, Y. W. Cheng, L. J. Wang, X. Li, *Ind. Eng. Chem. Res.* **2007**, *46*, 8980-8992; G. Cao, M. Pisu, M. Morbidelli, *Chemical Engineering Science* **1994**, *49*, 5775-5788.

[2] I. Hermans, E. S. Spier, U. Neuenschwander, N. Turra, A. Baiker, *Top. Catal.* **2009**, *52*, 1162-1174.

[3] A. K. Suresh, M. M. Sharma, T. Sridhar, *Ind. Eng. Chem. Res.* **2000**, *39*, 3958-3997; A. J. Hu, C. X. Lu, B. D. Li, *Progress in Chemistry* **2007**, *19*, 292-302.

[4] C. C. Guo, Q. Liu, X. T. Wang, H. Y. Hu, *Appl. Catal. A-Gen.* **2005**, *282*, 55-59.

[5] W. Partenheimer, *Catal. Today* **1995**, *23*, 69-158.

[6] R. A. Sheldon, J. K. Kochi, *Metal-Catalyzed Oxidations of Organic Compounds*, Academic Press, New York, **1981**; F. Haber, J. Weiss, *Naturwissenschaften* **1932**, *20*, 948-950.

[7] K. Blau, O. Kovacs, G. Lauterbach, M. Makhoul, W. Pritzkow, T. D. Tien, *Journal Fur Praktische Chemie* **1989**, *331*, 771-777.

[8] J. M. Thomas, R. Raja, *Chemical Communications* **2001**, 675-687; J. M. Thomas, R. Raja, G. Sankar, B. F. G. Johnson, D. W. Lewis, *Chem.-Eur. J.* **2001**, *7*, 2973-2978.

[9] R. Raja, J. M. Thomas, V. Dreyer, *Catal. Lett.* **2006**, *110*, 179-183; R. Raja, J. M. Thomas, *Solid State Sci.* **2006**, *8*, 326-331.

[10] B. Moden, B. Z. Zhan, J. Dakka, J. G. Santiesteban, E. Iglesia, *J. Catal.* **2006**, *239*, 390-401.

[11] B. Z. Zhan, B. Moden, J. Dakka, J. G. Santiesteban, E. Iglesia, *J. Catal.* **2007**, *245*, 316-325; B. Moden, L. Oliviero, J. Dakka, J. G. Santiesteban, E. Iglesia, *Journal of Physical Chemistry B* **2004**, *108*, 5552-5563.

[12] A. Ramanathan, M. S. Hamdy, R. Parton, T. Maschmeyer, J. C. Jansen, U. Hanefeld, *Appl. Catal. A-Gen.* **2009**, *355*, 78-82.

[13] G. C. Bond, *J. Chem. Technol. Biotechnol.* **1997**, *68*, 6-13; M. S. Wainwright, N. R. Foster, *Catal. Rev.-Sci. Eng.* **1979**, *19*, 211-292; V. Nikolov, D. Klissurski, A. Anastasov, *Catal. Rev.-Sci. Eng.* **1991**, *33*, 319-374.

[14] B. GrzybowskaSwierkosz, *Appl. Catal. A-Gen.* **1997**, *157*, 263-310.

[15] F. Rainone, L. Kiwi-Minsker, D. A. Bulushev, P. A. Buffat, A. Renken, *Appl. Catal. A-Gen.* **2003**, *244*, 251-263; F. Cavani, F. Trifiro, *Appl. Catal. A-Gen.* **1997**, *157*, 195-221; Y. I. Pyatnitsky, N. I. Ilchenko, *Catal. Today* **1996**, *32*, 21-28; G. C. Bond, *J. Catal.* **1989**, *116*, 531-539.

[16] SISAS, **1989**.

[17] T. Förster, S. A. Schunk, A. Jentys, J. A. Lercher, *Chem. Commun..* **2010**, submitted for publication.

[18] H. Witossek, E. Bratz, *Chem. Eng. Technol.* **1997**, *20*, 429-433; E. Yacoubgeorge, E. Bratz, H. Tiltscher, *J. Non-Cryst. Solids* **1994**, *167*, 9-15.

[19] T. Förster, S. Scholz, Y. Zhu, J. A. Lercher, *Microporous and Mesoporous Materials* **2010**, submitted for publication.

[20] G. B. Shulpin, D. Attanasio, L. Suber, *J. Catal.* **1993**, *142*, 147-152.

[21] S. K. Bhargava, D. B. Akolekar, *Journal Of Colloid And Interface Science* **2005**, *281*, 171-178.

[22] W. Partenheimer, *J. Mol. Catal. A-Chem.* **2003**, *206*, 105-119; W. Partenheimer, *J. Mol. Catal. A-Chem.* **2003**, *206*, 131-144.

[23] R. G. Pearson, *Abstracts of Papers of the American Chemical Society* **1986**, *192*, 157.

Chapter 5

Investigation of the kinetic description of the selective liquid phase oxidation of *o*-xylene

The detailed kinetic description of the liquid phase oxidation of o-xylene under solvent free conditions over polysiloxane supported Co or Mn catalysts revealed two pathways, a direct oxidation by the transition metal and an autocatalytic route for the initiation of the reaction leading to the primary product 2-methylbenzyl hydroperoxide. Both transition metals enhance the formation as well as the decomposition of the hydroperoxide. The simulation indicated furthermore that the formation of o-toluic acid only proceeds via oxidation of o-tolualdeyhde and was barely affected by the transition metal. The main effects of the catalyst are the formation and the decomposition of the intermediate hydroperoxide.

5.1. Introduction

The selective oxidation of alkyl substituted aromatics is an intensively studied area in the field of catalysis. [1] Due to the large potential of carboxylic acids in polymer chemistry, an intensive effort was spent to gain knowledge of the processes occurring during the controlled (side chain) oxidation reaction of toluene and the xylene isomers. [2] Stoichiometric oxidizing compounds, like peroxides or acids, which were used in earlier times, are currently replaced by environmentally friendly compounds with the goal of using molecular oxygen from air due to its ubiquitary availability.

The mechanism of the liquid phase oxidation of alkyl aromatics is described with a catalyst modified free radical chain mechanism consisting of initiation, propagation and termination. [3] In the initiation step benzylic radicals are formed and oxygen is introduced during the propagation by the formation of peroxy radicals, which react to peroxides by hydrogen abstraction from further alkyl groups of the aromatics. The termination is caused by the recombination of radicals. The primary formed peroxides tend to decompose slowly into hydroxy radicals and a carboxy radical at temperatures above 323 K. [3]

Kinetic studies of selective liquid phase oxidation reactions of alkyl substituted aromatics mainly focus on the description of homogeneous initiator systems. The oxidation of *p*-xylene was studied by Sun *et al.* in a liquid phase process using cobalt, manganese and bromine sources. [4] In this work the number of fitting parameters was kept as low as possible by assuming equal reactivities of all occurring peroxy radicals in terms of H abstraction and termination behaviour. Reaction steps containing radicals were neglected in the kinetic model.

Hoorn *et al.* proposed an extended model for the selective oxidation of toluene proceeding via peroxides and peroxy radicals. [5] The reactive radical intermediates were eliminated in the calculation by assuming a steady state for the radical concentration. Based on this work the oxidation of toluene to benzoic acid in a liquid phase reaction under batch conditions by using a cobalt stearate catalyst system was illustrated by Gizli *et al.*, [6] who compared three different reaction networks. They proposed that the description by the formation of benzyl radicals was supposed to be the most reasonable. In the postulated reaction network the intermediates benzyl alcohol and benzaldehyde are formulated but were not observed in notable quantities in the reaction mixtures and thus a simplification of the calculations was introduced.

We recently reported the function of transition metal containing hydrophobic polysiloxane catalysts in the selective oxidation of *o*-xylene. [23] The reaction was described to proceed via the formation of 2-methylbenzyl hydroperoxide as primary reaction product. Besides an acceleration of the reaction initiation, i.e. formation of hydroperoxide, the catalysts were shown to effectively decompose the hydroperoxide into the consecutive products *o*-tolualdehyde and 2-methylbenzyl alcohol. The final product observed was *o*-toluic acid formed by an oxidation of *o*-tolualdehyde, while a direct oxidation of 2-methylbenzyl alcohol to the acid was not observed.

Based on the reaction pathways postulated we developed a kinetic description for the reaction network of the selective liquid phase oxidation of *o*-xylene under solvent free conditions in this work. The catalysts applied were cobalt or manganese containing polysiloxane materials.

5.2. Experimental

5.2.1. Catalysts

The catalysts were prepared by a special method that allows the direct synthesis of spherical polysiloxane with the incorporation of the catalytically active transition metal.[7] A mixture of hydrolysable silane precursors and a transition metal source was injected into a water filled column. By the formation of stable droplets the spherical character of the resulting solid is assured. The synthesis procedure was performed at 333 K and dibutyltin dilaurate was added to the mixture as an accelerating component. The precursor compounds were tetraethyl orthosilicate (TEOS, >99%) and 3-aminopropyl-trimethoxysilane (APTMS, >97%) which were used in a ratio of 2 : 1. The transition metal was incorporated into the catalyst by the respective transition metal acetyl acetonate to the mixture. The resulting bead like materials were aged in water for 12 h at ambient temperature and washed with deionized water and *i*-propanol before they were dried by freeze drying.

The metal concentration was determined by atomic absorption spectroscopy (AAS) using a UNICAM Solaar M5 Spectrometer. Typically, 30-60 mg of the sample was dissolved in 0.5 ml of hydrofluoric acid (10%) at its boiling point (about 383 K).

5.2.2. Liquid phase oxidation of *o*-xylene

The liquid phase oxidation experiments of *o*-xylene were carried out in a bubble column reactor consisting of a 10 mm i.d. glass tube. The reactant (6 ml) and the catalyst (100 mg) were filled into the reactor without adding a solvent. For all experiments a pressure of 2.4 bar was used to prevent the liquid from foaming. To form small bubbles the gas was directed through a glass frit with openings of 2 µm. The reactor was divided into two zones, one heated to 445 K where the reaction was carried out followed by a zone cooled to 293 K in order to lower the partial pressure of the reactants and products. To prevent the discharge of the reactant via the gas phase leaving the reactor the inlet gas stream was saturated with reactant at 293 K, i.e. the same temperature as the gas stream leaving the reactor. After heating the reactant to the reaction temperature under nitrogen flow the reaction was started by adding a flow of synthetic air (50%) in nitrogen. The waste gas from the reactor was lead through a 0.1 M NaOH solution to determine the integral amount of CO_2 formed during the reaction by titration with hydrochloric acid.

During the reaction liquid samples were collected from the reactor by a syringe inserted from the top of the reactor. Hexachlorobenzene was used as internal standard. To quantify the concentration of each component in the reaction mixture a Shimadzu GC-2010 gas chromatograph equipped with a 30 m DB-5 column (0.25 mm inner diameter and 0.25 µm film thickness) and a FID detector was used. Tetradecane was added to each analyzed sample as internal GC standard. The concentration of 2-methylbenzyl hydroperoxide was determined by the procedure described by Shul´pin *et al.* [8] and in reference [9].

5.2.3. Simulation of kinetic equations

To calculate reaction rate constants (k) for the individual steps in the supposed reaction network the respective differential equations were solved using a 4th order Runge Kutta algorithm implemented in Berkeley Madonna.

5.2.4. Diffuse reflectance UV/Vis spectroscopy

To analyze the deposits formed on the catalyst surface during the reaction the materials were characterized by diffuse reflectance UV/Vis spectroscopy using an Anvantes AvaSpec-2048 spectrometer at ambient conditions. For spectra of used catalysts the samples were applied under reaction conditions at 445 K for 3 h and were removed from the reactant before the measurements. The reflectance R was normalized to polysiloxane samples without transition metals by the Kubelka Munk function $f(R) = (R-1)^2/2R$.

5.3. Results

5.3.1. Catalyst characterization

The chemical composition of the cobalt and manganese containing polysiloxane catalysts was analyzed by AAS and elemental analysis. The results are summarized in Table 5-1. For the synthesis TEOS and APTMS were used in a ratio of 2 : 1. The diameter of the spherical catalysts was 800 µm. The synthesized catalysts were freeze dried after the synthesis and directly used in the oxidation reaction without further treatment.

Table 5-1: Chemical composition of the Co and Mn containing catalysts.

Sample name	Metal loading (wt. %)	C content (wt. %)	Si content (wt. %)	N content (wt. %)	H content (wt. %)
Co-1.9	1.9	8.0	25.7	2.2	3.0
Mn-2.0	2.0	14.3	31.5	3.1	3.7

Catalysts loaded with Cobalt or Manganese were synthesized with metal concentrations of 2 wt. % each.

5.3.2. Thermal decomposition of the hydroperoxide

The primary product of the selective *o*-xylene oxidation under the applied conditions is 2-methylbenzyl hydroperoxide. As it is the only radical like species which can be detected on a macroscopic scale its quantification is crucial. Because of the low thermal stability, however, its concentration can not be determined directly via GC analysis as it will decompose thermally to 2-methylbenzyl alcohol and *o*-tolualdehyde already at temperatures around 473 K. To determine the ratio of 2-methylbenzyl hydroperoxide a solution containing 1 mol % 2-methylbenzyl hydroperoxide in *o*-xylene was prepared by oxidizing *o*-xylene at 398 K with synthetic air for 12 h. [10] Under these mild conditions only minor concentrations of 2-methylbenzyl alcohol and *o*-tolualdehyde were formed.

By ^{1}H-NMR spectroscopy of the solution their concentrations were determined. A ratio of 7:1 between *o*-tolualdehyde and 2-methylbenzyl alcohol, formed by the thermal decomposition of 2-methylbenzyl hydroperoxide in the GC inlet system was determined.

For the analysis of the liquid samples taken from the reactor each sample was divided into two parts. One was reduced with triphenyl phosphine to the alcohol (see Scheme 5-1) before each analysis.

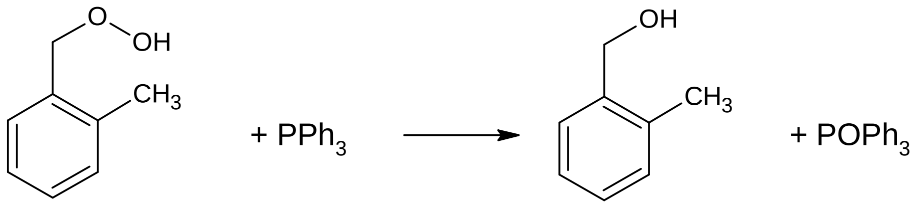

Scheme 5-1: Reduction of the 2-methylbenzyl hydroperoxide to 2-methylbenzyl alcohol by PPh_3.

A fraction was analyzed directly without any pretreatment. By using the thermal decomposition ratio of 2-methylbenzyl hydroperoxide, the concentrations of 2-methylbenzyl alcohol, *o*-tolualdehyde and 2-methylbenzyl hydroperoxide in the liquid samples were determined.

5.3.3. Oxidation of *o*-xylene with transition metal containing catalyst

The conversion of *o*-xylene was studied at 445 K and a total pressure of 2.4 bar. In all reactions an induction period was observed. Its duration was found to depend on the activity of the transition metal applied as catalysts.

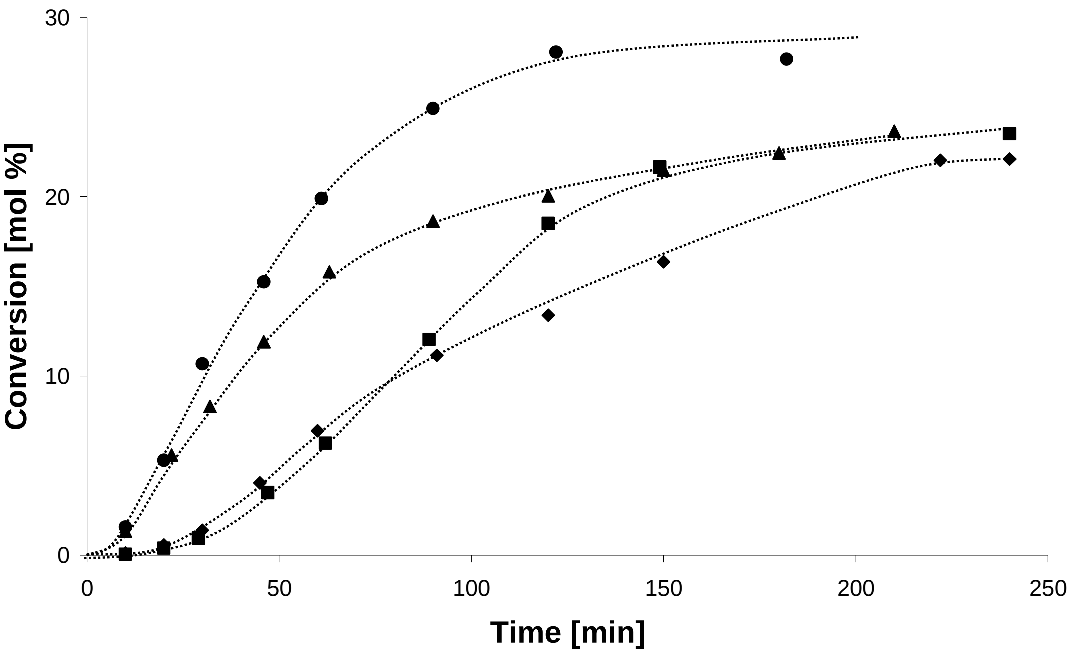

Figure 5-1: Conversion of *o*-xylene in dependence of the reaction time for different catalysts: Co-1.9 (♦), Mn-2.0 (■), Mn(III) acetyl acetonate (▲) and Co(II) acetyl acetonate (●) (reaction conditions: 445 K, total pressure 2.4 bar).

Figure 5-1 shows the conversion of *o*-xylene in dependence of the reaction time for heterogeneous cobalt and manganese polysiloxane catalysts compared to homogeneous acetyl acetonate systems. The sigmoid shapes of the conversion plots observed are typical for radical based reactions. In the starting phase the conversion increases slowly until a certain point (ca. 2 mol % conversion) is reached. This induction period is a characteristic for radical chain reactions because a certain concentration of radicals is necessary to reach a sufficient overall reaction rate. This feature is more pronounced for the examined heterogeneous systems compared to the solved (homogeneous) systems. The duration of this induction phase was shown to linearly depend on the concentration of cobalt in the catalyst. [9] After this initiation phase the conversion increases to a level of about 20 mol % before the rate drops down. The polysiloxane based catalysts show a longer induction period because the transition metal concentration is lower compared to the homogeneous analogues.

Upon the tested transition metals were cobalt, manganese, copper and vanadium. All show activity in the selective oxidation of *o*-xylene. The most promising activity was observed when cobalt or manganese containing catalysts were employed, therefore, the further studies focussed on these two transition metals.

Typically the selectivity to oxygenates produced from of *o*-xylene lead to product distributions as displayed in Figure 5-2. Firstly 2-methylbenzyl hydroperoxide, 2-methylbenzyl alcohol and *o*-tolualdehyde were formed. The selectivity towards *o*-toluic acid only increases when the conversion exceeds 3 mol %. 2-methylbenzyl hydroperoxide, 2-methylbenzyl alcohol and *o*-tolualdehyde were formed as primary reaction products. This is indicated by the positive initial slopes of their yield curves, while *o*-toluic acid was formed as a secondary reaction product.

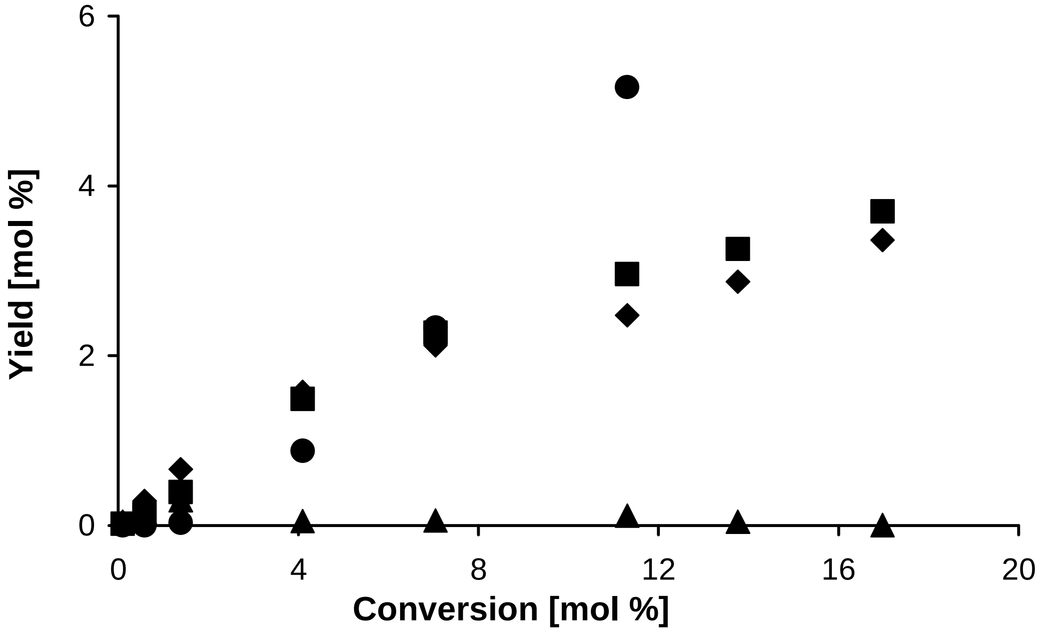

Figure 5-2: Yields of *o*-tolualdehyde (♦), 2-methylbenzyl alcohol (■), 2-methylbenzyl hydroperoxide (▲) and *o*-toluic acid (●) as function of the *o*-xylene conversion (reaction conditions: 445 K, 100 mg 1.9 wt. % Co catalyst, total pressure 2.4 bar).

In the case of Co catalysis a more pronounced tendency for the formation of *o*-tolualdehyde was observed whereas Mn tended to form more 2-methylbenzyl alcohol. Besides the mentioned main products phthalide and further oxygenates such as *o*-xylene dimers, an ester of *o*-toluic acid and 2-methylbenzyl alcohol, formiates of 2-methylbenzyl alcohol, toluene and phthalic anhydride were formed. The formation of total oxidation product CO_2 was detected in integral yields of maximum 0.5 mol % in all conducted experiments and thus was neglected for any further interpretation.

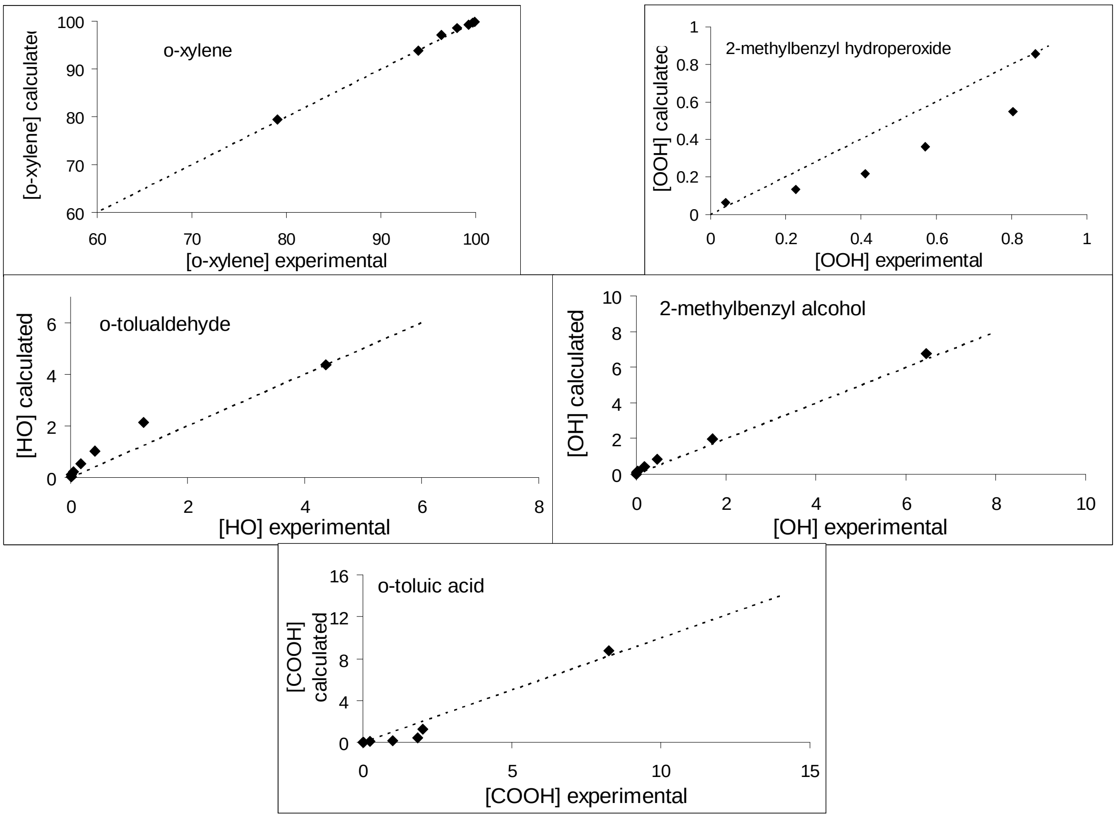

Figure 5-3: Correlation of experimental concentrations and calculated concentrations by simulation when no catalyst was used at 445 K.

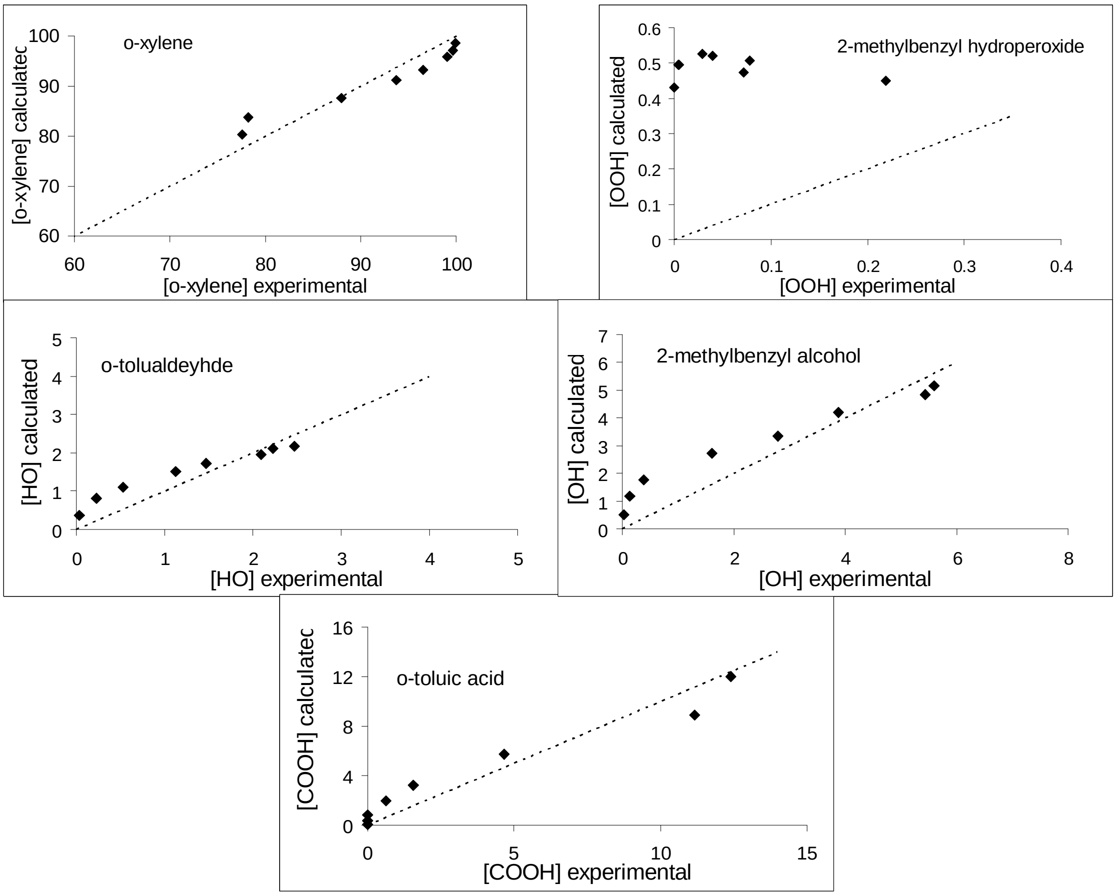

Figure 5-4: Correlation of experimental concentrations and calculated concentrations by simulation for the Mn-2.0 catalyst at 445 K.

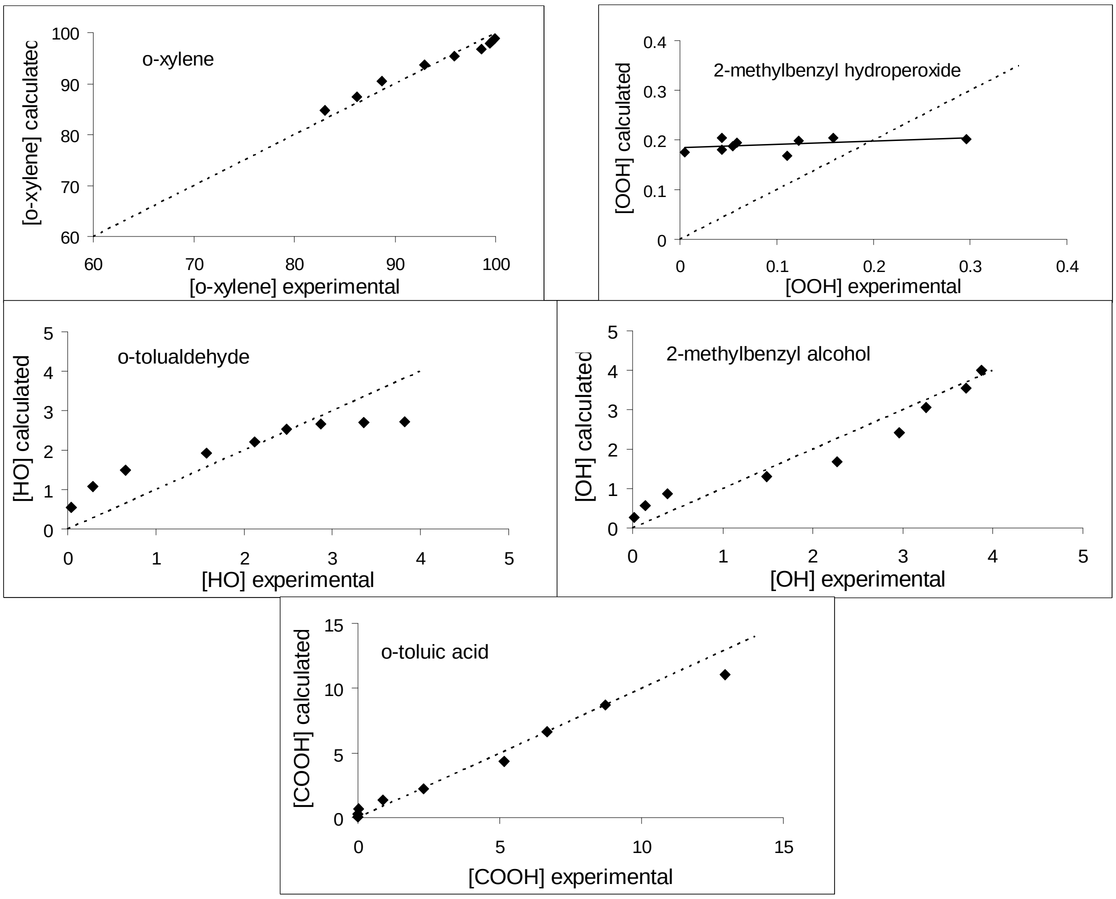

Figure 5-5: Correlation of experimental concentrations and calculated concentrations by simulation for the Co-1.9 catalyst at 445 K.

The parity plots (Figure 5-3, Figure 5-4 and Figure 5-5) show that the concentrations of *o*-xylene, *o*-tolualdehyde, 2-methylbenzyl alcohol and *o*-toluic acid are simulated in good agreement to the experimental data. The radical representing 2-methylbenzyl hydroperoxide is not fitting perfectly with the experimental data but only the trend is in agreement. This phenomenon is observed more pronounced the higher the reaction temperature was. At temperatures below 445 K the profile of the experimental and simulated 2-methylbenzyl hydroperoxide are satisfactory similar.

5.3.4. Analysis of surface species

The color of Co containing catalysts changes from blue to grayish blue after drying because of the deposition of reaction products. To study the residual oxidation products on the catalyst surface samples of used catalysts were investigated by diffuse reflectance UV/Vis spectroscopy.

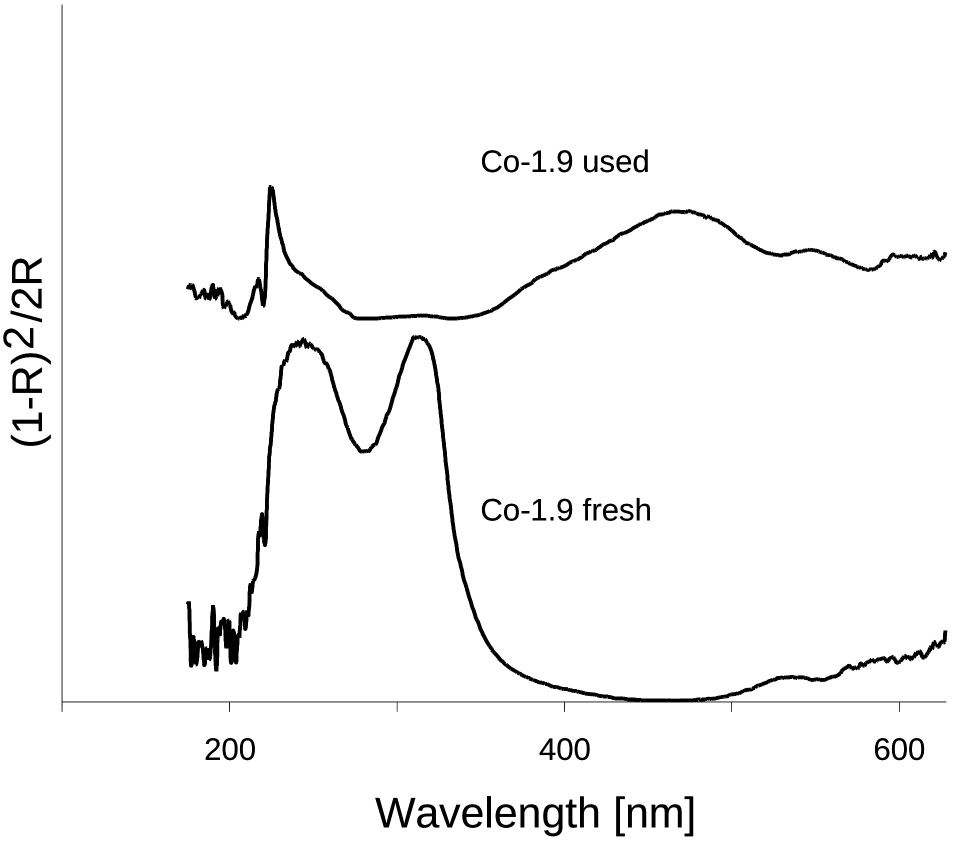

Figure 5-6: Diffuse reflectance UV/Vis spectra of fresh and used cobalt containing catalysts. The used catalysts were gained from the reactor after different reaction times.

From the spectra (see Figure 5-6) it can be seen that the two bands at 245 and 315 nm which correspond to Co^{2+} are still present but are less intensive after the reaction. [11] This is due to the presence of aromatic deposits on the catalyst surface. The peak at 225 nm and the broad band in the range of 360 to 550 nm correspond to the deposits which are colored yellow on the catalyst surface during the *o*-xylene oxidation reaction.

An accumulation of reaction products on the surface of the spheres was observed. In our earlier work we showed that CO adsorbs to transition metal in the polysiloxane support. When catalysts were investigated after their use in the oxidation reaction no CO adsorption was observed when the materials were only dried before adsorption. Additionally, the presence of carbonate bands proved that *o*-toluic acid covered the transition metal. The coverage was reversible as the transition metals were accessible for CO when they were washed with *o*-xylene before CO adsorption. The deposit on the surface of the employed cobalt catalysts used at 445 K was analyzed at conversions of 3.5 mol % and 15 mol %. For this purpose the reaction was stopped and the deposit was extracted from the catalyst's surface in acetone under stirring followed by GC analysis of the resulting solution. An overview of the composition of the precipitate is displayed in Figure 5-7.

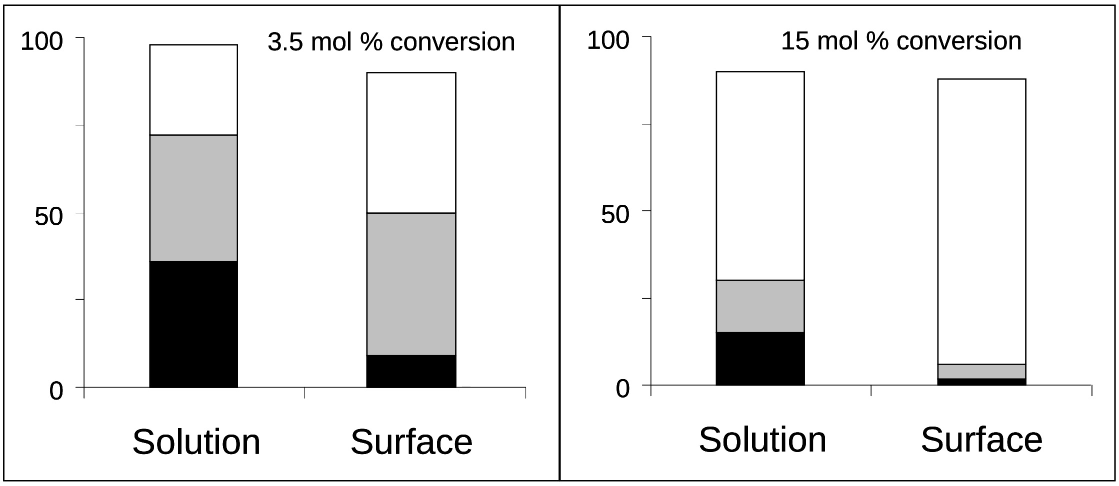

Figure 5-7: Selectivities towards the oxygenates *o*-tolualdehyde (black), 2-methylbenzyl alcohol (grey) and *o*-toluic acid (white) in the reaction solution compared to the catalyst surface at conversion levels of 3.5 and 15 mol % respectively (reaction conditions: 445 K, 100 mg Co-1.9 catalyst, 10% O_2).

The composition of the deposit shows that the largest fraction was *o*-toluic acid. The balance to 100% is made by phthalide and the ester of *o*-toluic acid and 2-methylbenzyl alcohol. Compared to the composition of the reaction mixture in the liquid phase it can be observed that the concentrations of oxygenates on the catalyst surface is different. On the surface a pronounced agglomeration of *o*-toluic acid was observed, i.e. the selectivity in the liquid phase and in the surface residue was increased from 26 to 40 mol% at

3.5 mol % conversion and even from 60 to 82 mol % at 15 mol % conversion. In contrast the concentrations of *o*-tolualdehyde and 2-methylbenzyl alcohol were decreased compared to the selectivity in the reaction mixture.

5.3.5. Temperature dependence of the oxidation reaction

To determine the influence of the reaction temperature on the rate of reaction when cobalt or manganese catalysts were applied the temperature was varied at a total pressure of 2.4 bar.

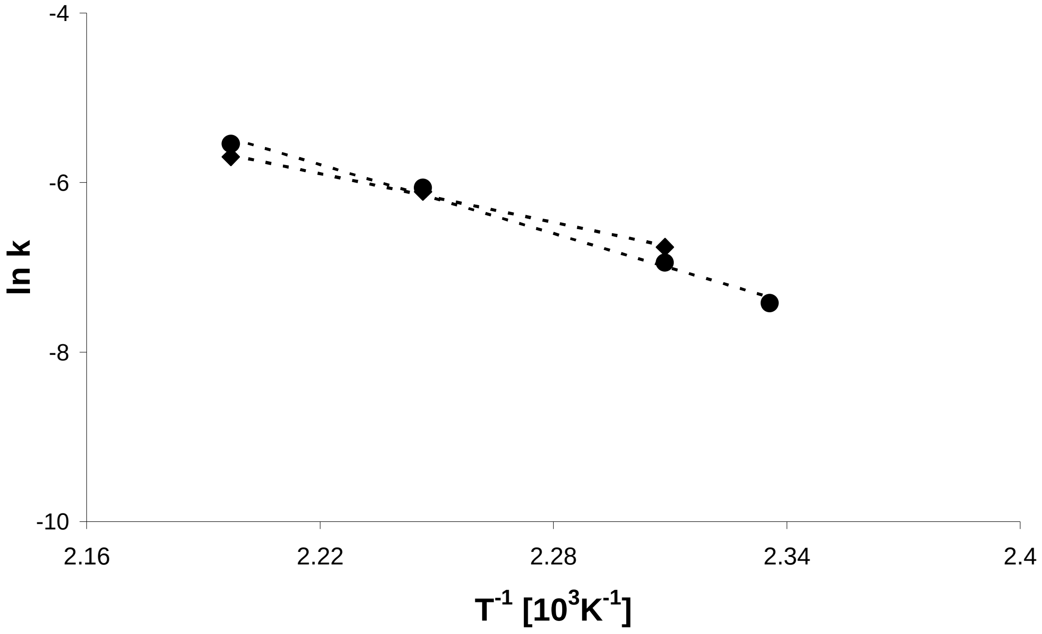

Figure 5-8: Arrhenius plot for the Co-1.9 catalyst (●) and Mn-2.0 (♦). The reaction conditions were 445 K, 100 mg catalyst, 10% O_2.

The activation energy derived from the slope in the Arrhenius plot for the use of Cobalt was determined to 112 kJ/mol. In the case of Manganese the activation energy was 80 kJ/mol.

5.3.6. Selectivities of different catalyst systems

To compare the resulting selectivity towards each oxygenate the yields of the components were compared at levels of equal *o*-xylene conversion for different catalysts. The reaction temperature was constant at 445 K and further reaction parameters were remained constant. The selectivities in Table 5-2 are reached at *o*-xylene conversion of 5 mol %.

Table 5-2: Oxygenate selectivity at 5 mol % conversion of *o*-xylene for applied transition metal catalysts (reaction conditions: 445 K, 10% O_2).

	Co-1.9	$Co(acac)_2$	Mn-2.0	$Mn(acac)_3$
o-tolualdehyde	35	39	28	30
2-methylbenzyl alcohol	35	27	40	42
2-methylbenzyl hydroperoxide	2	2	2	1
o-toluic acid	26	21	26	26

It can be seen that the manganese catalysts shift the selectivity in the direction of 2-methylbenzyl alcohol. Compared to the manganese systems the cobalt catalysts enhance the formation of *o*-tolualdehyde.

5.3.7. Kinetic analysis of the reaction network of the selective *o*-xylene oxidation

Based on the interpretation of the selectivity towards detected products a reaction network for the selective oxidation of *o*-xylene was deduced which is displayed in the scheme shown in Figure 5-9.

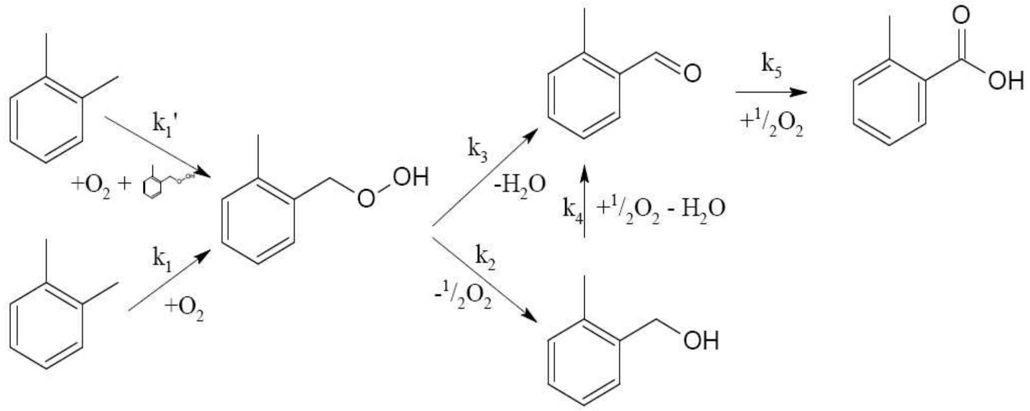

Figure 5-9: Proposed reaction network for the oxidation of *o*-xylene.

The first step in the oxidation reaction is the formation of radicals leading to 2-methylbenzyl hydroperoxide (k_1 and k_1'), the only radical like species that could be quantified during the reaction. Its formation is described by two routes to be able to implement the autocatalytic character of the radical based reaction step. From the hydroperoxide two pathways are possible. One route is the formation of *o*-tolualdehyde directly from the hydroperoxide (k_3). Alternatively the reaction to 2-methylbenzyl alcohol is feasible (k_2), which itself can be further oxidized to the aldehyde (k_4). The formation of *o*-toluic acid is supposed to proceed only via *o*-tolualdehyde (k_5).

Mathematically the reaction network is described by the following differential equation ((1)-(5)):

$$\frac{d(ox)}{dt} = -k_1[o-xylene] - k_1'[o-xylene] \qquad (1)$$

$$\frac{d(OOH)}{dt} = -k_1'[o-xylene][OOH] + k_1[o-xylene] - k_2[OOH] - k_3[OOH] \qquad (2)$$

$$\frac{d(OH)}{dt} = k_2[OOH] - k_4[OH] \qquad (3)$$

$$\frac{d(HO)}{dt} = k_3[OOH] + k_4[OH] - k_5[HO] \qquad (4)$$

$$\frac{d(COOH)}{dt} = k_5[HO] \tag{5}$$

The rate constants were determined by solving the differential equations (1) to (5) by numerical simulations. An overview of the received rate constants is presented in Table 5-3. The transition metal containing polysiloxane catalysts were compared to their homogeneously solved counterparts.

Table 5-3: Calculated k values for different catalysts (reaction conditions: 445 K, total pressure 2.4 bar).

	k_1 [min^{-1}]	k_1'[min^{-1} mol%$^{-1}$]	k_2 [min^{-1}]	k_3 [min^{-1}]	k_4 [min^{-1}]	k_5 [min^{-1}]
No catalyst	0.0004	0.0002	0.0140	0.0219	0.0006	0.0193
Co-1.9	0.0005	0.0001	0.1591	0.3688	0.0033	0.0280
Co(acac)$_2$	0.0001	0.0003	0.2563	0.6000	0.0074	0.0840
Mn-2.0	0.0002	0.0001	0.1511	0.1242	0.0110	0.0500
Mn(acac)$_3$	0.0009	0.0009	0.2347	0.1203	0.0200	0.0387

The formation of 2-methylbenzyl hydroperoxide (the sum of k_1 and k_1') was increased over both supported transition metal systems compared to the uncatalyzed reference. A particular trend of an acceleration of one of the two initiation pathways was not observed. It is notable that for both types of transition metal the decomposition of 2-methylbenzyl hydroperoxide was accelerated (k_2 and k_3). The favored product in the case of manganese was 2-methylbenzyl alcohol which results in a higher ratio of k_2 and k_3. The further oxidation of the alcohol to *o*-tolualdehyde was also increased by the manganese system. Both types of transition metal accelerated the oxidation of *o*-tolualdehyde to *o*-toluic acid as it can be seen in k_5. The effect on this was minor compared to the acceleration of the decomposition of the hydroperoxide.

5.4. Discussion

The detailed analysis of the oxidation products confirms the assumption of a radical chain mechanism. The presence of an induction period is typical for autocatalytic radical chain reactions supports. As evidence 2-methylbenzyl hydroperoxide which is the only radical analogue compound that can be detected under the applied conditions was quantified and included in the reaction network in difference to current literature. Although the concentrations of the hydroperoxide species can not be described very accurately by the simulated network the trend is in good agreement with the determined concentrations.

The reason for the discrepancy of the simulated and experimentally determined concentrations of 2-methylbenzyl hydroperoxide can be explained by the very low concentration of this species compared to those of the consecutive products which causes a relatively low weight during the iteration of mathematical simulations leading to wrong absolute concentrations. Furthermore determination of its concentration is performed by an indirect method. This may cause an error in the absolute hydroperoxide concentration. The actual hydroperoxide concentration might be higher as the determined. Additionally, the stability of this species is relatively low compared to the other occurring compounds. This may also cause an error in the determination of the concentration because a certain fraction might already be decomposed when the determination of the concentration is performed. A further explanation is the presence of alternative reaction pathways of the hydroperoxide decomposition. These can include the direct reaction with formed oxygenates in a product catalyzed decomposition. The reaction products would certainly be *o*-xylene or other stable radical based products which can not be determined. The introduction of further reaction pathways and thus fitting parameters could solve this problem but would result in a large number of parameters and an over parameterization is very likely.

Radical reactions are often autocatalytic, i.e., the reaction rate increases when a sufficient concentration of radicals is formed. For the calculation of the rate constants for the oxidation from *o*-xylene to 2-methylbenzyl alcohol two pathways, an autocatalytic

(k_1') and a catalytic route (k_1) were included. The second reaction pathway, the direct formation of radicals from *o*-xylene via a catalytic reaction (k_1), was included as for autocatalytic reactions an initial level of radicals is necessary to start and to describe the direct formation of radicals by interaction with the catalyst. 2-methylbenzyl hydroperoxide can react to *o*-tolualdehyde via dehydration (k_3) and to 2-methylbenzyl alcohol via the decomposition of 2-methylbenzyl hydroperoxide (k_2). The alcohol can be further oxidized to *o*-tolualdehyde (k_4), whereas a direct route to *o*-toluic acid from 2-methylbenzyl alcohol is not reasonable under the examined radical conditions. Consequently, the only pathway leading to *o*-toluic acid is the oxidation of *o*-tolualdehyde (k_5). The balance of the radicals supports this suggestion as there is no direct path from 2-methylbenzyl alcohol to *o*-toluic acid.

Differences in selectivities between cobalt and manganese catalysis towards the decomposition products of 2-methylbenzyl hydroperoxide were shown to depend on the differences in the electronegativity. [9, 12] In general, manganese enhanced the formation of 2-methylbenzyl alcohol, whereas cobalt increased of the decomposition of 2-methylbenzyl hydroperoxide to *o*-tolualdehyde. This trend was confirmed by the analysis of the kinetics. In the case of Co^{2+} catalysis increased values for k_3 were determined compared to k_2. The trend was the opposite when Mn^{3+} was applied. Here k_2 was higher than k_3 corresponding to an enhanced formation of 2-methylbenzyl alcohol.

Both transition metals have in common that the oxidation step from 2-methylbenzyl alcohol to *o*-tolualdehyde was accelerated in comparison to the uncatalyzed reaction; in contrast in the uncatalyzed reaction the thermal decomposition of the 2-methylbenzyl hydroperoxide favored the direct formation of *o*-tolualdehyde, which reacts further to *o*-toluic acid. The oxidation of 2-methylbenzyl alcohol to *o*-tolualdehyde only occurs with a very low reaction rate in the case of the uncatalyzed reaction. This effect is more pronounced for Mn catalysis. When Co is used the decomposition already results in a higher concentration of *o*-tolualdehyde and the further oxidation of 2-methylbenzyl alcohol does not need to be fast.

The rate constant of the further oxidation of *o*-tolualdehyde to *o*-toluic acid was not significantly increased by the heterogeneous Co catalysts, while manganese enhanced the oxidation of *o*-tolualdehyde to *o*-toluic acid. This is an additional explanation for the low *o*-tolualdehyde to 2-methylbenzyl alcohol ratio reached with Mn^{3+}. The function of Co was mainly described as accelerating the initiation of the radical reaction and the decomposition of hydroperoxide species. [13] This was also observed here. Under industrial conditions an addition of Br sources increases the activity of the catalysts to enhance the oxidation to the acid.

The k values of the decomposition of 2-methylbenzyl hydroperoxide are two orders of magnitude higher than those for the formation of the hydroperoxide. This is in agreement with the observation of the initial formation of reaction products. It is observed that *o*-tolualdehyde and 2-methylbenzyl alcohol are formed from the beginning of the reaction although they are considered to be consecutive products. As the concentration of their reactant 2-methylbenzyl hydroperoxide is much smaller than the starting molecule of the 2-methylbenzyl hydroperoxide formation and the reaction rate is in the same order of magnitude the k values have to be significantly higher. It also should be mentioned that the rate constants of the decomposition are orders of magnitude higher than for the formation of 2-methylbenzyl hydroperoxide and thus the local concentration of the hydroperoxide can not be described by the reaction network perfectly.

When the conversion reaches a certain level (depending on the applied type of catalyst) a decrease in reaction rate is observed. In principle two explanations for this observation can be proposed. One is the blockage of the active sites of the catalyst. It was shown that this is not the case here. UV/Vis analysis and investigations of the deposits showed that oxygenates are accumulated on the catalyst surface and the biggest fraction is *o*-toluic acid. This forms carboxylates with the transition metal of the catalyst, as seen in IR, and decreases its accessibility; no CO could be adsorbed to the transition metal. But this feature only occurs if the materials are dried after reaction and prior to IR experiments. After washing in *o*-xylene which simulates the reaction procedure at least at low conversions very good all oxygenates are washed from the catalyst. No carboxylates were observed and CO was adsorbed to the transition metal. A reduction of the transition metal's accessibility can thus be neglected.

The second possibility which seems to be more likely here is the presence of oxygen containing organic compounds. In contact with radicals they are supposed to form more stable oxygen based radicals which by this hinder the propagation of the radical chain. Also a formation of oxygenates might lead to an annihilation of radicals reducing their concentration and so the reaction rate.

5.5.Conclusions

By fitting the concentration time dependence of reaction intermediates during the selective oxidation of *o*-xylene the rate constants for each reaction step of the reaction network was determined. Calculations proved that the model introduced earlier is correct and strengthened the observed selectivities. By assuming two pathways of the initial hydroperoxide formation the typical sigmoid conversion shapes could be described. The radical intermediate 2-methylbenzyl hydroperoxide could not be described very accurately because of its low concentration and rapid decomposition by the catalysts.

The means of simulating kinetic data offers an opportunity to understand the principle reactions occurring during the selective liquid phase oxidation of *o*-xylene. It could be shown that Mn^{3+} enhances the decomposition of the hydroperoxide to the alcohol but also increases the rate constant of its further oxidation to aldehyde.

5.6.Acknowledgments

The authors thank the German Bundesministerium für Bildung und Forschung (BMBF) for partial financial support of the presented work (project number 03X2007A). We are grateful to Dipl. Ing. M. Neukamm for conducting AAS measurements Dipl. Ing. X. Hecht for operational support and B. Sc. S. Pedron for experimental performance. Furthermore the authors acknowledge fruitful discussions in the framework of the network of excellence IDECAT.

5.7. References

[1] G. C. Bond, *J. Chem. Technol. Biotechnol.* **1997**, *68*, 6-13; B. Grzybowska Swierkosz, *Appl. Catal. A-Gen.* **1997**, *157*, 263-310; V. Nikolov, D. Klissurski, A. Anastasov, *Catal. Rev.-Sci. Eng.* **1991**, *33*, 319-374; M. S. Wainwright, N. R. Foster, *Catal. Rev.-Sci. Eng.* **1979**, *19*, 211-292; F. Cavani, N. Ballarini, S. Luciani, *Top. Catal.* **2009**, *52*, 935-947.

[2] Q. B. Wang, X. Li, L. J. Wang, Y. W. Cheng, G. Me, *Ind. Eng. Chem. Res.* **2005**, *44*, 261-266; P. Raghavendrachar, S. Ramachandran, *Ind. Eng. Chem. Res.* **1992**, *31*, 453-462; A. J. Hu, C. X. Lu, B. D. Li, *Progress in Chemistry* **2007**, *19*, 292-302; G. M. Cao, A. Servida, M. Pisu, M. Morbidelli, *Aiche Journal* **1994**, *40*, 1156-1166; S. W. Tang, B. Liang, *Ind. Eng. Chem. Res.* **2007**, *46*, 6442-6448.

[3] W. Partenheimer, *Catal. Today* **1995**, *23*, 69-158.

[4] W. Z. Sun, Y. Pan, L. Zhao, X. G. Zhou, *Chem. Eng. Technol.* **2008**, *31*, 1402-1409.

[5] J. A. A. Hoorn, J. Van Soolingen, G. F. Versteeg, *Chem. Eng. Res. Des.* **2005**, *83*, 187-195.

[6] A. Gizli, G. Aytimur, E. Alpay, S. Atalay, *Chem. Eng. Technol.* **2008**, *31*, 409-416.

[7] T. Förster, S. Scholz, Y. Zhu, J. A. Lercher, *Microporous and Mesoporous Materials* **2010**, submitted for publication; H. Witossek, E. Bratz, *Chem. Eng. Technol.* **1997**, *20*, 429-433; E. Yacoub-George, E. Bratz, H. Tiltscher, *J. Non-Cryst. Solids* **1994**, *167*, 9-15.

[8] G. B. Shulpin, D. Attanasio, L. Suber, *J. Catal.* **1993**, *142*, 147-152.

[9] T. Förster, S. A. Schunk, A. Jentys, J. A. Lercher, *Chem. Commun.* **2010**, submitted for publication.

[10] W. Pritzkow, R. Hofmann, *Journal Für Praktische Chemie* **1960**, *12*, 11-17.

[11] S. A. Chavan, D. Srinivas, P. Ratnasamy, *J. Catal.* **2001**, *204*, 409-419.

[12] W. Partenheimer, *J. Mol. Catal. A-Chem.* **2003**, *206*, 105-119.

Chapter 6

Summary and conclusions

The focus of this work was the synthesis of transition metal containing spherical polysiloxanes as catalysts for the selective oxidation of alkyl substituted aromatics. To optimize the catalytic performance of these materials the effect of the synthesis procedure was elucidated and fine tuned. By means of physicochemical characterization techniques the surface chemistry and the properties of the polysiloxanes were studied. Relevant properties were the chemical nature of interaction of the support with transition metals, the hydrophobicity of the materials and the accessibility of the catalytically active transition metal species. Besides the description of the catalyst's nature the selective liquid phase oxidation of *o*-xylene under solvent free conditions was investigated. The focus was the understanding of mechanistic details and the elucidation of the function of the catalyst. The development of a reaction network including all reaction intermediates was the fundament for the kinetic description of this network.

After the description of the motivation of this work in Chapter 1 a summary of the reaction principles of synthesis routes of polysiloxanes by the sol-gel process using hydrolysable silane precursors are overviewed in Chapter 2 of this thesis. The synthesis procedure is explained in detail because it allows the production of spherical polysiloxane particles in the millimeter range. Furthermore the principles of radical based liquid phase oxidations of alkyl substituted aromatics are summarized focusing on the industrially applied initiator systems.

The investigations on the synthesis procedure of spherical polysiloxane based catalysts in Chapter 3 described the structure and properties of the organically modified silica. It was shown that the incorporation of transition metals into the polysiloxane support was possible for a broad variety of metals including Co, Cu, Fe, V and Mn. For the synthesis of polysiloxane spheres by the present synthesis process the introduction of basic amino group containing silanes is necessary since the basicity is crucial to ensure a sufficient reaction rate. The rate of polycondensation is very important because the reaction volume is limited by the height of the water filled column in the present process. Additionally, the amino groups act as anchor for transition metals. IR spectroscopy confirmed the coordination of the transition metal by amino groups affixed to the polysiloxane network. The accessibility of incorporated transition metals, which is very important in terms of catalytic applications, was verified by adsorbing CO as a probe molecule. The presence of transition metals in the precursor mixture furthermore allowed a faster condensation of the silanes because of the formation of condensation nuclei. This resulted in a higher degree of condensation shown by ^{29}Si MAS NMR spectroscopy. A variation of the base concentration in the reaction mixture illustrated the function of the basic groups. By increasing the base concentration the specific surface area decreased giving evidence for a higher degree of condensation of the polysiloxane network. Also the type of amino source influenced the condensation behavior. The use of side groups with two amino groups increased the reaction rate due to their higher basicity and hydrophilicity. When the concentration of organic side groups was increased the hydrophobicity increased as more lipophil groups are located on the (inner) surface. By adsorption of water to the polysiloxane network the hydrophilicity was shown to be lower than an oxidic reference material. The hydrophobicity depended on the amount and the type of organic chains introduced into the polysiloxane. It was concluded that the present method allows the incorporation of a variety of transition metals into a hydrophobic polysiloxane matrix offering potential for catalytic applications. The relatively simple variation of the surface properties of the spherical polysiloxanes, additionally, offers a powerful tool to adjust the support to the specifications of the applied process.

In Chapter 4 the application of Co^{2+} or Mn^{3+} containing polysiloxane catalysts in the selective liquid phase oxidation of *o*-xylene under solvent free conditions was investigated. The reaction mechanism is described by a radical chain reaction. The function of the catalysts is the acceleration of the radical initiation and the decomposition of intermediately formed hydroperoxide species. From the linear correlation of the catalysts’ activity and the transition metal concentration it was concluded that the active center is the transition metal cation. The quantification of CO adsorption experiments, additionally, showed a linear correlation of the adsorption capacity and the cation concentration indicating that the metal loading of the catalyst does not change the accessibility and the local structure of the transition metal species. The catalysts were shown to effectively decompose 2-methylbenzyl hydroperoxide during the oxidation reaction of *o*-xylene to 2-methylbenzyl alcohol and *o*-tolualdehyde. Depending on the type of transition metal a more pronounced selectivity to one of the two decomposition products was observed. Co^{2+} enhanced the formation of *o*-tolualdehyde whereas in the case of Mn^{3+} 2-methylbenzyl alcohol was favored. The difference in reactivity is caused by the different electronegativities of the metals resulting in a different polarization of the intermediately formed metal oxygen bond. The overall activity of the polysiloxane based catalysts was higher than the reference system Co naphthenate. This was explained by the hydrophobicity of the polysiloxane support as interactions of the polar reaction products with this hydrophobic surface are weak reducing its retention in the pores. Toluene and mesitylene were also selectively oxidized over the investigated materials showing a general activity for the selective oxidation of alkyl substituted aromatics.

To further strengthen the conclusions drawn from the observations in the reaction network analysis the kinetic simulation of each reaction is described in Chapter 5. The description follows the network deduced from the reactivity analysis. As primary product 2-methylbenzyl hydroperoxide is formed from *o*-xylene. Consecutively it is decomposed to *o*-tolualdehyde and 2-methylbenzyl alcohol by the catalyst. The rate constant of the two decomposition pathways strongly depends on the transition metal of the catalyst as seen in the analysis of the reaction network in Chapter 4. Mn^{3+} enhances the formation of 2-methylbenzyl alcohol whereas Co^{2+} tends to form more *o*-tolualdehyde. This selectivity relation is reflected in the rate constants of the two decomposition pathways which both were orders of magnitude higher than those of the hydroperoxide formation. Additionally, it was confirmed by the calculations that the further oxidation to *o*-toluic acid proceeds via *o*-tolualdehyde and no direct route from 2-methylbenzyl alcohol is assumed. The initial reaction of *o*-xylene to 2-methylbenzyl hydroperoxide occurs via two pathways. A direct oxidation by the transition metal component and an autocatalytic route are used for the simulation. The function of the catalysts was shown to be the increase of rate of the initiation step and even more pronounced the acceleration of the hydroperoxide decomposition. In case of Mn catalysis the further oxidation of 2-methylbenzyl alcohol to *o*-tolualdehyde was accelerated and also the oxidation of *o*-tolualdehyde to *o*-toluic acid more pronounced than in the case of Co.

In summary, the studies described in this work show the effect of the systematic variation of the synthesis parameters during the production of polysiloxane supported catalysts on the material’s properties. The detailed characterization of polysiloxanes is summarized in Chapter 3. The application of Co or Mn containing catalysts for the selective liquid phase oxidation of *o*-xylene is the main focus of the Chapters 4 and 5. Knowledge of mechanistic aspects of tuned materials was gained by the detailed analysis of the reaction network by consideration of the individual reaction steps and by kinetic analysis. This work contributes to the understanding of radical chain oxidation reactions by elucidating the function of transition metals during this process.

Chapter 7

Zusammenfassung und Folgerungen

Der Schwerpunkt der vorliegenden Arbeit lag auf der Synthese übergangsmetallhaltiger, kugelförmiger Polysiloxane als Katalysatoren für die selektive Oxidation alkylsubstitierter Aromaten. Die Optimierung der Synthese und die exakte Kenntnis und Steuerung der Katalysatoreigenschaften sind von entscheidender Bedeutung für die Verbesserung der katalytischen Aktivität der Materialien. Mittels physiko-chemischer Charakterisierungsmethoden wurden die Chemie der Oberfläche und die Eigenschaften der Polysiloxane untersucht. Relevante Eigenschaften waren dabei die Interaktion der Übergangsmetalle mit den Trägermaterialien, die Hydrophobizität der Materialien und die Zugänglichkeit der katalytisch aktiven Übergangsmetalle. Neben der Beschreibung der Katalysatoren wurden diese in der selektiven Flüssigphasenoxidation von *o*-Xylol unter lösemittelfreien Bedingungen getestet. Der Schwerpunkt lag dabei auf dem Verständnis des Reaktionsmechanismus und der Aufgaben der Katalysatoren in diesem. Die Entwicklung eines Reaktionsnetzwerks, das sämtliche Intermediate der Reaktion beinhaltet, stellte das Fundament zur kinetischen Beschreibung der vorliegenden Prozesse dar.

Nach der Darlegung der Motivation für diese Arbeit in Kapitel 1 sind in Kapitel 2 dieser Arbeit die Grundlagen der Reaktionen hydrolysierbarer Silanverbindungen während des Sol-Gel Prozesses und die Prinzipien des in dieser Arbeit angewendeten Syntheseprozesses zusammengefasst. Die Grundlagen der Synthesemethode sind ausführlich erläutert, da dieses spezielle Verfahren die Herstellung kugelförmiger Polysiloxane im Millimetermaßstab ermöglicht. Außerdem sind die Grundlagen von Oxidationsreaktionen, die über Radikalketten ablaufen, beleuchtet. Der Fokus dabei auf industriell verwendete Initiatorsysteme gelegt.

Untersuchungen der Synthese der sphärischen Polysiloxan-Katalysatoren konnten die Struktur und die Eigenschaften der organisch modifizierten Materialien aufklären. Diese sind in Kapitel 3 dieser Arbeit zusammengefasst. Es wurde gezeigt, dass die Integration von Übergangsmetallen in die Polysiloxanmatrix für eine Vielzahl von Metallen möglich war, darunter Co, Cu, Fe, V und Mn. Für die Synthese der Polysiloxankugeln mittels der beschriebenen Methode erwiesen sich Silane mit Aminogruppen als notwendig, da diese eine ausreichend große Reaktionsgeschwindigkeit sicherstellen. Die Rate der Kondensation ist äußerst wichtig, da der Reaktionsraum durch die Höhe des verwendeten Reaktors begrenzt ist. Darüber hinaus fungieren die Aminogruppen, die an das Polysiloxannetzwerk gebunden sind, als Bindestelle für Übergangsmetalle. Die Zugänglichkeit der integrierten Übergangsmetalle, die im Hinblick auf katalytische Anwendungen sehr wichtig ist, wurde durch die Adsorption des Testmoleküls CO bestätigt. Die Anwesenheit von Übergangsmetallen in der Ausgangslösung führte ferner zur Beschleunigung der Kondensation der Silane, da sich Kondensationskeime ausbildeten. Diese führte zu einem höheren Grad der Kondensation, welcher durch ^{29}Si-MAS NMR-Spektroskopie gezeigt wurde. Durch Variation der Basenkonzentration der Reaktionsmischung konnte die Funktion der basischen Gruppen ermittelt werden. Eine Erhöhung der Basenkonzentration führte zu einer Reduzierung der spezifischen Oberfläche, die auf eine Zunahme des Kondensationsgrads schließen lässt. Auch die Art der Aminoquelle spielte eine Rolle für die Kondensation. Bei Verwendung organischer Gruppen mit zwei Aminofunktionalitäten stieg die Reaktionsgeschwindigkeit wegen der höheren Basizität und Hydrophilie. Eine Erhöhung der Konzentration organischer Seitengruppen ging einher mit einer Steigerung der Hydrophobie, da mehr lipophile Gruppen auf der (inneren) Oberfläche lokalisiert sind. Mittels Adsorption von Wasser konnte verdeutlicht werden, dass die Hydrophilie geringer ist als bei oxidischen Vergleichsmaterialien. Diese hing von der Konzentration und der Art der eingebauten organischen Gruppen ab. Es konnte gezeigt werden, dass die beschrieben Methode die Integration einer breiten Anzahl an Übergangsmetallen in eine hydrophobe Polysiloxanmatrix ermöglicht und somit großes Potential für katalytische Anwendungen besitzt. Die verhältnismäßig einfache Variation der Oberflächeneigenschaften der kugelförmigen Polysiloxane ermöglicht darüber hinaus ein mächtiges Werkzeug zur Abstimmung des Trägermaterials auf die Forderungen der jeweiligen Anwendung.

Kapitel 4 beschreibt die Anwendung Co^{2+}- und Mn^{3+}-haltiger Polysiloxankatalysatoren in der selektiven Flüssigphasenoxidation von *o*-Xylol unter lösemittelfreien Bedingungen. Der Reaktionsmechanismus dieser Oxidation wird durch einen Radikalketten-Mechanismus beschieben. Die Aufgaben des Katalysators bestehen dabei in der Beschleunigung der Radikal-Initiierung und der Zersetzung intermediär gebildeter Hydroperoxide. Aus der linearen Abhängigkeit der Katalysatoraktivität von der Übergangsmetallkonzentration wurde geschlossen, dass die Übergangsmetalle die aktiven Zentren sind. Die Quantifizierung der CO-Adsorption zeigte ferner, dass die Adsorptionskapazität linear von der Übergangsmetallkonzentration abhängt. Dies ist ein weiterer Hinweis dafür, dass die Metallbeladung der Katalysatoren die Zugänglichkeit und die lokale Struktur nicht verändert. Die Katalysatoren zersetzten während der Oxidationsreaktion von *o*-Xylol 2-Methylbenzylhydroperoxid effektiv zu *o*-Tolylaldehyd und 2-Methylbenzylalkohol. Abhängig vom Übergangsmetall war die Selektivität zu einem der beiden Zersetzungsprodukte mehr ausgeprägt. Co^{2+} bevorzugte die Bildung von *o*-Tolylaldehyd während Mn^{3+} die Zersetzung zu 2-Methylbenzylalkohol forcierte. Die unterschiedliche Reaktivität wurde mit den verschiedenen Elektronegativitäten der Metalle begründetet, die eine unterschiedliche Polarisierung der zwischenzeitlich gebildeten Metall-Sauerstoff-Bindung verursacht. Die Gesamtaktivität der Polysiloxankatalysatoren war größer als ein Referenzsystem Co-Naphthenat. Diese verbesserte Aktivität wurde durch die hydrophobe Oberfläche des Polysiloxanträgers erklärt. Die Interaktion dieser mit polaren Reaktionsprodukten ist äußerst schwach und verringert dadurch die Zurückhaltung der Produkte in den Poren des Katalysators. Toluol und Mesitylen konnten mit den beschriebenen Katalysatoren ebenfalls selektiv oxidiert werden. Dies zeigt, dass diese als allgemein aktive Materialien bezüglich der selektiven Oxidation alkylsubstituierter Aromaten angesehen werden können.

Um die Folgerungen, die aus den Beobachtungen der Analyse des Reaktionsnetzwerks gezogen wurden, zu belegen wurde in Kapitel 5 die einzelnen Reaktionen mittels eines kinetischen Modells beschreiben. Die Beschreibung folgt dabei dem Reaktionsnetzwerk, das aus der Untersuchung der Reaktivität abgeleitet wurde. Als Primärprodukt aus *o*-Xylol wurde 2-Methylbenzylhydroperoxid angenommen. Dieses wird katalytisch anschließend zu *o*-Tolylaldehyd oder 2-Methylbenzylalkohol zersetzt. Die Geschwindigkeitskonstante der beiden Zersetzungsrouten hängt dabei stark von der Art des verwendeten Übergangsmetalls ab, die bei der Analyse des Reaktionsnetzwerks in Kapitel 4 beschrieben wurde. Mn^{3+} beschleunigt die Bildung von 2-Methylbenzylalkohol während Co^{2+} zur Bildung von *o*-Tolylaldehyd tendiert. Diese Selektivitäten werden in den Ratenkonstanten der Zersetzungswege widergespiegelt, die in beiden Fällen um Größenordnungen größer sind als die der Bildung des Hydroperoxids. Darüber hinaus wurde durch die Berechnungen gezeigt, dass die Weiteroxidation zu *o*-Tolylsäure über *o*-Tolylaldehyd erfolgt und keine direkte Route von 2-Methylbenzylalkhohl ausgehend existiert. Die Initiierung der Reaktion des *o*-Xylol zu 2-Methylbenzylhydroperoxid erfolgt über zwei Pfade. Zum Einen wurde eine direkte Oxidation durch das Übergangsmetall und zusätzlich eine autokatalytische Route zur Simulation der Ratenkonstanten verwendet. Als Wirkungsweise des Katalysators wurden somit die Erhöhung der Bildungsrate des 2-Methylbenzylhydroperoxids und ferner dessen Zersetzung, die in größerem Maß beschleunigt wurde, bestimmt. Im Falle der Mn-Katalysatoren wurde die Oxidation von 2-Methylbenzylalkohol zu *o*-Tolylaldehyd und auch die Weiteroxidation dessen zur *o*-Tolylsäure in größerem Maße beschleunigt, als das für Co der Fall war.

Zusammenfassend lässt sich resümieren, dass die beschriebenen Studien den Einfluss der systematischen Variation der Synthesebedingungen auf die Eigenschaften der Polysiloxane darstellen. Die detaillierte Charakterisierung der Polysiloxane ist in Kapitel 3 zusammengefasst. Die Anwendung Co- oder Mn-haltiger Katalysatoren für die selektive Flüssigphasenoxidation von *o*-Xylol ist der Hauptteil der Arbeiten in den Kapiteln 4 und 5. Verständnis mechanistischer Aspekte bei Verwendung optimierter Katalysatoren wurde aus der genauen Analyse des Reaktionsnetzwerks unter Berücksichtigung der einzelnen Reaktionen und der Kinetik gewonnen. Durch die Beschreibung der Funktion der Katalysatoren trägt diese Arbeit zum Verständnis von Radikalkettenreaktionen bei.

Curriculum Vitae

Tobias Förster was born in Munich on October 8th, 1980. He visited the Gisela-Gymnasium München until June 2000, when he graduated and received his Abitur (general qualification for university entrance). After civilian service until July 2001, he took up chemistry studies at the Technische Universität München, majoring in catalysis and reaction engineering. In 2006, Tobias Förster joined the group of Johannes A. Lercher (Chair for technical chemistry II) for his Diploma thesis entitled “Investigation on the Dealumination Kinetics of HZSM-5 Zeolite by Steaming Treatment”. After graduation as “Diplom-Chemiker” (master degree) in August 2006, he stayed in the group of Johannes A. Lercher as a PhD student at the Technische Universität München. His work was focused on the transition metal containing polysiloxane based catalysts for selective oxidation reactions.

List of publications

One step synthesis of organofunctionalized transition metal containing porous silica spheres, T. Förster, S. Scholz, Y. Zhu, J. A. Lercher, *Microporous and Mesoporous Materials*, **2011**, accepted for publication.

Co and Mn polysiloxanes as unique initiator-catalyst-systems for the selective liquid phase oxidation of *o*-xylene, T. Förster, S. A. Schunk, A. Jentys, J. A. Lercher, *Chemical Communications*, **2011**, submitted for publication.

Selective liquid phase oxidation of *o*-xylene with gaseous oxygen by transition metal containing polysiloxane initiator-catalyst-systems, T. Förster, S. A. Schunk, A. Jentys, J. A. Lercher, *Journal of the American Chemical Society*, **2011**, submitted for publication.

List of presentations

Selective oxidation of alkyl aromatics by silica supported transition metal catalysts, (Poster) T. Förster, A. Jentys, J.A. Lercher, 42. Jahrestreffen Deutscher Katalytiker, **2009**, Weimar, Germany.

Continuous preparation of functionalized porous silica spheres, (Poster) S. Scholz, T. Förster, J.A. Lercher, 21. Deutsche Zeolithtagung, **2009**, Kiel, Germany.

Silica based transition metal materials as heterogeneous catalysts for the selective liquid phase oxidation of alkyl aromatics, (Poster) T. Förster, S. A. Schnk, A. Jentys J.A. Lercher, 43. Jahrestreffen Deutscher Katalytiker, **2010**, Weimar, Germany and 4th IDECAT Conference on Catalysis, **2010**, Porquerolles, France.